

1992

Yield pillar design for United States longwall mining.

Po Tsang

Follow this and additional works at: <https://researchrepository.wvu.edu/etd>

Recommended Citation

Tsang, Po, "Yield pillar design for United States longwall mining." (1992). *Graduate Theses, Dissertations, and Problem Reports*. 9916.

<https://researchrepository.wvu.edu/etd/9916>

This Thesis is protected by copyright and/or related rights. It has been brought to you by the The Research Repository @ WVU with permission from the rights-holder(s). You are free to use this Thesis in any way that is permitted by the copyright and related rights legislation that applies to your use. For other uses you must obtain permission from the rights-holder(s) directly, unless additional rights are indicated by a Creative Commons license in the record and/ or on the work itself. This Thesis has been accepted for inclusion in WVU Graduate Theses, Dissertations, and Problem Reports collection by an authorized administrator of The Research Repository @ WVU. For more information, please contact researchrepository@mail.wvu.edu.

INFORMATION TO USERS

This manuscript has been reproduced from the microfilm master. UMI films the text directly from the original or copy submitted. Thus, some thesis and dissertation copies are in typewriter face, while others may be from any type of computer printer.

The quality of this reproduction is dependent upon the quality of the copy submitted. Broken or indistinct print, colored or poor quality illustrations and photographs, print bleedthrough, substandard margins, and improper alignment can adversely affect reproduction.

In the unlikely event that the author did not send UMI a complete manuscript and there are missing pages, these will be noted. Also, if unauthorized copyright material had to be removed, a note will indicate the deletion.

Oversize materials (e.g., maps, drawings, charts) are reproduced by sectioning the original, beginning at the upper left-hand corner and continuing from left to right in equal sections with small overlaps. Each original is also photographed in one exposure and is included in reduced form at the back of the book.

Photographs included in the original manuscript have been reproduced xerographically in this copy. Higher quality 6" x 9" black and white photographic prints are available for any photographs or illustrations appearing in this copy for an additional charge. Contact UMI directly to order.

U·M·I

University Microfilms International
A Bell & Howell Information Company
300 North Zeeb Road, Ann Arbor, MI 48106-1346 USA
313/761-4700 800/521-0600

Order Number 9409890

Yield pillar design for U.S. longwall mining

Tsang, Po, Ph.D.

West Virginia University, 1992

Copyright ©1994 by Tsang, Po. All rights reserved.

U·M·I
300 N. Zeeb Rd.
Ann Arbor, MI 48106

YIELD PILLAR DESIGN FOR U.S. LONGWALL MINING

by

Po Tsang, M.S. Mining Engineering

A Dissertation

Submitted to the Faculty of

Department of Mining Engineering

College of Mineral and Energy Resources

West Virginia University

In Partial Fulfillment of the Requirements

for the Degree of

Doctor of Philosophy

in

Mining Engineering

Morgantown, West Virginia

October 1992

ABSTRACT

The longwall mining in U.S. has continuously set both the world production and safety records over the years. In order to ensure the future success of longwall mining, continuous improvement on this new mining technology is very important. This study deals with the problems related to longwall pillar design by proposing a new pillar design method based on the "yield pillar" concept.

In order to simplify the geological and mining conditions, the new pillar design method classifies the in-situ roof and floor conditions into four different categories: 1) strong roof and strong floor, 2) strong roof and weak floor, 3) weak roof and strong floor, and 4) weak roof and weak floor conditions. According to different roof and floor conditions, the new method can be used to design various types of three-entry system for longwall panel development. Comparison among different types of design indicates that the stiff-yield pillar design is the most favorable design and can be used as an alternative, especially under deeper cover.

The new pillar design method is developed based on the finite element model simulation, stability study and nonlinear regression analysis. The finite element model used in this study considers the material properties and time-dependent behaviors of rock. To better organize the finite element model simulation, the orthogonal experiment design is used in this study to arrange the finite element models and proved

to be very effective. Using the finite element model simulation, the functions and mechanisms of the "yield pillar" have been studied. The important variables that affect the stability of longwall entry-pillar system are identified also.

In this study, the new pillar design method has been also compared with the other available longwall pillar design methods. In addition, an application example is used to illustrate the basic design procedures involved in the new pillar design method.

ACKNOWLEDGEMENTS

The research effort represented in this dissertation was made possible through the contributions of many persons. With respect and gratitude, the author is deeply indebted to all members of his research committee: Dr. A. W. Khair, Dr. C. Mark, Dr. H. J. Siriwardane and Dr. N. T. Sivaneri for their supports and invaluable suggestions during this research work. Their guidance, concern, and positive thinking will long be remembered and appreciated.

Sincere gratitude and appreciation is expressed to Dr. S. S. Peng, Chairman of his advisory committee, for initially suggesting the problem, and for his supervision, interest, and interesting discussions provided throughout this research. His guidance has been invaluable to the completion of this dissertation, and is greatly appreciated.

The author also expresses heartfelt appreciations to his fellow students and staffs of COMER for their help.

An acknowledgement is also due to his family. Their generosity and understanding is overwhelming, their support literally made this research effort feasible. And to his wife, Silvia; and daughter, Julia, the author sincerely thanks for providing the motivation and inspiration that made it all worthwhile.

Finally, the author expresses his deepest appreciation and affection for the support, encouragement, and patience of his parents, Ke-Chin Tsang and Xiao-Yu Huang. The author owes special thanks to his mother-in-law, Manly Yang, who has unselfishly supported him and his family during this study.

TABLE OF CONTENTS

	<u>Page</u>
ABSTRACT	i
ACKNOWLEDGMENTS	ii
TABLE OF CONTENTS	iii
LIST OF TABLES	iv
LIST OF FIGURES	vi
LIST OF SYMBOLS	xi
1. INTRODUCTION	1
2. LITERATURE REVIEW	5
2.1. Two Pillar Design Concepts	5
2.2. Pillar Load Consideration	6
2.2.1 Room-And-Pillar Mining	6
2.2.2 Longwall Mining	8
2.2.3 Abutment Load Distribution	11
2.3. Pillar Strength Consideration	13
2.3.1 Size Effect	13
2.3.2 Shape Effect	14
2.4. Standard Procedure of Conventional Pillar Design	19
2.5. Yield Pillar Practice	20
2.6. Summary	24
3. ROOF AND FLOOR CLASSIFICATION SYSTEM FOR YIELD PILLAR DESIGN	29
3.1 Variables Affected Performance of Entry-Pillar System	29
3.2 Purpose of Developing A Roof and Floor Classification System	30
3.3 Roof and Floor Classification Method	31
3.3.1 Introduction	31
3.3.2 Principle of Classification System	32
3.3.3 Selection of Classification Indexes	33
3.3.4 Classification Procedures	34
3.4 Roof and Floor Conditions in Underground Coal Mines	43

	<u>Page</u>
4. MECHANISM OF YIELD PILLAR	45
4.1 Introduction	45
4.2 Finite Element Modeling	45
4.2.1 Finite Element Method Consideration	46
4.2.2 A Typical Finite Element Model	47
4.3 Stability Criteria of Entry-Pillar System	50
4.4 Mechanism of Yield Pillar	51
4.5 Model Simulation	52
4.5.1 Strong Roof and Strong Floor Condition	56
4.5.2 Strong Roof and Weak Floor Condition	64
4.6 Conclusions	75
5. SIGNIFICANCE ANALYSIS ON VARIABLES AFFECTING PERFORMANCE OF LONGWALL CHAIN PILLAR	77
5.1 Introduction	77
5.2 Variables Considered in Significance Analysis	78
5.3 Orthogonal Experiment Design for Finite Element Model	80
5.4 Finite Element Model	83
5.5 Results And Discussion	90
5.5.1 Stability Indexes	90
5.5.2 Maximum Variance Analysis	91
6. DEVELOPMENT OF NEW PILLAR DESIGN METHOD	100
6.1 Introduction	100
6.2 3-Level Orthogonal Experiment Design for Finite Element Modeling	101
6.3 The Strong Roof and Strong Floor Conditions	104
6.3.1 Introduction	104
6.3.2 Regression Model	106
6.3.3 Design of Three-Entry System under the Strong Roof and Strong Floor Conditions	108
6.4 The Strong Roof and Weak Floor Conditions	115
6.4.1 Introduction	115
6.4.2 Regression Model	117
6.4.3 Design of Three-Entry System under the Strong Roof and Weak Floor Conditions	118
6.5 The Weak Roof and Strong Floor Conditions	122
6.5.1 Introduction	122

	<u>Page</u>
6.5.2 Regression Model	125
6.5.3 Design of Three-Entry System under the Weak Roof and Strong Floor Conditions	126
6.6 The Weak Roof and Weak Floor Conditions	127
6.6.1 Introduction	127
6.6.2 Regression Model	131
6.6.3 Design of Three-Entry System under the Weak Roof and Weak Floor Conditions	133
6.7 Summary	138
7. COMPARISON STUDY AND APPLICATION	139
7.1 Introduction	139
7.2 Design Procedures	139
7.2.1 Classification of In-situ Roof and Floor Conditions	141
7.2.2 Use of Corresponding Equations for Determining Suitable Pillar Size	142
7.3 Application Example	143
7.4 Comparison Study	147
7.5 Summary	151
8. CONCLUSIONS	152
REFERENCES	155
VITA	160
APPROVAL PAGE	

LIST OF TABLES

<u>Table</u>	<u>Page</u>
3.1 Raw Data Matrix for the Cluster Analysis	35
3.2 Weighting Factors for the Classification Variables	38
3.3 Mean Vector of Each Group	41
3.4 Standardized Mean Vector of Each Group	41
4.1 Reduction Factors for Gob Materials	50
4.2 Rock Mechanical Properties	55
4.3 Recommended Pillar Size under the Strong Roof and Strong Floor Condition	63
4.4 Recommended Pillar Size under the Strong Roof and Weak Floor Condition	75
5.1 Variables Considered in Different Pillar Design Methods	79
5.2 Finite Element Models Designed by A 2-Level Orthogonal Experiment Plan	81
5.3 Rock Mechanical Properties	87
5.4 Database for Finite Element Model Analysis	89
5.5 Orthogonal Experiment Design for 2-Level 14 Variables	92
6.1 3-Level Orthogonal Experiment Design for 10 Variables	103
6.2 Database for Finite Element Modeling under Strong Roof and Strong Floor Condition	105
6.3 Input Data for Comparison Study under Strong Roof and Strong Floor Condition	112

<u>Table</u>	<u>Page</u>
6.4 Database for Finite Element Modeling under Strong Roof and Weak Floor Condition	116
6.5 Input Data for Comparison Study under Strong Roof and Weak Floor Condition	119
6.6 Database for Finite Element Modeling under Weak Roof and Strong Floor Condition	124
6.7 Input Data for Comparison Study under Weak Roof and Strong Floor Condition	126
6.8 Database for Finite Element Modeling under Weak Roof and Weak Floor Condition	132
6.9 Input Data for Comparison Study under Weak Roof and Weak Floor Condition	133
7.1 Mechanical Properties of Related Rocks	143
7.2 Classification Variables of New Samples	144
7.3 Euclidean Distances between New Samples and Centers of the Predefined Groups	144

LIST OF FIGURES

<u>Figure</u>	<u>Page</u>
2.1 A typical room-and-pillar mining layout(after Peng, 1986)	7
2.2 Supercritical longwall panel(after King and Whittaker, 1971)	9
2.3 Subcritical longwall panel(after King and Whittaker, 1971)	9
2.4 Abutment load distribution proposed by Wilson (after Carr and Wilson)	12
2.5 Theoretical vertical stress distribution in coal pillars(after Wilson, 1983)	18
2.6 Parallel-room method	21
2.7 Time-control method	22
2.8 Compounded-time-control method	23
2.9 Two-entry system, yield pillar design	25
2.10 Three-entry system, stiff-yield pillar design	25
2.11 Four-entry system, yield-stiff-yield pillar design	26
2.12 Five-entry system, yield-stiff-stiff-yield pillar design	26
2.13 Five-entry system, full-yield pillar design	27
3.1 Schematic diagram for the cluster analysis	37
4.1 A typical longwall panel layout	48
4.2 A typical 2-D finite element model	49
4.3 Geological column used in finite element models for simulating the strong roof and strong floor conditions	53

<u>Figure</u>	<u>Page</u>
4.4 Geological column used in finite element models for the simulating strong roof and weak floor conditions	54
4.5 Yield zone changes with yield pillar size under the strong floor conditions after the 2nd panel mining	57
4.6 Yield zone changes with stiff pillar size under the strong floor conditions after the 2nd panel mining	58
4.7 Changes of floor safety factor with yield pillar width before the 2nd panel mining while stiff pillar is 120 ft. wide	59
4.8 Changes of floor safety factor width stiff pillar width before the 2nd panel mining while yield pillar is 15 ft. wide	59
4.9 Maximum entry convergence in entry 2 changes with yield pillar width before the 2nd panel mining	61
4.10 Maximum entry convergence in entry 2 changes with stiff pillar width before the 2nd panel mining	61
4.11 Average vertical strain in yield pillar before the 2nd panel mining while stiff pillar is 60 ft. wide	62
4.12 Maximum tensile stress in roof of entry 2 before the 2nd panel mining	62
4.13 Stiff and yield pillar designs under strong roof and weak floor condition	65
4.14 Yield zone development under the weak floor condition for conventional pillar design	66
4.15 Yield zone changes with yield pillar size under the weak floor conditions	68

<u>Figure</u>	<u>Page</u>
4.16 Yield zone changes with stiff pillar size under the weak floor conditions	69
4.17 Floor safety factor changes with yield pillar width under weak floor condition when stiff pillar is 120 ft. wide	71
4.18 Floor safety factor changes with stiff pillar width under weak floor condition when yield pillar is 20 ft. wide	71
4.19 Maximum entry convergence changes with yield pillar width	73
4.20 Maximum entry convergence changes with stiff pillar width	73
4.21 Pillar vertical strain changes with yield pillar width under weak floor condition when stiff pillar is 100 ft. wide	74
4.22 Maximum tensile stress in entry 2 when stiff pillar is 120 ft. wide	74
5.1 A typical longwall layout	84
5.2 Cross-section A-A used in finite element analysis	86
5.3 A typical geological column	88
5.4 Effect of variable on yield zone in Pillar 1	94
5.5 Effect of variable on yield zone in Pillar 2	94
5.6 Effect of variable on the maximum entry convergence in the entry-pillar system	96
5.7 Effect of variable on the maximum roof tensile stress in the entry-pillar system	96
5.8 Effect of variable on the minimum safety factor of the roof	97
5.9 Effect of variable on the minimum safety factor of the floor	97

<u>Figure</u>	<u>Page</u>
5.10 Effect of variable on average safety factor of pillars	98
5.11 Effect of variable on overall stability of the entry-pillar system	98
6.1 Stiff-stiff pillar design	109
6.2 Yield-yield pillar design	109
6.3 Combination of a stiff and a yield pillar design	110
6.4 Total pillar width vs depth of cover for both stiff-yield and yield-stiff pillar designs under strong roof and strong floor condition	113
6.5 Maximum tensile stress in roof vs depth of cover for both stiff-yield and yield-stiff pillar designs under strong roof and strong floor condition	113
6.6 Total pillar width vs depth of cover for stiff-stiff, yield-yield and stiff-yield pillar designs under strong roof and strong floor conditions	114
6.7 Maximum tensile stress in roof vs depth of cover for stiff-stiff, yield-yield and stiff-yield pillar designs under the strong roof and strong floor conditions	114
6.8 Total pillar width vs depth of cover for both stiff-yield and yield-stiff pillar designs under the strong roof and weak floor conditions	120
6.9 Minimum safety factor of floor vs depth of cover for both stiff-yield and yield-stiff pillar designs under the strong roof and weak floor condition	120
6.10 Maximum tensile stress in roof vs depth of cover for both stiff-yield and yield-stiff pillar designs under strong roof and weak floor condition	120

<u>Figure</u>	<u>Page</u>
6.11 Total pillar width vs depth of cover for stiff-stiff, yield-yield and stiff-yield pillar designs under strong roof and weak floor condition	120
6.12 Minimum safety factor of floor vs depth of cover for stiff-stiff, yield-yield and stiff-yield pillar designs under strong roof and weak floor condition	123
6.13 Maximum tensile stress in roof vs depth of cover for stiff-stiff, yield-yield and stiff-yield pillar designs under strong roof and strong floor condition	123
6.14 Total pillar width vs depth of cover for both stiff-yield and yield-stiff pillar designs under weak roof and strong floor condition	128
6.15 Minimum safety factor of roof vs depth of cover for both stiff-yield and yield-stiff pillar designs under weak roof and strong floor condition	128
6.16 Maximum tensile stress in floor vs depth of cover for both stiff-yield and yield-stiff pillar designs under weak roof and strong floor condition	129
6.17 Total pillar width vs depth of cover for stiff-stiff, yield-yield and stiff-yield pillar designs under weak roof and strong floor condition	129
6.18 Minimum safety factor of roof vs depth of cover for stiff-stiff, yield-yield and stiff-yield pillar designs under weak roof and strong floor condition	130
6.19 Maximum tensile stress in floor vs depth of cover for stiff-stiff, yield-yield and stiff-yield pillar designs under weak roof and strong floor condition	130
6.20 Total pillar width vs depth of cover for both stiff-yield and yield-stiff pillar designs under	

<u>Figure</u>	<u>Page</u>
weak roof and weak floor condition	135
6.21 Minimum safety factor of roof vs depth of cover for both stiff-yield and yield-stiff pillar designs under weak roof and weak floor condition	135
6.22 Minimum safety factor of floor vs depth of cover for both stiff-yield and yield-stiff pillar designs under weak roof and weak floor condition	136
6.23 Total pillar width vs depth of cover for stiff-stiff, yield-yield and stiff-yield pillar designs under weak roof and weak floor condition	136
6.24 Minimum safety factor of roof vs depth of cover for stiff-stiff, yield-yield and stiff-yield pillar designs under weak roof and weak floor condition	137
6.25 Minimum safety factor of floor vs depth of cover for stiff-stiff, yield-yield and stiff-yield pillar designs under weak roof and weak floor condition	137
7.1 Design Procedures	140
7.2 Total pillar width of stiff-stiff predicted by the different design methods for a three-entry system	149
7.3 Total pillar width of stiff-yield predicted by the different design methods for a three-entry system	150

CHAPTER 1

INTRODUCTION

After decades of longwalling coal in the U.S., improvements are still continuous on this new mining technology. The average daily production of the longwall panels has increased from several hundred tons to several thousand tons, on average three to six times of that produced ten years ago(Combs, 1992).

In 1991, there were a total of 93 operable longwall systems, with 27 companies operating in 12 states. Longwall operators had added 4 longwall faces in 1991, and the newly installed faces are much longer, wider and deeper than 10 years ago(Merritt, 1992). At present, longwall mines produce more than 37% of all underground coal, up from less than 31% just 5 years ago(Sanda, 1991). The growth of longwall mining has been spurred by an explosion in productivity, which has doubled since 1985(Combs, 1990). On the other hand, the increased demand of coal in utility and nonutility markets and exports has boosted coal production increasing at an annual rate of 1.2% in the 1980's(Sprouls, 1989). Overall, the latest industry forecast calls for coal production to expand at an average of 1.5 percent annually during the 1990's(Quenon, 1989). In 1990, the production reached one-billion-ton annual production level for the U. S. coal industry, setting the all time record(Sprouls, 1991).

The statistics have shown that longwall mining holds the promise of high

production at low cost under suitable operating conditions (Britton, 1986). In addition, the accident rates of longwall mining on a per-ton basis are one-third lower than room-and-pillar mining(Pappas, 1987). Because of its better production and safety records, longwalls have been called "the salvation of the large deep mines in America," and the production of longwall mining is expected to double in the 1990's(Eyer, 1989).

The current success in longwall mining is mainly attributed to the continuous improvement on mining technology and better geological and mining conditions. As the future longwall mining goes deeper, both geological and mining conditions become more complicated. Therefore, to select suitable longwall equipment and design proper longwall panels in accordance with geological and mining conditions present will have a great impact on the future success of the longwall mining in the U.S..

The key to a proper longwall panel design is to design a suitable longwall entry-pillar system that provides safe accesses for ventilation, coal and supplies transportation, man trips, and escape ways and keeps longwall mining in safe, high productivity and low cost bases. An improper designed longwall panel usually leads to an unstable entry-pillar system and causes serious ground control problems, such as roof falls, floor heaves, and pillar bumps. All these problems can greatly increase production cost and will become more severe as the longwall mining goes deeper. Sometimes, they may result in a significant loss of coal resources.

To solve these problems, a longwall entry-pillar system must be designed to fit

specific geological and mining conditions, and such design should maintain stable entries and pillars in the system that serve for transportation, ventilation and escape ways. Traditionally, pillars in the longwall entry-pillar system are designed to minimize the interaction between the entries and the adjacent mining activities. For this purpose, pillars in the system are designed as stiff pillars that will support the whole overburden load plus additional abutment loads. Therefore, the deeper the mining activity goes, the bigger the pillar size becomes. Large pillar means longer pillar length and frequently lead to insufficient quantities of air being delivered to the entry development faces, and slow down of longwall advance rate due to excessive tramming time in mining cycle and reduces the overall efficiency of longwall mining. When the longwall mining is conducted at great depth, the pillars become so big that they may not meet the ventilation and production requirements. On the other hand, longwall chain pillars are left unretrieved after longwall mining, the bigger chain pillars become, the lower coal recovery is. All of these problems from the traditional pillar design concept can result in unprofitable mining operations.

In order to reduce production cost while maintaining the health and safety standards for the miners, it is important now to search for a new approach to mine design problems. Application of yield pillar seems to be a very promising approach. Yield pillars reportedly have been very successful in controlling ground control problems in potash, salt, and trona mines. However, due to its complex geological conditions,

several questions have to be answered before the concept can be successfully applied to underground coal mines: What is the mechanism behind the yield pillar technique? Does the yield pillar concept really work in coal mines, and if it does, is it applicable under all types of geological and mining conditions? If applicable, what should be the proper method for yield pillar design?

This study is designed to address these very important issues. The results from the study will assist coal operators to evaluate whether a yield pillar design is feasible in their mines and if so, how they should design the mine layout.

CHAPTER 2

LITERATURE REVIEW

Pillar design is probably one of the oldest ground control problems in underground mining. Ever since coal mining began, tremendous efforts have been made to develop the more accurate and realistic design methods that can be used to design a safe pillar under various geological and mining conditions. Up to now, there are two pillar design concepts used in mining practice (Tsang and Peng, 1989): one is the traditional pillar design concept while the other which is relatively new is called the yield pillar design concept.

2.1 Two Pillar Design Concepts

The traditional pillar design, based on the ultimate strength theory, assumes that the stresses within a pillar are uniformly distributed and pillar will fail once the average stress reaches its strength. In order to design a safe pillar, both pillar load and strength are considered. The result from this concept is to design a stiff pillar that will support the whole overburden tributary to it such that it minimizes the interaction between entries and adjacent mining activities. In contrast, the yield pillar design concept takes the material's progressive failure into consideration. Since in reality the stresses inside a pillar and the surrounding materials are not uniformly distributed, failure is always

initiated at the critically stressed regions, propagates and leads to final collapse. Based on this design concept, a pillar can be designed to yield properly during its service life period and transfer its load to adjacent stiff pillars or surrounding rocks, and still maintain a stable entry-pillar system. Therefore, under the same geological and mining conditions, the yield pillar design concept tends to design a smaller pillar than the traditional concept.

Conceptually, the traditional pillar design is quite simple and straight forward. A successful pillar design depends on the accuracy of calculation of pillar load and pillar strength. To achieve this goal, researchers have been focusing mainly on; 1) determining pillar loading, and 2) estimating pillar strength. On the other hand, the yield pillar design based on a more realistic assumption and more or less on try-and-error bases, has been practiced in underground coal mines for many years.

2.2 Pillar Load Consideration

There are several approaches available for estimating pillar load, or average pillar stress. Basically, there are two types of loading conditions, each of them is related to different mining methods in underground coal mines.

2.2.1 Room-And-Pillar Mining

For room-and-pillar mining, the pillar load is calculated based on so called

tributary area loading concept(Peng, 1986) in the U.S.. According to this concept, a pillar supports uniformly the weight of the rock overlying the pillar and one-half the width of rooms or entries on each side of the pillar. Thus in a typical room-and-pillar

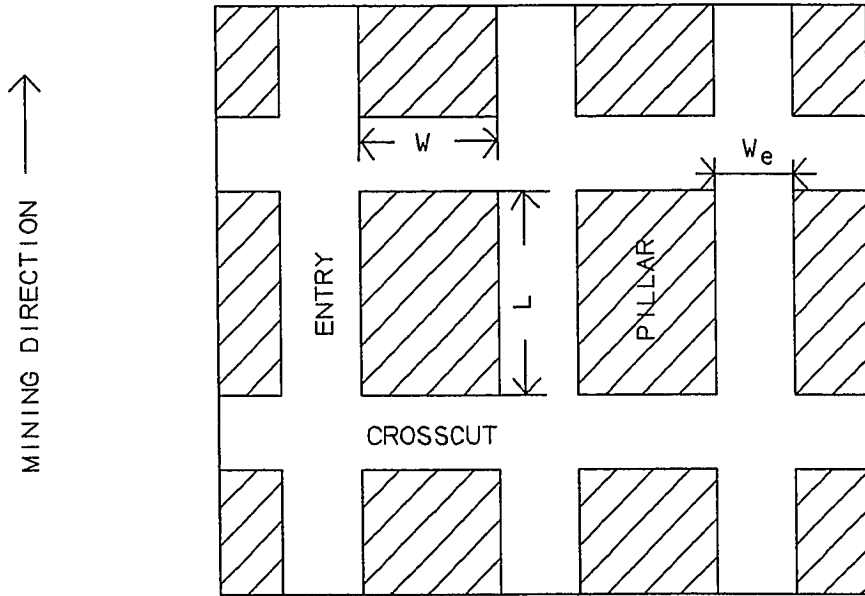


Figure 2.1. A typical room-and-pillar mining layout(after Peng, 1986).

mining layout(Fig.2.1), the average stress on a pillar can be calculated by the following equation.

$$S_p = \frac{(W+W_e)(L+W_e)}{WL} \times h\gamma \quad (2.1)$$

Where S_p is the average pillar stress, W and L are the width and the length of the pillar, respectively. W_e is the entry or room width, h is the overburden depth, and γ

is the unit weight of the overburden. In general, this method can approximately determine the pillar load in room-and-pillar mining without pillar retreating.

2.2.2 Longwall Mining

For longwall mining, pillars, in addition to the load defined by the tributary area loading concept, are subjected to abutment loads on one or two sides due to the presence of gob areas in one or two sides, respectively(Figs. 2.2 and 2.3). Usually, the longwall chain pillar experience two types of load during its service life: One is development load, which is present right after the development of longwall panel, and the other is abutment load attributable to the presence of gob areas in one or two sides, depending on the characteristics of the roof strata and their sequence(Peng and Chiang, 1984). Therefore, to accurately estimate the chain pillar load is very important for designing a proper longwall chain pillar system.

The development load is due to the weight of overburden directly above the pillars and entries, and can be estimated by the tributary area loading concept(Eq.2.1, and Fig.2.1).

The abutment loads occur when portions of the weight of overburden that have been supported by the excavated longwall panel are transferred to the pillars(Fig. 2.2). The abutment loads are further divided into side abutment load and front abutment load(Mark and Bieniawski, 1987). In order to calculate the side abutment loads, an

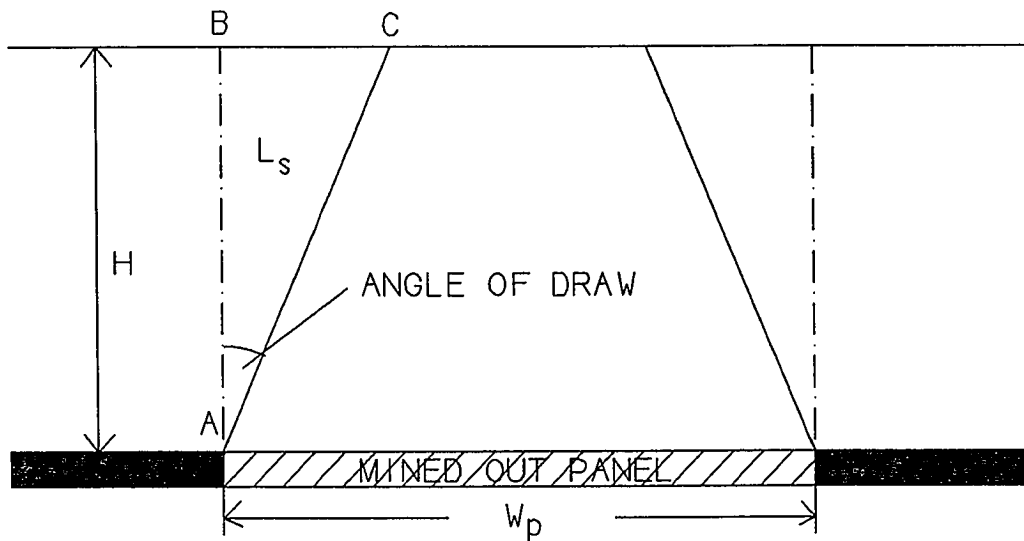


Figure 2.2. Supercritical longwall panel(after King and Whittaker, 1971).

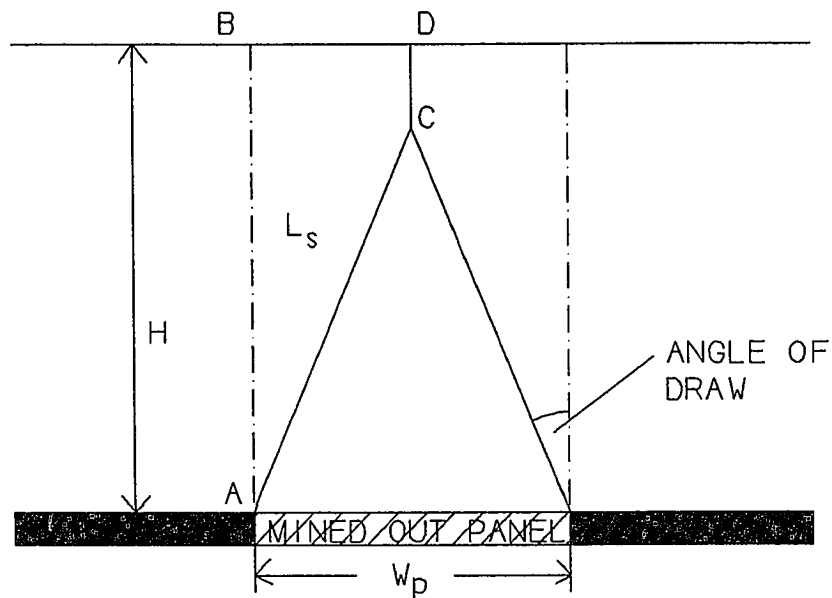


Figure 2.3. Subcritical longwall panel(after King and Whittaker, 1971).

analytical approach for estimating the pillar load has been proposed by King and

Whittaker(1971). They assumed that the additional load supported by a pillar is the volume of rock enclosed between the vertical line AB and the inclined line AC from the edge of the pillar(Fig. 2.2). The angle measured from the vertical line AB might be, according to King and Whittaker(1971), equals to the angle of draw used in subsidence analysis. For calculating the side abutment load, the following two equations have been developed by considering simple geometry:

For critical and supercritical panels where the panel width $W_p \geq 2h \tan(\beta)$ (Fig. 2.2);

$$L_s = \frac{h^2 \gamma \tan(\beta)}{2} \quad (2.2)$$

For subcritical panels where the panel width $W_p < 2h \tan(\beta)$ (Fig. 2.3).

$$L_s = \left(\frac{hW_p}{2} - \frac{W_p^2}{8 \tan(\beta)} \right) \gamma \quad (2.3)$$

Where L_s is the side abutment load, h is the overburden depth, γ is the average unit weight of the overburden, β is the angle of draw, and W_p is the width of longwall panel.

Therefore, whether or not the side abutment load can be accurately estimated depends heavily on the angle of draw. The magnitude of the front abutments load is much more difficult to determine analytically than that of the side abutment load. Some researchers have used three-dimensional numerical modeling to analyze the problem(Hsiung and Peng, 1985; Kripakov, 1986) while others have used field measured

data to estimate the front abutment pressure. Mark(1987) had presented the following formula to estimate the front abutment pressure based on the in-situ field measurement,

$$L_f = F_h(L_s) \quad (2.4)$$

where L_f is the front abutment load, F_h is front abutment factor. By relating the front abutment load to the side abutment load, the total loads on the longwall chain pillars can be determined.

2.2.3 Abutment Load Distribution

Since the stress in the pillars nearby the longwall panel is not uniformly distributed, it will affect the longwall chain pillar design. For this reason, the stress distribution within the abutment influence zone has been studied by many researchers in the past. The width of the abutment influence zone D which is defined as the distance from the panel edge within which abutment stress increase can be detected was analyzed according to field measurements by Peng and Chiang(1984). They obtained an equation as follows;

$$D = 9.3 \times \sqrt{h} \quad (2.5)$$

where D is abutment influence zone, h is overburden depth.

In order to estimate the percentage of total front or side abutment load that is carried by each pillar, the distribution of abutment pressure within the abutment influence zone must be known. Different distribution functions of side abutment

pressure have been developed by a few researchers (Mark, 1987; Carr and Wilson, 1982). Among them, Carr and Wilson's distribution function is a typical one. By considering the area of AOB equivalent to COD in Fig. 2.4, they presented the distribution of side abutment pressure as an exponential function;

$$\sigma - q = (\bar{\sigma} - q)e^{-\frac{x}{c}} \tag{2.6}$$

where σ is stress at any point measured x ft. from the edge of chain pillar, $\bar{\sigma}$ is peak stress, c is a constant while q is average overburden stress. By using Eq.2.6, the stress in or load carried by each chain-pillar in a longwall entry system can be determined.

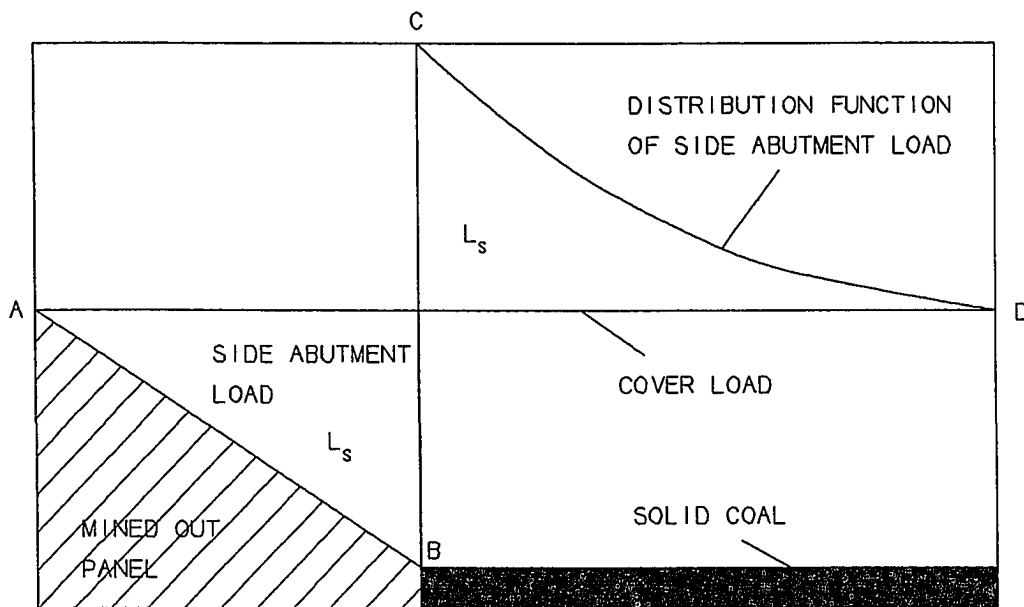


Figure 2.4. Abutment load distribution proposed by Wilson(after Carr and Wilson, 1982)

2.3 Pillar Strength Consideration

On the other hand, there have been more efforts spent on the development of pillar strength formula. Researches have shown that the strength of pillar is affected by both the size and shape of pillar.

2.3.1 Size Effect

The relationship between the size and strength of testing samples can be represented in a general form by Evans(1961);

$$S_1 = K_1 d^{-a} \quad (2.7)$$

where S_1 is the uniaxial compressive strength of the cubical pillar, d is the side length of the specimen, K_1 and a are constants.

The values of the constant a range from 0.38 to 0.66(Peng, 1978) with 0.5 being the average. To consider the in-situ pillar strength, the concept of the "critical size strength"(Bieniawski, 1986) for rock masses is very important in practical design. The critical size is defined as that specimen size beyond which a continued increase in specimen width causes no significant decrease in strength. The critical sizes have been determined for different coal by Bieniawski(1975) and Hustrulid(1976). By combining the laboratory data and field measurement, the following equation was proposed by Hustrulid(1976):

For cubic pillar having the height > 36 inches.

$$S_1 = \frac{K_1}{\sqrt{36}} \quad (2.8)$$

For cubic pillars having the height < 36 inches.

$$S_1 = \frac{K_1}{\sqrt{H}} \quad (2.9)$$

Where S_1 is the uniaxial compressive strength of the cubical pillars, H is the pillar height, inches; and K_1 is a constant.

In the above equations, the constant K_1 must be determined for actual pillar material, and is calculated as shown by Gaddy(1956).

$$K_1 = \sigma_c \sqrt{D} \quad (2.10)$$

Where σ_c is the uniaxial compressive strength of the rock specimen in the laboratory, and D is the specimen size.

2.3.2 Shape Effect

In addition to the size effect, coal strength is affected by the specimen geometry and shape. To understand this phenomenon, extensive laboratory and in-situ investigations have been conducted. As a result, a number of strength formulae has been proposed to estimate pillar strength.

Based on elasticity considerations and laboratory tests, Obert and Duvall(1967) proposed the following formula:

$$S_p = S_1 \left(0.778 + 0.222 \frac{W}{H} \right) \quad (2.11)$$

Where S_p is the pillar strength, S_1 is the uniaxial compressive strength of a cubical specimen, and W and H are pillar width and height.

For laboratory tested specimens Holland(1973) found that the strength of coal varies with the square root of the least lateral dimension divided by its height. He then(1964) extended the work by Gaddy(1956), and proposed the following formula:

$$S_p = K_1 \frac{\sqrt{W}}{H} \quad (2.12)$$

Where K_1 is the Gaddy factor, determined from Eq. 2.10.

In 1967, Salamon and Munro conducted a field survey in South Africa. Based on the results, they developed the following equation to estimate the pillar strength.

$$S_p = \frac{K_1 W^{0.46}}{12 H^{0.66}} \quad (2.13)$$

Researchers have found that the strength of sampling material in the laboratory is quite different from the one in in-situ due to difference in loading conditions and material structure. To take these effects into account, the following equation was proposed by Bieniawski(1984).

$$S_p = S_1 \left(0.64 + 0.36 \frac{W}{H} \right) \quad (2.14)$$

Where S_1 is the strength of cubical specimen of critical size or greater(e.g., about 3 ft.

for coal), W is the pillar width, and H is the pillar height.

In addition to the strength formulae discussed above, Wilson's(1972) formula is unique in that it is based on the concept of material progressive failure. Wilson hypothesized that a remanent pillar flanked on both sides by the gob contains two zones; a yield zone around the edges and a core at the center enclosed by the yield zone. The pillar core is relatively undisturbed or an intact zone which will carry the main pillar loading. The stress in the yield zone is not uniformly distributed, and the yield zone only provides confinement to the pillar core and carries much less pillar load. Soon after a pillar is developed, the greatest stress in the pillar is found at the boundary between the yield zone and the core(Fig. 2.5a). As additional longwall loadings are applied to, the average stress in the pillar core increases until it equals the peak stress at the yield boundary. Up until this point, which Wilson(1983) calls the "Limit Roadway Stability"(Fig. 2.5b), both the pillar and entries adjacent to it are stable. Further loading of the pillar causes the yield zone to expand. Finally the "Ultimate Limit"(Fig. 2.5c) is reached when the entire core yields. Any additional loads will now be transferred to the adjacent pillars. Wilson(1983) provided equations for determining the stress distribution in the pillar at both the LRS and UL for two different "boundary conditions"; one where the roof and floor are strong(or rigid) and the other where yielding takes place all around the entries. The load-bearing capacity of the pillar(or pillar strength) can be determined by integrating the stress distributions over the area

of pillar for different loading conditions.

For strong roof and floor conditions.

$$\sigma_v = p^* q e^{\frac{X}{h}} \quad (2.15)$$

$$\bar{\sigma} = Kq + \sigma_o \quad (2.16)$$

$$X_b = \frac{h}{F} \ln \frac{q}{p^*} \quad (2.17)$$

For weak roof and floor conditions.

$$\sigma_v = Kp^* \left(2 \frac{X}{M} + 1\right)^{K-1} \quad (2.18)$$

$$\bar{\sigma} = Kq + \sigma_o \quad (2.19)$$

$$X_b = \frac{h}{2} \left(\frac{q}{p^*} \frac{1}{K-1} - 1 \right) \quad (2.20)$$

Where σ_v is the vertical stress within the pillar, psi; $q = h\gamma$ is the cover stress, M is the height of extraction of the opening, σ_o is the unconfined compressive strength of in-situ strata, X_b is width of yield zone, p^* is the failed coal strength, $\bar{\sigma}$ is the peak stress, X is the distance from rib side, ft., K is the triaxial stress factor, and F is a constant.

Both K and F can be determined from the following equations;

$$K = \frac{1 + \sin\theta}{1 - \sin\theta} \quad (2.21)$$

$$F = \frac{K-1}{\sqrt{K}} + \left(\frac{K-1}{\sqrt{K}} \right)^2 \tan^{-1} \sqrt{K} \quad (2.22)$$

where θ is the angle of internal friction, and \tan^{-1} is in radian.

Different formula described above are developed for different purposes. Each

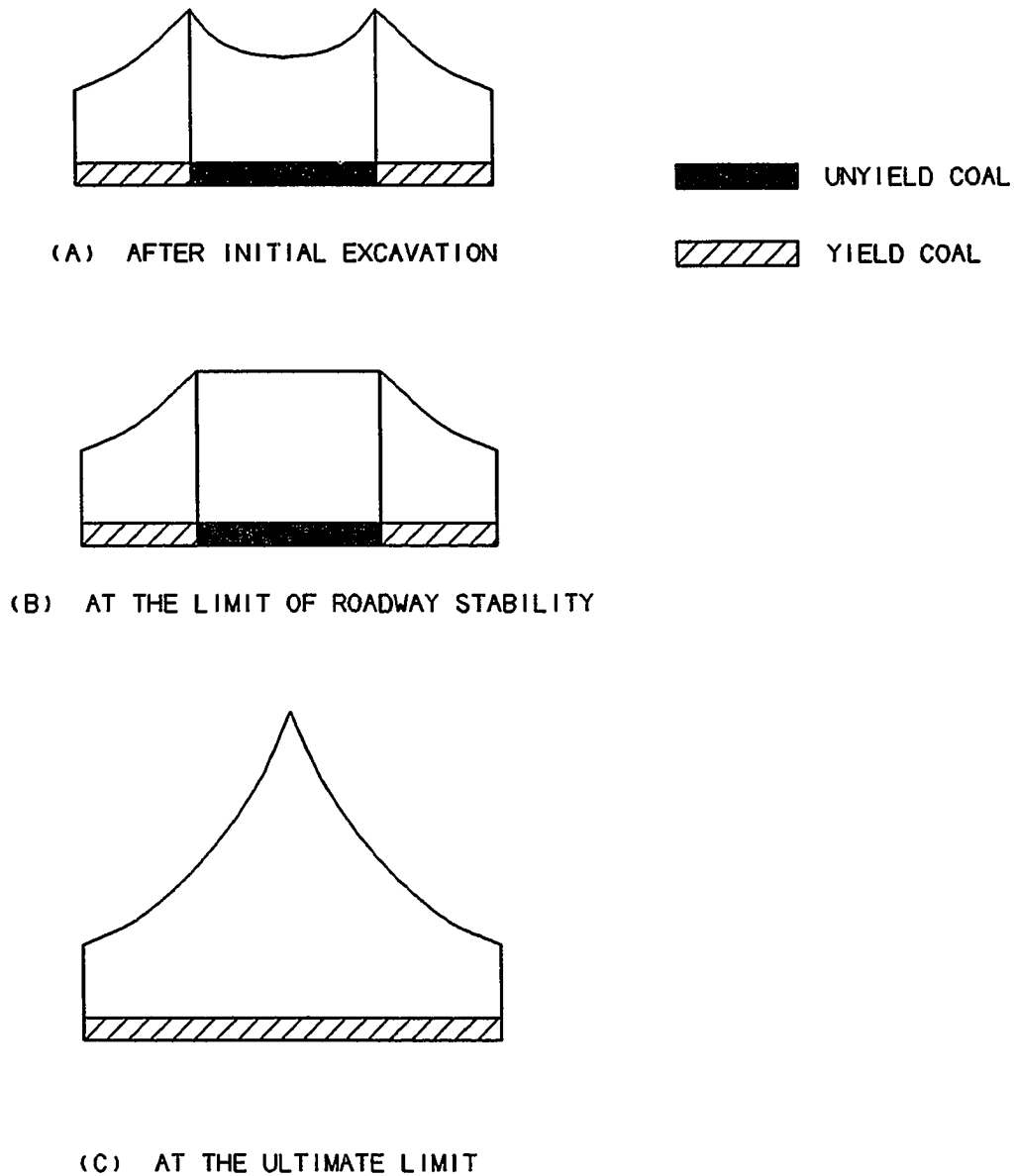


Figure 2.5. Theoretical vertical stress distribution in coal pillars(after Wilson, 1983).

of them may fit certain geological and mining conditions, but not others, simply because of complexity and variety of in-situ geological and mining conditions encountered in underground coal mines.

2.4 Standard Procedures of Conventional Pillar Design

The standard procedures for the conventional pillar design consist of three basic steps: (1) determining the pillar loads, (2) estimating the pillar strength, and (3) calculating the safety factor. Although the safety factor has been calculated in different ways for each method. Basically it is defined as the ratio of pillar strength to its load and must be larger than 1.0. Therefore, all of those pillar design methods attempt to determine the dimension of a stiff pillar.

However, there is a unique longwall chain pillar design method which is developed by Hsiung and Peng(1985). The method was developed from numerical modeling described by Hsiung(1984). In the development of the method, Hsiung used three-dimensional finite element models to simulate the pillars at various stages of longwall mining. The parameters varied by Hsiung in the models included overburden depth, pillar width, compressive strength of coal, panel dimensions, Young's modulus of the roof and floor, and thickness of main and immediate roofs. Using the pillar stability as a design criteria, Hsiung performed multivariable statistical analysis to relate the modeled geological , mechanical, and geometric parameters to the pillar stability. The final results is presented by a simple equation which predicts pillar width as a function of seven parameters:

$$\log W = -4.686 \times 10^{-3} \frac{E_i}{E_c} - 4.04 \times 10^{-3} \frac{E_m}{E_c} - 3.33 \times 10^{-2} \log \frac{E_f}{E_c} - 7.29 \times 10^{-2} \log \sigma_c + 0.5144 \log h + 4.94 \times 10^{-2} \log \frac{L}{2} + 0.1941 \log W \quad (2.22)$$

Where W is pillar width, E_c , E_f , E_i , E_m are Young's modulus of the coal, floor, immediate roof, and main roof, respectively. W_p and L are panel width and length, respectively, σ_c is uniaxial compressive strength of coal, and h is seam depth.

2.5 Yield Pillar Practice

The yield pillar concept was first introduced by Holland in 1963. Later, his work was reviewed by several other researchers (Adler and Sun, 1968; Britton, 1980). However, the application of yield pillars has not been widely accepted in the coal industry and no related research has ever been attempted. Reluctance of adopting yield pillars may be attributed partly to a lack of understanding on the fundamental aspect of yield pillars and partly to suspicion whether or not the yield pillars can be used in such complex geological conditions as that found in the coal mines.

Although yield pillars are not completely accepted by the coal industry, they are widely used in potash, salt, and trona mines. Several techniques utilizing the yield pillar concept have been introduced by Serata (1976, 1982) to control stress distribution around the openings and reportedly have achieved great success in potash, salt, and trona mines. They are:

1. Parallel-room method. It requires the creation of an entry parallel to the preceding failed entry with a yield pillar in between (Fig. 2.6). Protection of the succeeding entry is provided by the development of a so-called

secondary stress envelope around the entire structure of the entry system.

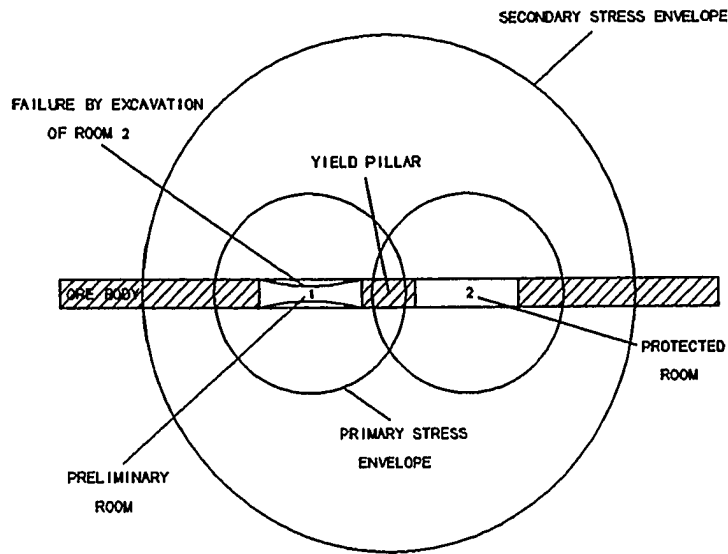


Figure 2.6. Parallel-room method.

- 2) Time-control method. It involves a specific time-controlled sequence in the excavation of a group of entries. Two "control entries" are driven parallel to each other and allowed to deteriorate (Fig. 2.7). The width of the pillar left between them should be such that the pillar is strain-hardened. The extent of pillar strain-hardening is a function of time. A "protected entry" is formed by excavation between the "control entries." The pillars between the "protected entry" and "control entries" are expected to yield immediately after they are isolated.
- 3) Compounded-time-control method. This is a special case of the time-control method (Fig. 2.8). Instead of a three-entry system in the time-

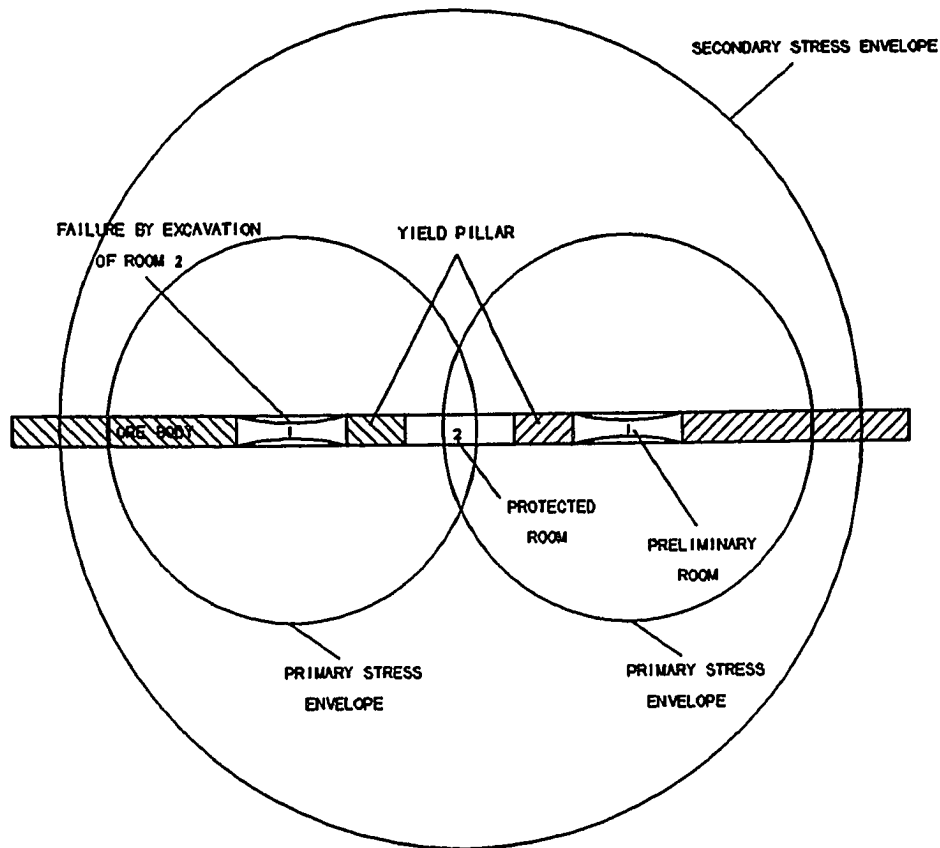


Figure 2.7. Time-control method.

control method, multi-entry systems may be excavated using compounded time-control methods and more than one designed entry may be protected.

According to Serata(1976), the parallel-room method is suitable for weak geological conditions with possible bed separations, while time-control and compounded-time-control methods are most applicable to extremely weak geological conditions. However, the applicability of the three techniques to the often complex coal mine

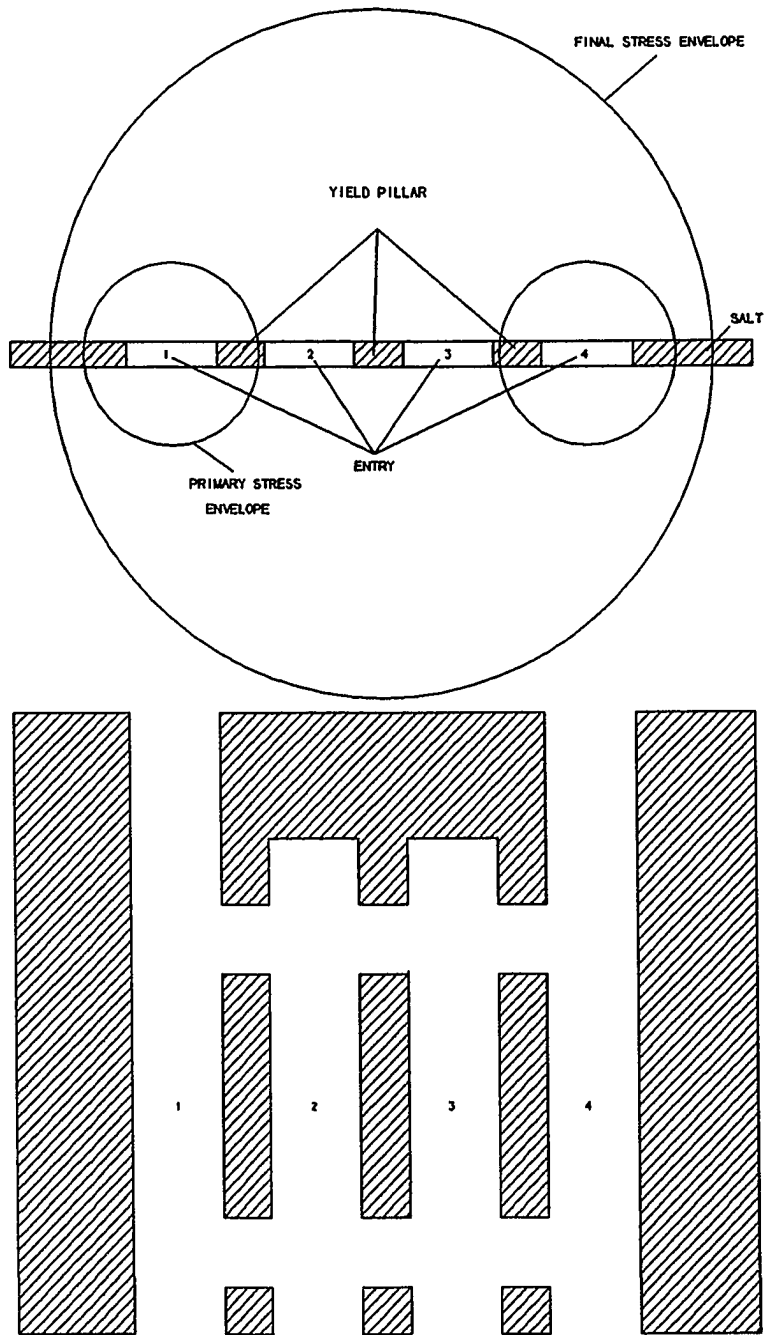


Figure 2.8. Compounded-time-control method.

conditions has not been verified.

A recent application of yield pillar in coal mines at great depth has been

successfully carried out at four of the mines operated by Jim Walter Resources(Carr, et al., 1984, 1985; Gauna, et al., 1985). The longwall development entries created by employing the original abutment pillar design in these mines were subjected to severe floor heave such that the entries were completely closed in some extreme cases. Under this situation, yield-abutment-yield pillar design have been tried. The original severe floor heave in the entries due to inadequate size of abutment pillars was reduced significantly. In addition to the improvement of the entry stability, a yield-abutment-yield pillar design offered an increase in recovery and production efficiency. Barton(1989) conducted a field survey in three longwall entry-pillar systems in Kentucky and indicated that the yield pillar system combined with heavy artificial support may be a viable ground control alternative for deep-cover multi-entry longwall system. The yield pillar experiments had also been carried out by others(Dahl, 1972; DeMarco, M. J., 1988; Haramy, 1989). The results have shown that yield pillar design have improved the stability of the entry-pillar system and increased coal recovery. Tests of yield pillar designs have included 2-entry, 3-entry, 4-entry, and 5-entry system as shown in Figs. 2.9 to 2.13. However, up to now, there is no uniform design method for yield pillar in the U.S. longwall mining.

2.6 Summary

As described earlier, although researchers have developed a number of pillar

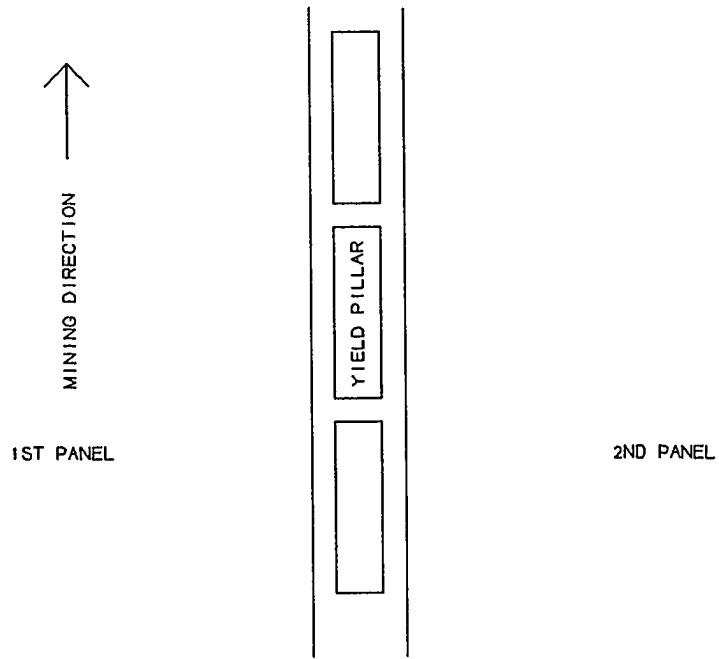


Figure 2.9. Two-entry system, yield pillar design.

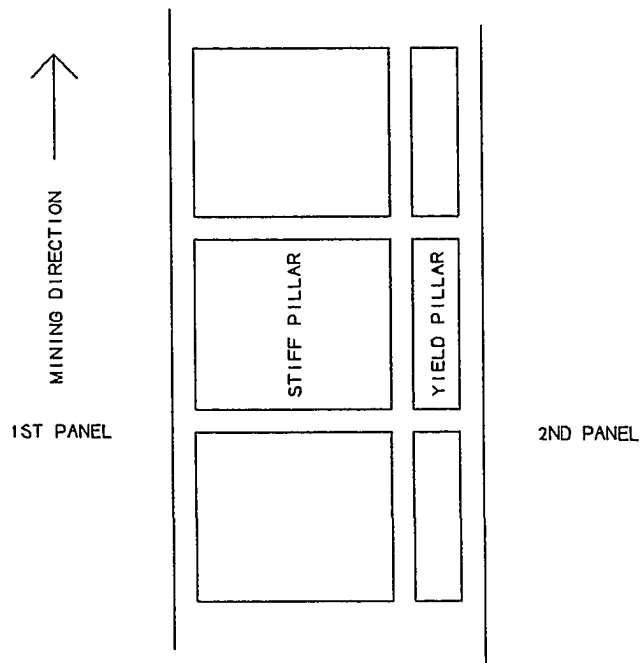


Figure 2.10. Three-entry system, stiff-yield pillar design.

design methods each of them has its own merits and short comings. Overall, the

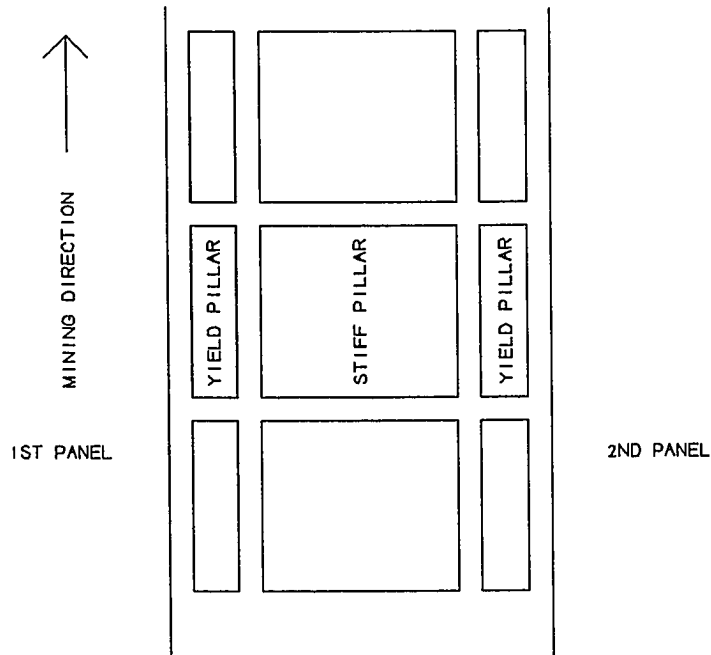


Figure 2.11. Four-entry system, yield-stiff-yield pillar design.

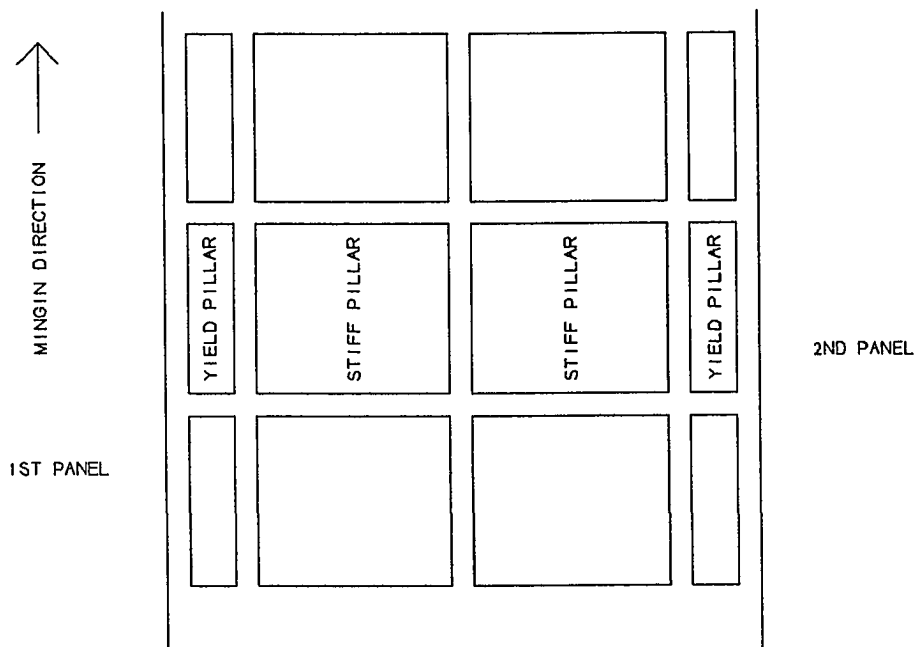


Figure 2.12. Five-entry system, yield-stiff-stiff-yield pillar design.

following characteristics can be observed:

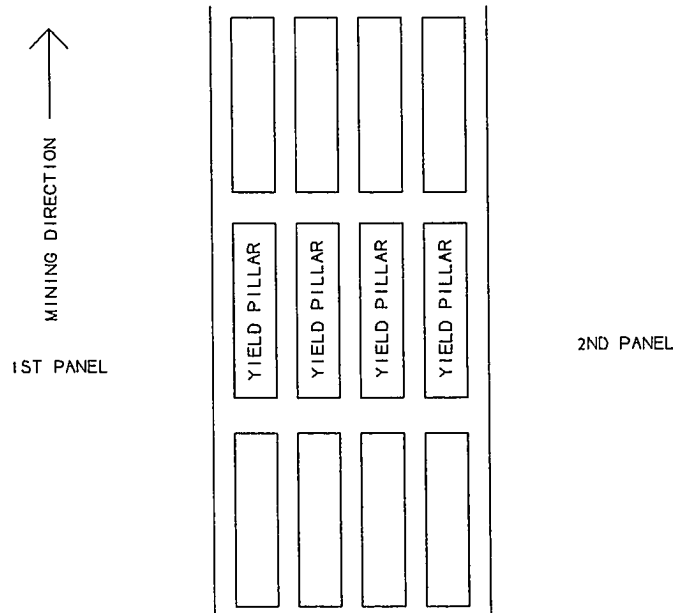


Figure 2.13. Five-entry system, full-yield pillar design.

- 1) Without exception, all conventional pillar design methods consider the pillar stability only.
- 2) To determine pillar loadings, the conventional methods for longwall pillar design assume that a pillar is subjected to vertical pressure only and that the vertical stresses within a pillar are uniformly distributed.
- 3) All the pillar design methods attempt to design a stiff pillar, even though the progressive failure of pillar has been recognized by most researchers as more realistic in describing the failure mechanisms of underground structures.
- 4) No methods have considered the deterioration of material properties as the time elapses.

- 5) Although yield pillars have been practically used in underground coal mines, there is no uniform design method to design a yield pillar. Most practical application of the yield pillars remain at the stage of trial and error.

However, years of mining practice have shown clearly that a stable pillar does not necessarily promise a stable entry system. Further, researches have proven that both vertical and lateral pressures exist in underground coal mines. The magnitude of the lateral stress may vary from zero to a value greater than the vertical stress. Additionally, the stresses within a pillar are not uniformly distributed. Based on this information that previous researchers have discovered, the conventional pillar design method eventually will have some limitations on its applications. It can not deal with some ground control problems, such as coal bumps, floor heave, cutter roof, etc. The problems will become more severe when the mining activity goes deeper. Therefore, a new pillar design method based on structure stability analysis that provides an alternative for deeper coal mines will be very significant and meaningful.

CHAPTER 3
ROOF AND FLOOR CLASSIFICATION SYSTEM
FOR YIELD PILLAR DESIGN

3.1 Variables Affecting Performance of Entry-Pillar System

The stability of an entry-pillar system in underground coal mines is mainly affected by geological and mining conditions as well as mechanical properties of rocks surrounding the entry-pillar system. The geological conditions refer to area topography, faults, joints, tectonic force, geostratigraphy, etc.. The mining conditions involve mining method, mine layout, ground control plan, and equipments used for extracting coal. The mechanical properties of rock, such as Young's modulus, Poisson's ratio, compressive strength, cohesion strength, internal friction angle, are totally controlled by the mother nature.

In order to ensure the stability of an entry-pillar system in the underground coal mine, the design of the entry-pillar system has to consider the geological and mining conditions and mechanical properties of rocks. This involves many variables each of which will affect the stability of the entry-pillar system to a different degree. Some of them may have significant effects on the stability of the entry-pillar system under certain geological and mining conditions while the others may not. The role of each of the variables also varies with other conditions. For example, the design of an entry-

pillar system for an underground coal mine with a strong roof and strong floor condition, coal strength is a decisive factor(or variable) because coal is the weakest element. When a mine has a weak floor as its immediate floor, such as mudstone or fireclay, coal strength may not be important, rather the strength of the immediate floor will decide the stability of the entry-pillar system. Very often, the variables are also related to each other.

3.2 Purpose of Developing A Roof and Floor Classification System

Since geological and mining conditions in coal mines vary from place to place and from time to time, if all these variables are considered, it will make the design of an entry-pillar system an extremely difficult task. Fortunately, the mining practice has demonstrated that very often, the stability of an entry-pillar system is dominated by several important variables under certain roof and floor conditions, and the effects from the remaining variables, in general, are insignificant and can be neglected. As a result, the design criteria for an entry-pillar system will also vary with different roof and floor conditions. Therefore, an entry-pillar system can be designed safely based on different design criteria. In order to simplify the yield pillar design problem and reduce the number of design criteria needed for each type of roof and floor conditions without affecting the accuracy, a classification system has to be developed to identify each type of roof and floor conditions. The classification system would help us establish a typical

study case within a similar roof and floor condition, and to evaluate the design criteria for yield pillar design method. It also will help us summarize and extract relevant information from large multivariate data sets. Consequently the results from these typical case studies can be used for yield pillar design within a similar geological condition.

3.3 Roof and Floor Classification Method

3.3.1 Introduction

As mentioned earlier, large multivariate data sets can prove difficult to comprehend. In such cases summarizing and extracting relevant information are necessary in order to simplify the study cases. To achieve this goal, it is often useful to consider dividing a set of objects into classes in such a way that ensures that objects within a class are similar to one another. In recent years, much attention has been devoted to this activity, which has usually been referred to as 'classification' or 'cluster analysis', and the methodology has been applied in many diverse disciplines. Application of classification in geomechanics design has come into vogue with the popularization of RMR and Q system of rock mass classification (Bieniawski, 1976). Since then, a score of classification models for different geo-technical situations including mining applications have been developed and used throughout the world for decision making purposes (Bieniawski, 1979, Franklin, 1975 and Barton, 1976, and Rutledge and Preston,

1978).

Classification is in fact a pattern recognition process, where, once some predefined classes have been established, a new sample can be recognized as a member of one of those classes by using a decision rule. Each of the predefined class has to have typical characteristics that will distinguish itself from the others. In this case, the physical system, rock, has some measurable characteristics. Initial selection of the number of characteristics depends on the specific applications and theoretical knowledge of that particular area, or even application of heuristic knowledge in the absence of any theoretical development. In order to design a stable entry-pillar system for an underground coal mine, it is very important to know what kind of roof and floor conditions are encountered there. Since both mining practice and numerical model analysis have proven that the performance of an entry-pillar system under either strong roof and floor condition or strong roof and weak floor condition can be different (Tsang and Peng, 1989), roof and floor strata are classified into either strong or weak rock group in this part of study.

3.3.2 Principle of Classification System

From ground control point of view, the mechanical properties of coal and surrounding rocks, and interaction among roof, floor, and pillar are very important factors that affect the stability of the entry-pillar system. Whether a rock is strong or

weak not only depends on rock strength but also its stress level. For example, a rock with a low strength does not necessarily fail if it is under a low stress level in comparison with its strength. On the other hand, a rock with high strength can still fail under a high stress level. So the word "strong" or "weak" is only a relative term. Therefore, it is essential for a classification system to classify rocks based on its stress level and strength properties. The classification system proposed here considers both strength properties and stress conditions of a rock during pattern recognition process. This way a strong rock is so defined when it is subjected to a relatively lower stress level than its strength and will not yield or fail under general mining condition. A weak rock, in contrast with a strong rock, has a relatively high stress level than its strength. Based on this principle, a data base was established. The data base collected data from more than 50 coal mines of varying mining depth, rock type, rock properties, and statistical information. It provides input data for both classification of mine roof and floor, and for finite element modeling study later.

3.3.3 Selection of Classification Variables

In general, the roof or floor of an entry-pillar system can fail under either tension or shear depending on stress level and strength properties. In order to consider both stress level and strength properties of rock in the classification system, the following five classification variables have been chosen for classification of mine roof and floor rocks:

$h\gamma/C$ (the ratio of mining depth multiplied by the average unit weight of the overburden divided by the cohesion strength of the rock), E (Young's modulus of the rock), ϕ (internal friction angle of the rock), T (tensile strength of the rock), and ν (Poisson's ratio of the rock). The variables $h\gamma/C$ indicates the stress level and the internal friction angle are used to examine the possibility of shear failure of rock. The tensile strength, T , is used to estimate the possibility of tensile failure. The Young's modulus and Poisson's ratio consider the deformability of rock.

3.3.4 Classification Procedures

A total of fifty-five samples were selected from the data base for cluster analysis (Table 3.1). A complete schematic diagram of different stages involved in the process of the cluster analysis is given in Figure 3.1. The process consists of two parts; 1) cluster analysis for establishing the predefined strata groups, and 2) classification of new samples into one of the predefined groups. For cluster analysis, seven basic stages are involved.

Stage 1. Pre-processing raw data

For cluster analysis purpose, the raw data listed in Table 3.1 is converted into a standardized data matrix by the following standardizing function.

$$S_{ij} = \frac{X_{ij} - X_{jmin}}{X_{jmax} - X_{jmin}} \quad \begin{matrix} i(1, \dots, n) \\ j(1, \dots, m) \end{matrix} \quad (3.1)$$

Where S_{ij} is the value of j th variable of the i th sample in standardized data matrix, X_{ij}

Table 3.1. Raw Data Matrix for the Cluster Analysis

Sample Number	Classification Variables				
	$h\gamma/C$	E, Young's Modulus (10^6 psi)	ν , Poisson's Ratio	ϕ , Internal Friction Angle (degree)	T, Tensile Strength (psi)
1	0.083	1.765	0.105	42.9	1175.0
2	0.074	1.219	0.121	44.3	1282.0
3	0.170	3.150	0.205	24.2	455.0
4	0.375	2.410	0.162	20.5	219.0
5	0.365	1.786	0.158	24.5	746.0
6	0.107	1.735	0.200	23.0	109.8
7	0.171	1.706	0.153	44.1	1455.0
8	0.172	1.703	0.157	28.6	612.0
9	0.092	4.685	0.240	42.0	1252.2
10	0.618	1.588	0.167	29.9	715.0
11	0.497	1.214	0.200	21.4	966.0
12	1.608	1.150	0.231	15.0	927.0
13	0.085	2.986	0.205	39.9	1152.0
14	1.370	0.916	0.170	43.3	1432.0
15	0.451	0.913	0.380	43.8	750.0
16	0.205	0.835	0.210	34.0	1191.0
17	0.082	0.834	0.178	22.8	170.2
18	2.377	0.816	0.432	20.5	525.0
19	0.611	0.540	0.300	26.0	480.0
20	2.301	0.405	0.415	20.0	438.0
21	0.501	0.346	0.320	30.0	564.0
22	0.422	0.470	0.160	43.0	525.2
23	0.408	0.487	0.150	34.0	499.4
24	0.501	0.756	0.202	27.0	537.8
25	1.804	0.647	0.351	21.0	723.8
26	2.424	0.815	0.260	19.9	984.4
27	2.421	0.940	0.160	23.5	642.0
28	1.807	0.115	0.311	24.0	727.0
29	4.006	0.195	0.405	35.0	442.0
30	2.421	0.798	0.160	24.5	446.0
31	0.901	0.966	0.260	27.0	305.0
32	3.102	1.088	0.231	18.0	547.0

Table 3.1. Continue

33	3.101	0.285	0.320	31.5	532.0
34	2.001	0.081	0.150	34.0	415.0
35	2.422	0.077	0.461	27.0	219.0
36	2.902	0.076	0.425	34.1	198.0
37	1.531	0.371	0.351	27.5	575.0
38	2.109	0.067	0.451	26.0	205.0
39	1.203	0.840	0.201	26.7	959.0
40	1.302	0.508	0.190	24.2	874.0
41	1.405	0.610	0.189	29.0	319.0
42	1.511	2.742	0.175	39.2	800.0
43	1.601	1.803	0.155	35.5	642.0
44	1.702	1.921	0.150	34.1	726.0
45	1.202	1.400	0.200	36.7	959.0
46	1.321	0.871	0.190	24.2	521.0
47	1.411	0.600	0.180	31.2	319.0
48	1.504	0.703	0.170	27.1	603.0
49	1.602	2.121	0.160	28.7	1143.0
50	1.721	0.918	0.150	23.0	726.0
51	1.201	1.402	0.210	26.7	959.0
52	1.301	0.499	0.180	24.2	510.0
53	1.409	0.623	0.185	32.0	319.0
54	1.503	0.728	0.165	23.0	620.0
55	1.601	1.408	0.160	44.5	992.0
Maximum	4.006	4.685	0.461	44.5	1455.0
Minimum	0.074	0.067	0.105	15.0	109.8
Average	1.293	1.102	0.228	29.6	675.1
STD	0.925	0.872	0.093	7.7	330.3

Classification System

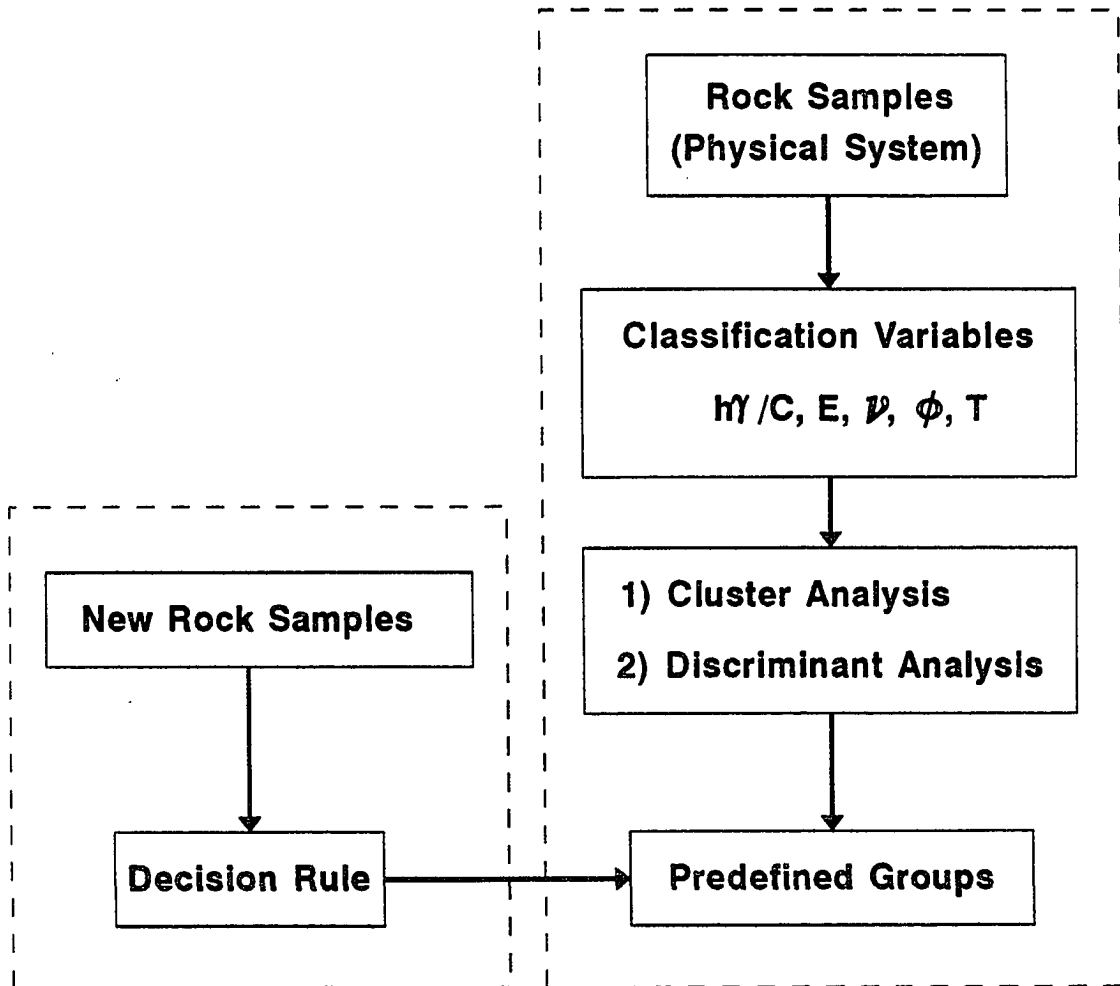


Figure 3.1. Schematic diagram for the cluster analysis.

is the value of the j th variable of the i th sample in raw data matrix, X_{jmin} and X_{jmax} are the minimum and the maximum value of j th variable respectively. The standardization of the raw data matrix is done because of two reasons: (1) to convert the raw data to dimensionless units, so that the arbitrary effects are removed. (2) the value of each variable varies in different ranges, the standardization makes variables contribution more equally to the similarities among samples.

Stage 2. Assignment of Weight Factor

Since each variable affects the performance of an entry-pillar system in a different degree, a weighting factor was assigned for each variable based on importance and is listed in Table 3.2.

$$Z_{ij} = S_{ij} W_j \tag{3.2}$$

Where Z_{ij} is the value of the j th variable of the i th sample in the weighted data matrix, and W_j is the weighting factor for the j th variable

Table 3.2. Weighting Factors for the Classification Variables

Variable	hy/C	E	v	ϕ	T
Weighting Factors	4	2	1	1	1

Stage 3: Estimate the Initial Classification Centers

For simplicity, the roof and floor rock will be classified into two groups only:

strong rock or weak rock. The initial classification center for both groups can be estimated by the following equation:

$$C_{kj} = \frac{Z_{jmax} + Z_{jmin}}{K}(k - 0.5) \quad \begin{matrix} k = 1, \dots, K \\ j = 1, \dots, m \end{matrix} \quad (3.3)$$

Where C_{kj} is the center of the j th variable of the k th group, K is the number of the rock groups, Z_{jmax} and Z_{jmin} are the maximum and minimum values of the j th variable in standardized data matrix. The initial center serves as a starting point for cluster analysis, and will not affect the final results.

Stage 4. Sample Grouping

Once the initial center of each group is assigned, the Euclidean distance, one of the commonly used measures of the dissimilarity between the i th and j th objects, is used to determine to which group each sample belongs. Euclidean distance is calculated by;

$$D_{ik} = \sqrt{\sum_{j=1}^m (Z_{ij} - C_{kj})^2} \quad \begin{matrix} i = 1, \dots, n \\ k = 1, \dots, K \end{matrix} \quad (3.4)$$

where D_{ik} denotes the distance between the i th sample and the center of the k th group. A sample will be grouped into one particular group for which the sample has the shortest Euclidean distance between itself and the center of that group. This rule is also known as Nearest Neighbor Rule.

Stage 5: Re-evaluation of the New Center of Each Group

After all the samples have been grouped, the new center of each group is re-evaluated by the following equation.

$$C_{kj} = \frac{\sum_{i=1}^{L_k} Z_{ij}}{L_k} \quad (3.5)$$

Where Z_{ij} is the element of the k th group, and L_k is the total number of elements in the k th group. Obviously, the new center will be different from the initial evaluation. The center of each group denotes average value of each variable within its own group.

Stage 6: Finding the Final Classification Group

In order to find the final classification group, steps 4 and 5, i.e., sample grouping and re-evaluation of the new centers are repeated until there are no further changes in the centers of the groups. Then the values from the latest evaluation on the center of each group are considered as the final and a set of predefined classes is established. The cluster analysis was performed on WVNET mainframe computer. The results are listed in Tables 3.3 and 3.4. Table 3.3 shows the average value of each variable in different group. The average values in Table 3.3 are converted into standardized data by using Eq. 3.1 and listed in Table 3.4. They represent the characteristics of each predefined group. According to the results from the cluster analysis (Table 3.3), a strong rock or stratum is usually under lower stress in comparison with its strength because of a lower value of hy/C , 0.88 and a higher tensile strength, 734 psi. The Young's modulus and internal friction angle of a strong rock or stratum are larger than a weak rock while

its Poisson's ratio is much lower than a weak rock.

Table 3-3. Mean Vector of Each Group

Group	No. of Samples	Group Center(Classification Variables)				
		$h\gamma/C$	E (10^6 psi)	ν	ϕ (degree)	T (psi)
Strong Rock	40	0.876	1.323	0.195	30.9	733.8
Weak Rock	15	2.514	0.457	0.324	25.6	503.2

Table 3-4. Standardized Mean Vector of Each Group

Group	No. of Samples	Group Center(Classification Variables)				
		$h\gamma/C$	E	ν	ϕ	T
Strong Rock	40	0.204	0.272	0.253	0.542	0.464
Weak Rock	15	0.621	0.084	0.615	0.359	0.292

Stage 7. Discriminant Analysis

In order to verify whether or not the classification results are acceptable, one of the most widely used multivariate procedures in earth science, called discriminant function method, is used for analysis of the classification results(Potter, Shimp, and Witters, 1963). According to the method, if two groups data are from two clusters or two groups of points in multivariate space, there must be a plane in the multivariate

space along which two clusters have the greatest separation while simultaneously each cluster has the least inflation. The plane is represented by the following discriminant function;

$$R = \lambda_1 X_1 + \lambda_2 X_2 + \dots + \lambda_m X_m \quad (3.6)$$

where λ is the coefficients of the discriminant function. They can be determined by solving the following equation:

$$[S_p^2] \times [\lambda] = [D] \quad (3.7)$$

Where $[S_p^2]$ is a $m \times m$ matrix of pooled variances and covariances of the m variables, and $[D]$ is the vector of group center difference between the two groups.

The first step of testing the significance of a discriminant function is to measure the separation or distinctness of the two groups. This is done by computing the distance between the centroids, or multivariate means, of the groups. In a multivariate space, the standardized squared distance is represented by

$$D^2 = [D]' [S_p^2]^{-1} [D] \quad (3.8)$$

This measure of difference between the means of two multivariate groups is called Mahalanobis' distance. The significance of Mahalanobis' distance was tested by using an F statistics. The null hypothesis tested by this statistic is that the multivariate means are equal, or that the distance between them is zero. That is,

$$H_0 : [D_i] = 0 \quad (3.9)$$

against

$$H_o : [D_i] > 0 \quad (3.10)$$

The F statistics is calculated by

$$F = \frac{n_a+n_b-m-1}{(n_a+n_b-2)m} \times \frac{n_a n_b}{n_a+n_b} \times D^2 \quad (3.11)$$

$$= 53.967 > F_{0.05,5,49}$$

with m and $(n_a + n_b - m - 1)$ degrees of freedom. Where n_a and n_b are number of samples in the two tested groups, and m is the number of variables. Based on the F statistics, the null hypothesis was rejected. Therefore, the two groups are well separated in the multivariate space. From statistics point of view, the classification results from cluster analysis are acceptable.

Once the predefined groups are established, new samples will be classified into one of the two predefined groups based on Euclidean distances between each new sample and centers of each of the predefined groups. Again, the nearest neighbor rule is used to determine to which group a new sample belongs.

3.4 Roof and Floor Conditions in Underground Coal Mines

Based on this classification system, a total of four types of roof and floor conditions can be established for finite element model analysis; 1) strong roof and strong floor conditions, 2) strong roof and weak floor conditions, 3) weak roof and strong floor conditions, and 4) weak roof and weak floor conditions. In each group, weak strata and

pillar will affect the performance of an entry-pillar system. Therefore, in yield pillar design more attention should be focused on the weakest elements. Thus, the design criteria can be selected based on the stabilities of the weakest elements in an entry-pillar system. The classification system quantitatively defines each type of roof and floor condition, and will be helpful in establishing pillar design formula and simplifying the design procedures.

CHAPTER 4

MECHANISM OF YIELD PILLAR

4.1 Introduction

At present, there are two pillar design concepts used in mining practice, i.e., conventional and yield pillar design concepts. Usually, a stiff pillar designed by the conventional concept is always larger in size than a yield pillar designed by the yield pillar concept under the same geological and mining conditions. Therefore a stiff pillar has a higher safety factor(S.F.). But the deeper the mining activity goes, the bigger the pillar is required and results in more loss of coal resources. Sometimes if a stiff pillar is under-designed, it may cause potential ground control problems, such as roof fall and floor heave, especially when the floor and/or roof strata are weaker than the coal. Currently, yield pillars have been used to eliminate those ground control problems. Since a yield pillar is usually smaller than a stiff pillar, coal recovery increases also. But the mechanisms and functions of yield pillar are still poorly understood. This chapter will address these questions.

4.2 Finite Element Modeling

In the mining operation, pillar performance depends mainly on the mechanical properties of coal pillar itself and the surrounding rocks, and interactions among roof,

floor, and pillar. In order to study the mechanisms of the yield pillar, it is very important to evaluate the effects of each factor on pillar performance. By incorporating all these factors in the study of yield pillar mechanism, the difficulties encountered in the analytical method will be increased tremendously. Such study would become almost impossible to do if a numerical model simulation is not implemented. The finite element method, one of the commonly used numerical modeling methods in rock and earth engineering, is selected and used in this study to simulate yield pillar performance under various geological and mining conditions. The finite element method is used to analyze stress condition in roof, coal and floor, and to understand the processes of the stress redistribution within the areas of interest.

4.2.1 Finite Element Method Consideration

The 2-D finite element method used in this study considers both time-dependent behavior and plastic failure of rock. The Mohr-Coulomb yield criterion is employed in the finite element analysis;

$$\tau = C + \sigma \tan \phi \quad (5.1)$$

where τ is the shear strength, C is the cohesion, σ is the normal stress acting on the failure plane, and ϕ is the angle of internal friction.

For simulating the time-dependent behavior of rock material, the following empirical creep law is chosen;

$$\varepsilon(\sigma, t) = a \sigma^b t^d \quad (5.2)$$

where a , b and d are material constants, σ is applied stress, ϵ is creep strain, and t is elapse time. NASTRAN program(NASTRAN,1986) was used in this study because the program's ability and accuracy.

4.2.2 A Typical Finite Element Model

A commonly used longwall layout which consists of three entries and two pillars on each side of the panel was simulated(Fig.4.1). The finite element models were constructed to study pillar performance before and after the second panel mining, i.e. at cross-section of A-A and B-B, respectively. Figure 4.2 shows a typical 2-D finite element model used in the study. The isotropical quadrilateral elements were used. The element size varied from 5 by 4.5 ft to 20 by 40 ft. Both the side and bottom boundaries of the model were roller-constrained. An additional stress was imposed on top of the model to simulate the remaining overburden. The width of stiff and yield pillar varied from case to case. To consider the gob effect in the model, an approach similar to Peng(1980) and Hsiung(1984) was adopted. According to them, the gob effect can be considered by systematically reducing the gob material property such as unit weight, Young's modulus, and Poisson's ratio. The reduction factors used in this study are listed in Table 4.1. The maximum gob height at the center of the gob area was equal to six times of mining height. Such a large scale finite element modeling enables us to simulate in-situ mining operation and evaluate the pillar performance in

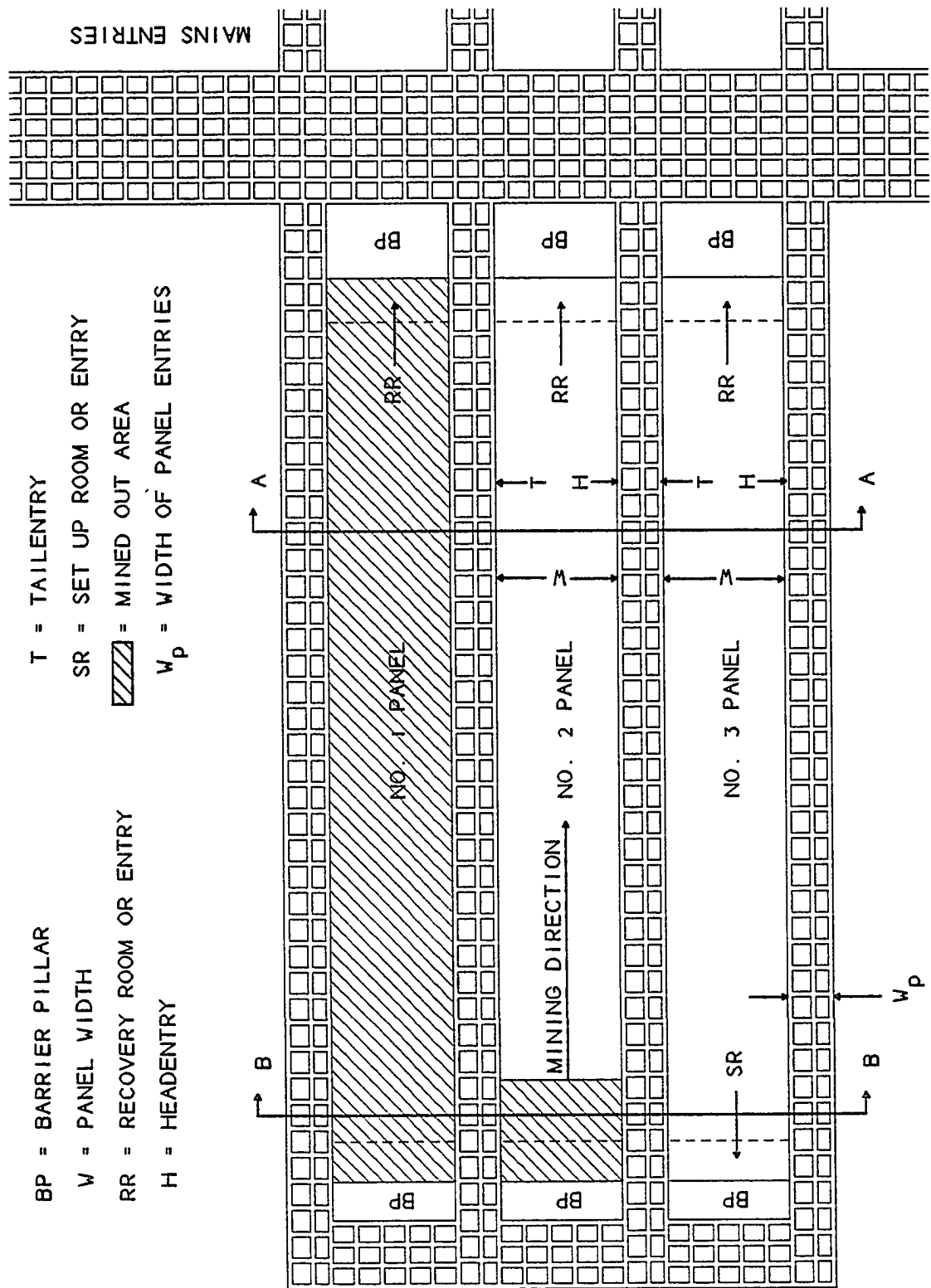


Figure 4.1. A typical longwall panel layout.

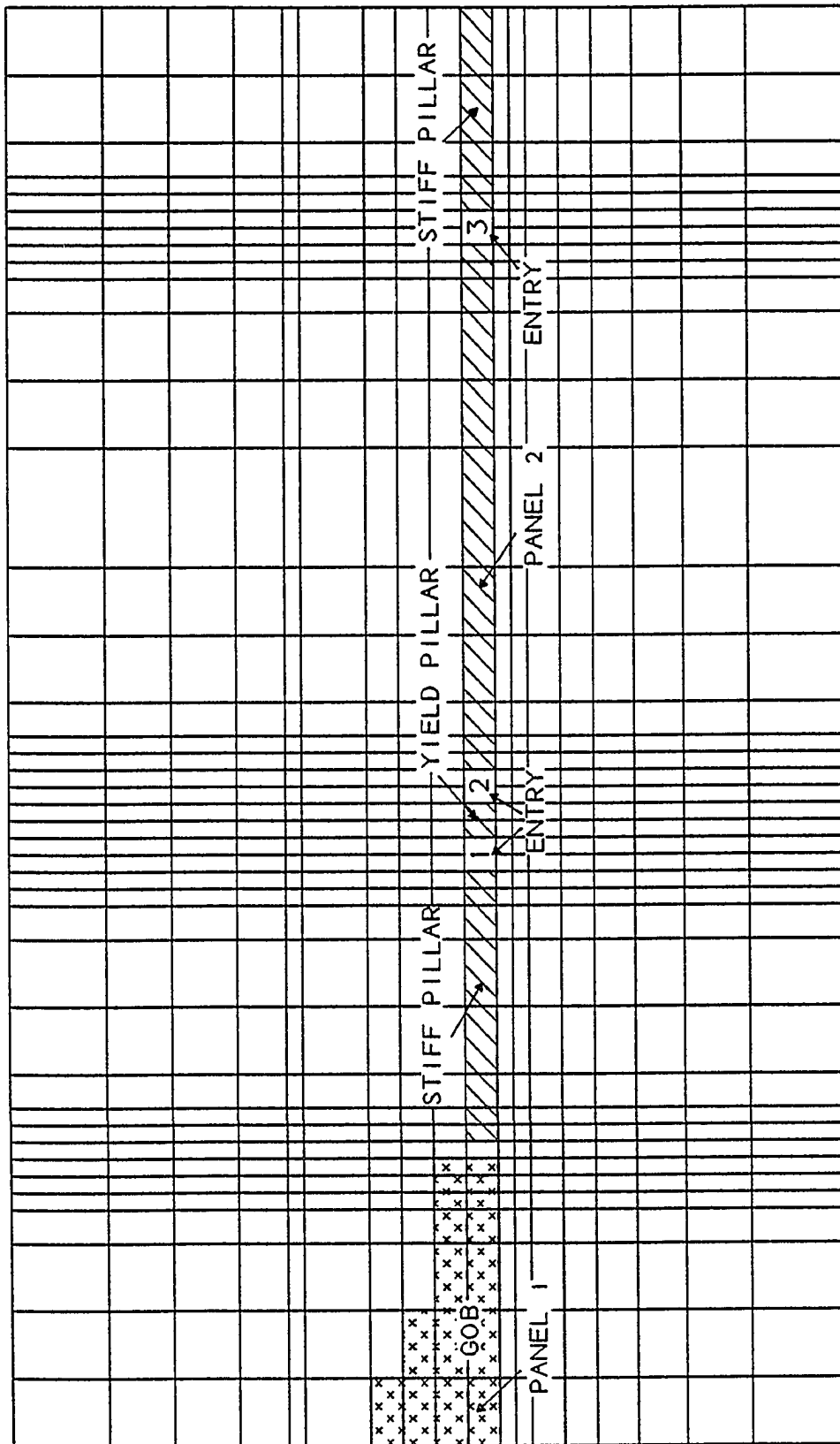


Figure 4.2. A typical 2-D finite element model.

a more realistic manner.

Table 4.1. Reduction Factors for Gob Materials

Gob Material	Reduction Factor		
	Young's Modulus	Poisson's Ratio	Density
Well Packed Gob	1/20	1/3	2/3
Packed Gob	1/40	1/5	2/3
Loosely Packed Gob	1/60	1/10	2/3

4.3 Stability Criteria of Entry-Pillar System

In underground coal mines, ground control concerns mainly the stability of coal pillar and room or entry. The stability problem for pillar is pillar failure whereas those for entries and rooms are all types of roof falls, rib falls and floor heave. During its service life period, all element(i.e., pillar or entry) must be stable in order to keep the whole entry-pillar system stable for continuous coal production. If anyone of them fails, a normal production will not be feasible. Therefore the design of an entry-pillar system should consider the stability of entry and pillar simultaneously. In this study the maximum entry convergence, average yield pillar strain, maximum tensile stress in the roof and S.F. of roof, pillar and floor are used as stability criteria for evaluating the performance of the entry-pillar system.

4.4 Mechanics of Yield Pillar

Yield pillar design, contrary to the traditional concept of pillar design, is used to design a relatively small pillar under given geological conditions, and the designed pillar is expected to yield right after its development. Thus, its original load is transferred to the adjacent pillars or gob. Yield pillars have been used in several coal mines and demonstrated that it can improve entry stability and eliminate the floor heave problems. But its design is more or less based on trials and errors mainly because the mechanisms and application limitations of yield pillar are still not well understood.

It is well known from the field practice that the duration of yielding of coal and rocks before collapse depends on the initial loading and material properties. As long as the rate of yielding is in the safe range, the overall stability condition for the entry-pillar system can be maintained for a given length of time, e.g., the required service life time. For safe mining operations, a yield pillar must satisfy two basic requirements: (1) it yields properly after development, so that its load can be transferred, and (2) it should sustain and maintain good working conditions in the adjacent entries for the intended service life period. If a pillar satisfies both requirements it is defined as a stable yield pillar(or functionable yield pillar). If a pillar only satisfies the first one, it is an unstable yield pillar(or an unfunctionable yield pillar).

A yield pillar, in general, is less stable than a stiff one. But considering the overall stability condition, a yield pillar or a combination of yield and stiff pillar design

may provide the best results, and it may be the only alternative design for certain geological conditions(e.g., deep coal mine). The whole purpose of the yield pillar design is to design the stable(or functionable) yield pillars in an entry-pillar system.

4.5 Model Simulation

In this section, the mechanisms and design criteria of yield pillar are discussed based on the geological conditions in a southern West Virginia mine. The overburden of the mine ranged from 1000 to 1200 ft. The overall roof and floor were stronger than the coal except in certain area where localized weak floor condition had caused floor to heave up in the head-entry. By using the classification system developed early(Chapter 3), both the strong roof and strong floor, and the strong roof and weak floor conditions, i.e., Category 1 and 2, were encountered in this mine. To consider all the possible geological conditions, both yield and stiff pillar designs were evaluated under the strong roof and strong floor, and the strong roof and weak floor conditions. In the yield pillar design, the chain pillars consisted of one yield and one stiff pillar. Whereas in the conventional design, it consisted of two stiff pillars, the pillar width of which were 70 and 50 ft., respectively. Figures 4.3 and 4.4 show the geological columns used in finite element modeling for both the strong roof and strong floor, and the strong roof and weak floor conditions. The material properties of immediate roof and floor for the two conditions are listed in Table 4.2 also.

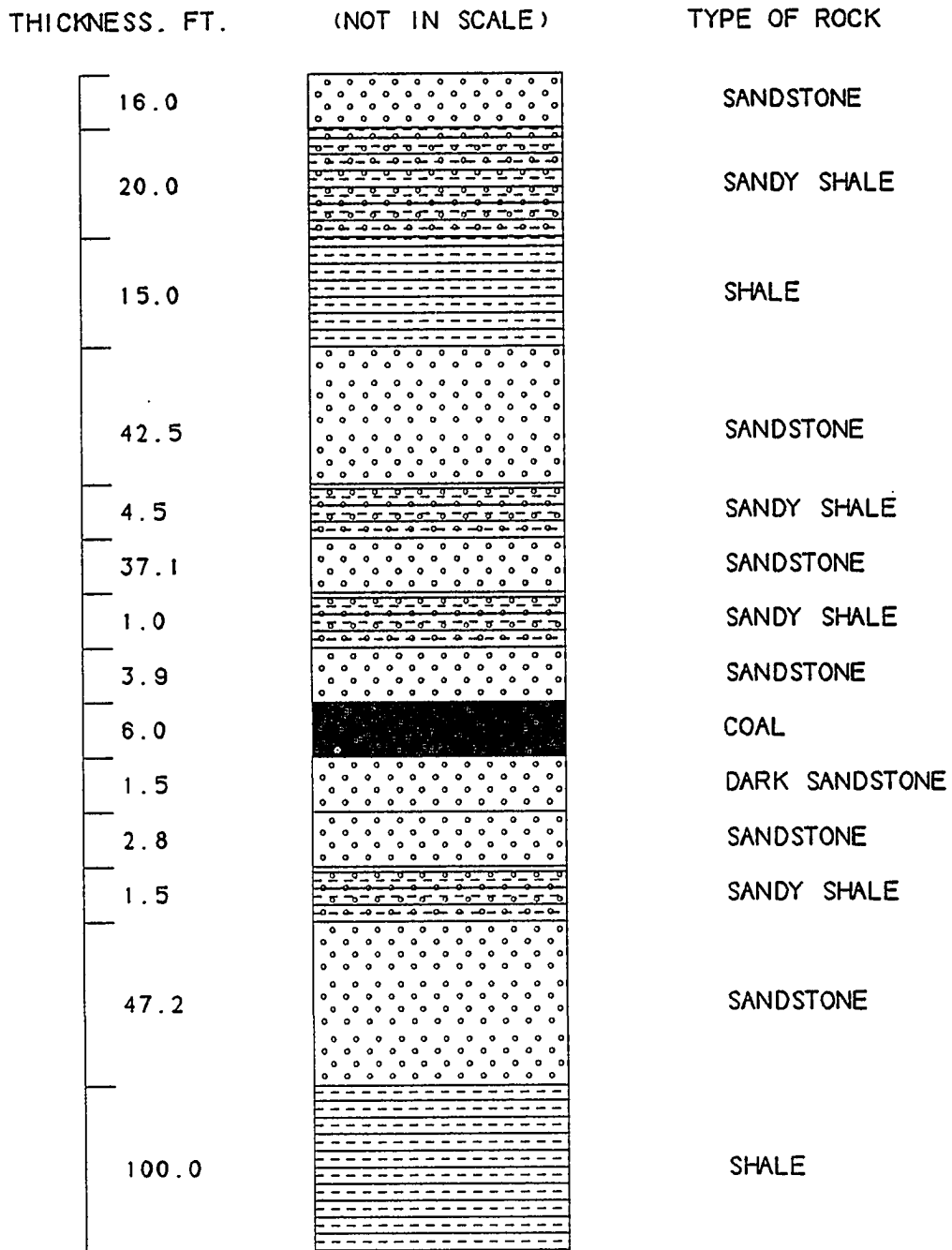


Figure 4.3. Geological column used in finite element models for simulating the strong roof and strong floor conditions.

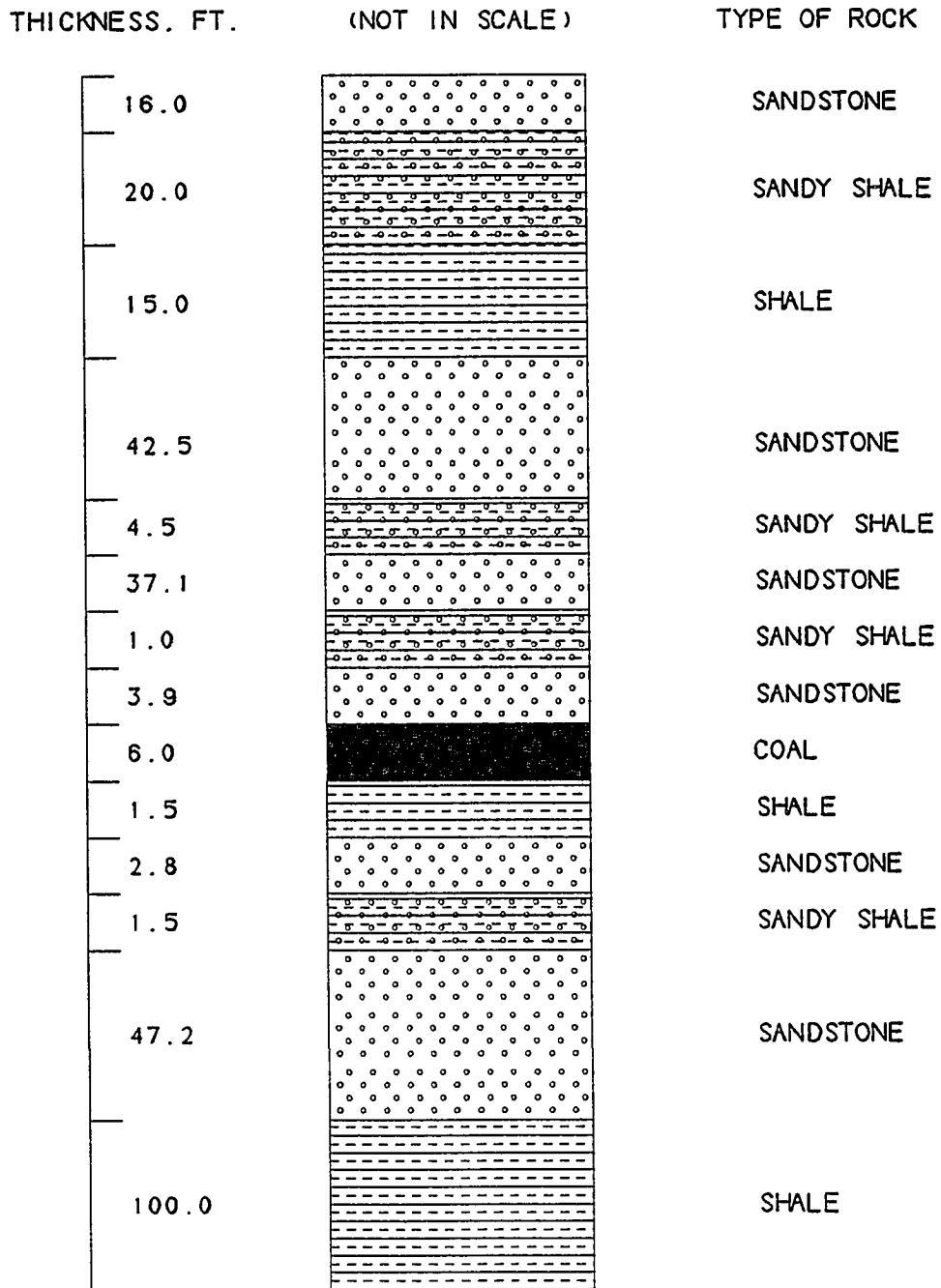


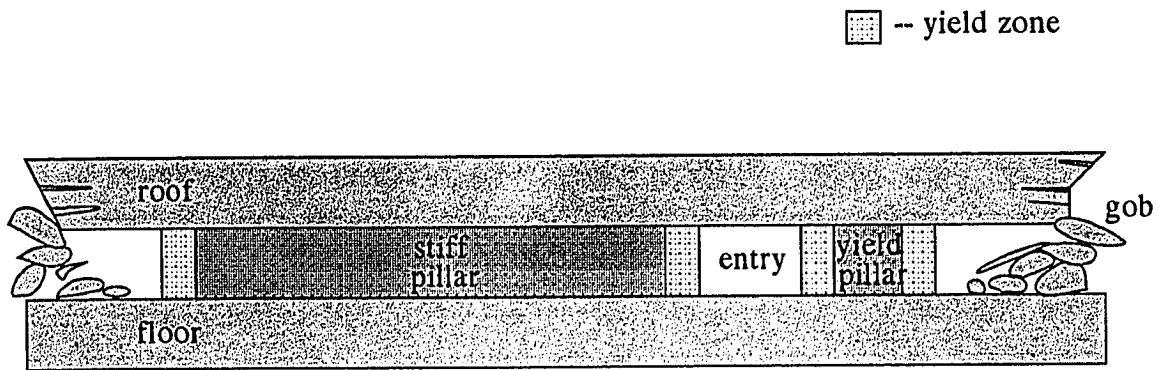
Figure 4.4. Geological column used in finite element models for simulating the strong roof and weak floor conditions.

Table 4.2. Rock Mechanical Properties

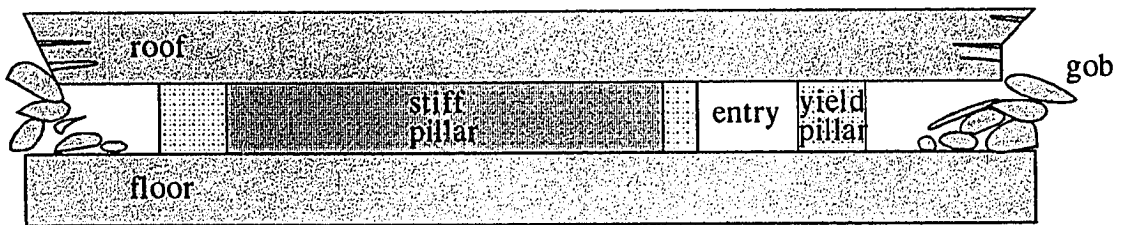
Type of Rock	Young's Modulus (10 ⁶ psi)	Poisson's Ratio	Unit Weight (pcf)	Compressive Strength (psi)	Tensile Strength (psi)	Internal Friction Angle	Depth of Cover (ft)
overall roof and floor condition, category 1							
Immediate Roof	4.8	0.15	159	11616	1094	40°	1000
Immediate Floor	3.05	0.16	167	10414	726	40°	1006
localized weak floor condition, category 2							
Immediate Roof	4.8	0.15	159	11616	1094	40°	1000
Immediate Floor	1.79	0.21	170	1200	1046	30°	1006

4.5.1 Strong Roof and Strong Floor Condition

In the case of a strong roof and strong floor condition, a total of 650 to 720 elements was used, and more than 20 models were constructed. The width of stiff and yield pillar in the models were varied from 60 to 120 ft. and 5 to 30 ft., respectively. The entries were 20 ft. wide. Figures 4.5 and 4.6 show the yield zone changes with the width of the stiff and yield pillars. Since the roof and floor are strong, there is no yield zone observed in either the roof or floor. When the yield pillar width is less than 25 ft. and stiff pillar is 120 ft., the yield pillar yields totally(Figs. 4.5 and 4.7). If the yield pillar is 15 ft., the stiff pillar will yield totally when its width is less than 70 ft.(Figs. 4.6 and 4.8). The yield zone, in general, increases when the size of the stiff and yield pillar reduces. There is a tendency that the S.F. of the floor under the yield pillar increases with decrease in the width of the yield pillar while that under the stiff pillar decrease very slightly(Fig. 4.7). The trend indicates load transformation from the yield pillar to the stiff pillar. Because the results of this study show load increasing on the stiff pillar and decreasing on the yield pillar. The yield pillar width plays a very important role in the design. Decreasing its size will increase the S.F. up to 96% of the floor under it with minimum effect on the floor under the stiff pillar. However, the effect caused by changing the stiff pillar width on average S.F. of the floor under both stiff and yield pillars(Fig. 4.8) is not as significant as the yield pillar(within 8%). The same thing is true for the roof. The possible reason is that the stiff pillar in this case is large enough



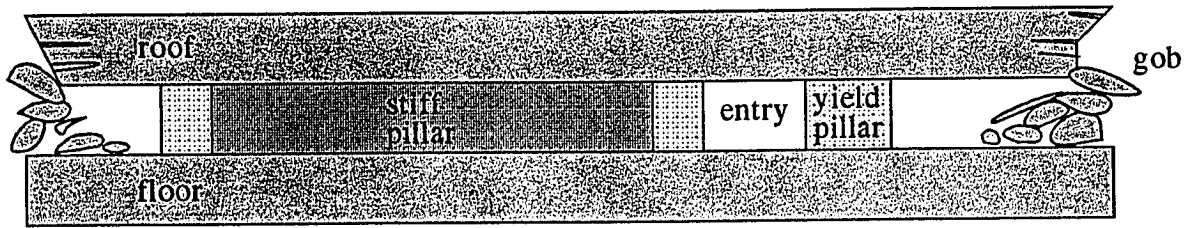
a) Stiff pillar is 120-ft wide, yield pillar is 30-ft wide.



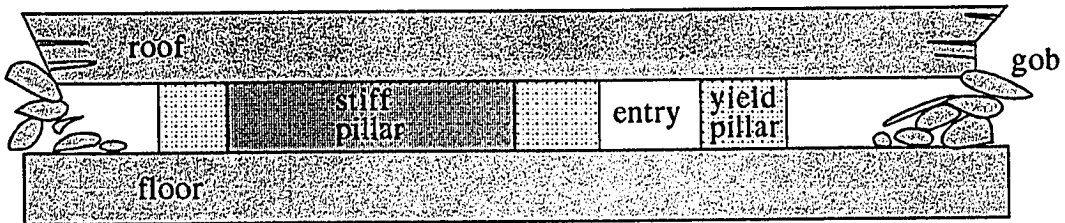
b) Stiff pillar is 120-ft wide, yield pillar is 10-ft wide.

Figure 4.5. Yield zone changes with yield pillar size under the strong floor conditions after the 2nd panel mining.

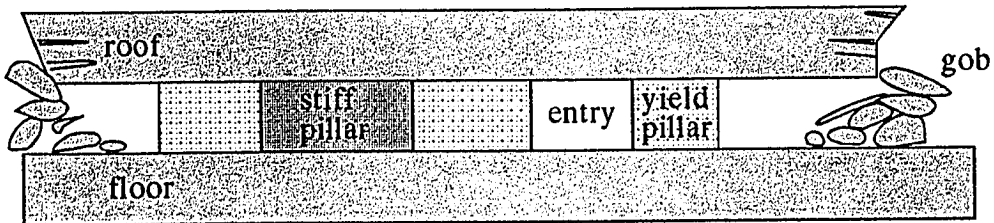
▣ -- yield zone



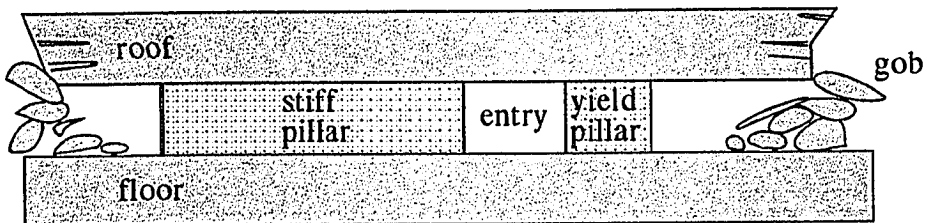
a) Stiff pillar is 120-ft wide, yield pillar is 20-ft wide.



b) Stiff pillar is 100-ft wide, yield pillar is 15-ft wide.



c) Stiff pillar is 80-ft wide, yield pillar is 15-ft wide.



d) Stiff pillar is 60-ft wide, yield pillar is 15-ft wide.

Figure 4.6. Yield zone changes with stiff pillar size under the strong floor conditions after the 2nd panel mining.

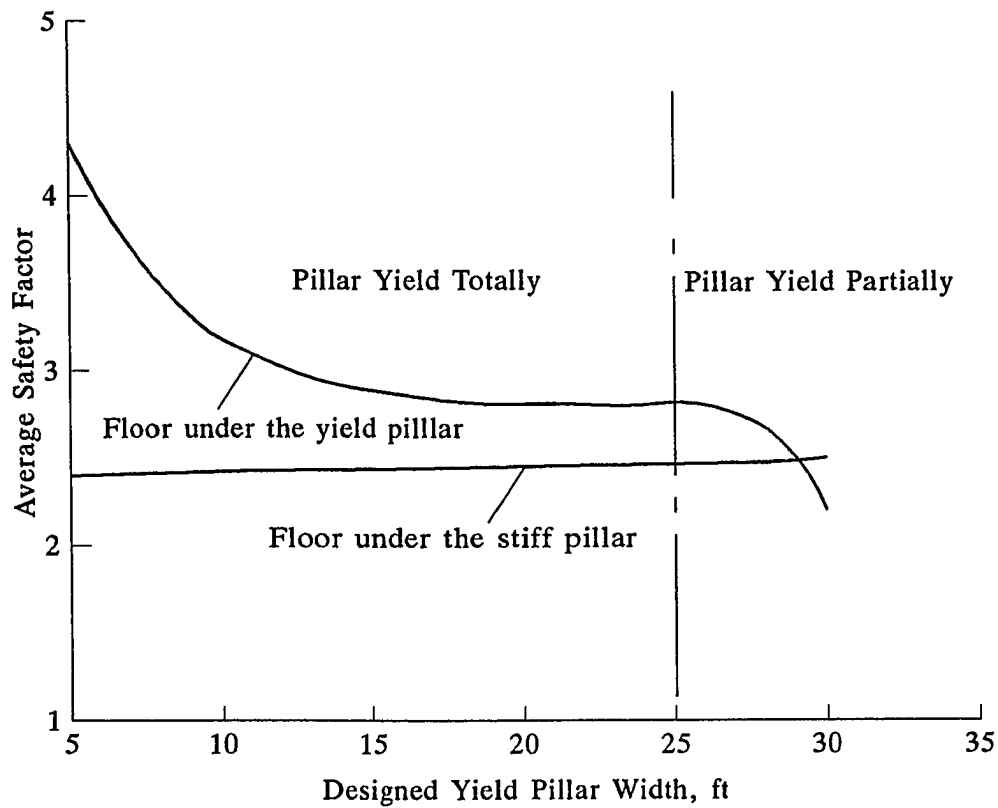


Figure 4.7. Changes of floor safety factor with yield pillar width before the 2nd panel mining while stiff pillar is 120 ft. wide.

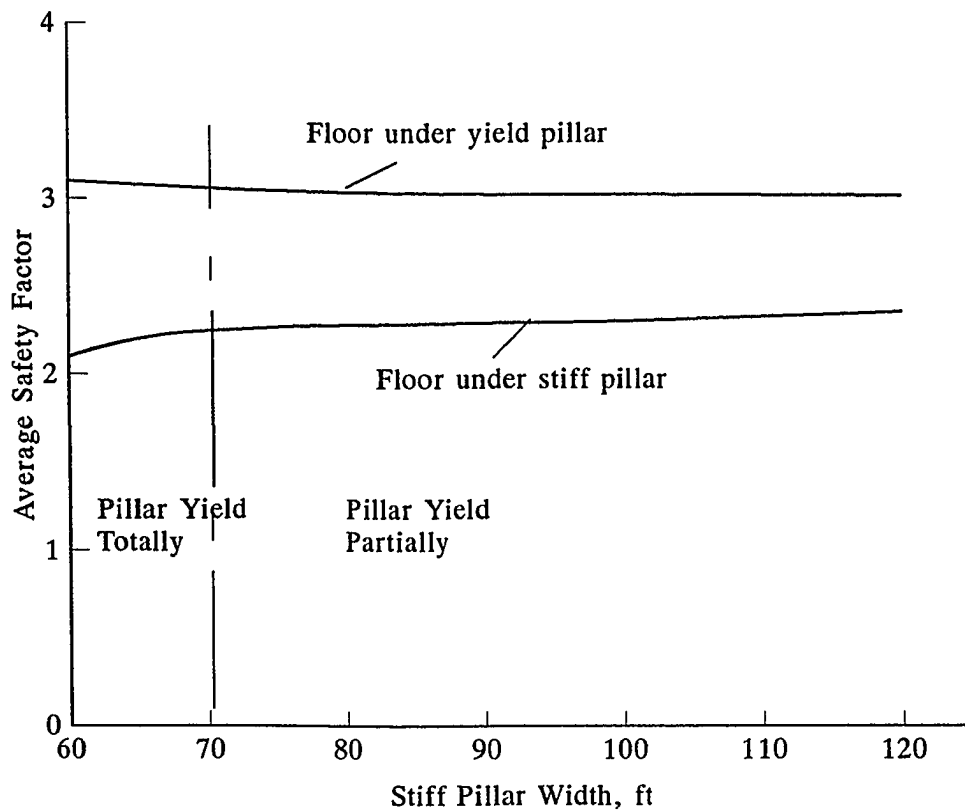


Figure 4.8. Changes of floor safety factor with stiff pillar width before the 2nd panel mining while yield pillar is 15 ft. wide.

to carry the transferred load. The results also show that a functionable yield pillar should yield substantially. If a designed yield pillar(>25 ft.) is strong and only yields partially, the original load will not be transferred. Rather, the load is imposed on the floor through the unyielding pillar. At the same time, if the floor strata under the pillar are weak, it may yield and be squeezed out easily, and causes the floor heave problem in the entry. This will be discussed later under the weak floor condition. Conversely, if the roof is weaker than the coal, roof separation and roof falls also may happen in the entry. According to this study, the most critical stress condition before the second panel mining occurs in the entry 2(Fig. 4.2). Therefore, its stability will ensure the stability of the entry-pillar system. Figs. 4.9 and 4.10 show that the maximum entry convergence for different pillar designs changes with time. The entry convergence for all pillar designs increases rapidly in the first 10 to 30 days, but slows down and becomes stable later in the service life period. Usually, the maximum entry convergence increases with decreasing width of the yield and stiff pillar. To evaluate the stability of the yield pillar, the average yield pillar strain is used. Similarly the yield pillar yields rapidly and slows down after 30 days. Although the average safety factor of the yield pillar in most cases is less than 1.0 but larger than 0.85, its average vertical strain becomes stabilized(Fig. 4.11). Since both entry convergence and pillar strain are stable during the service life time except the first 10 to 30 days, it seems that the entry-pillar system will be stable under any of these designs. Therefore, by considering these factors

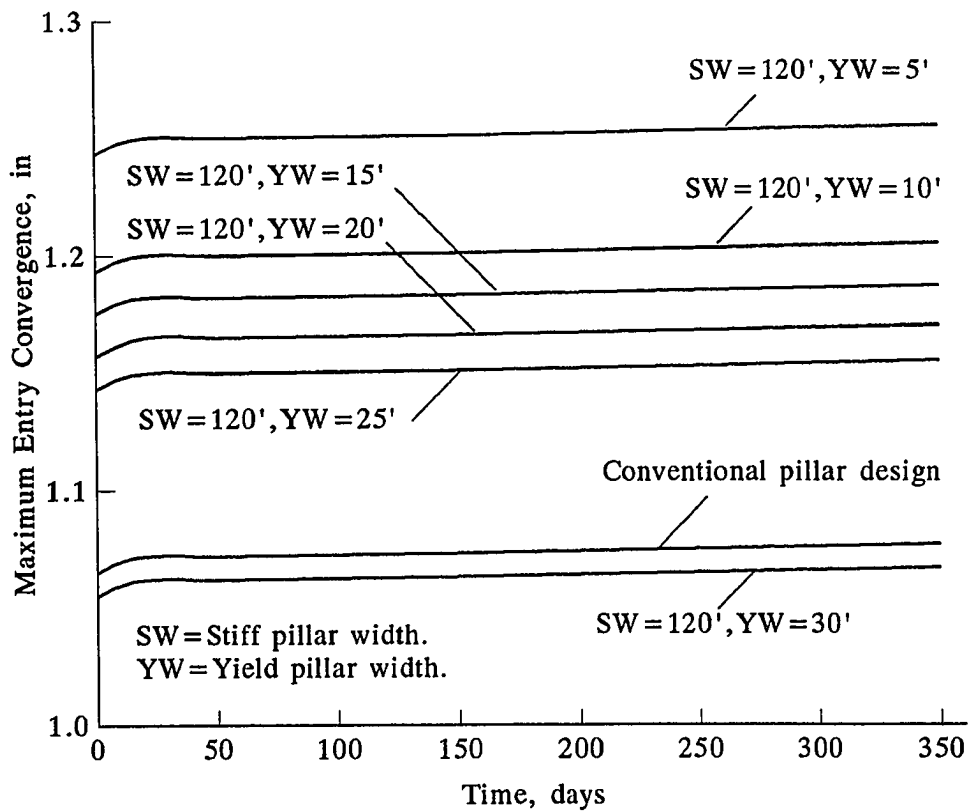


Figure 4.9. Maximum entry convergence in entry 2 changes with yield pillar width before the 2nd panel mining.

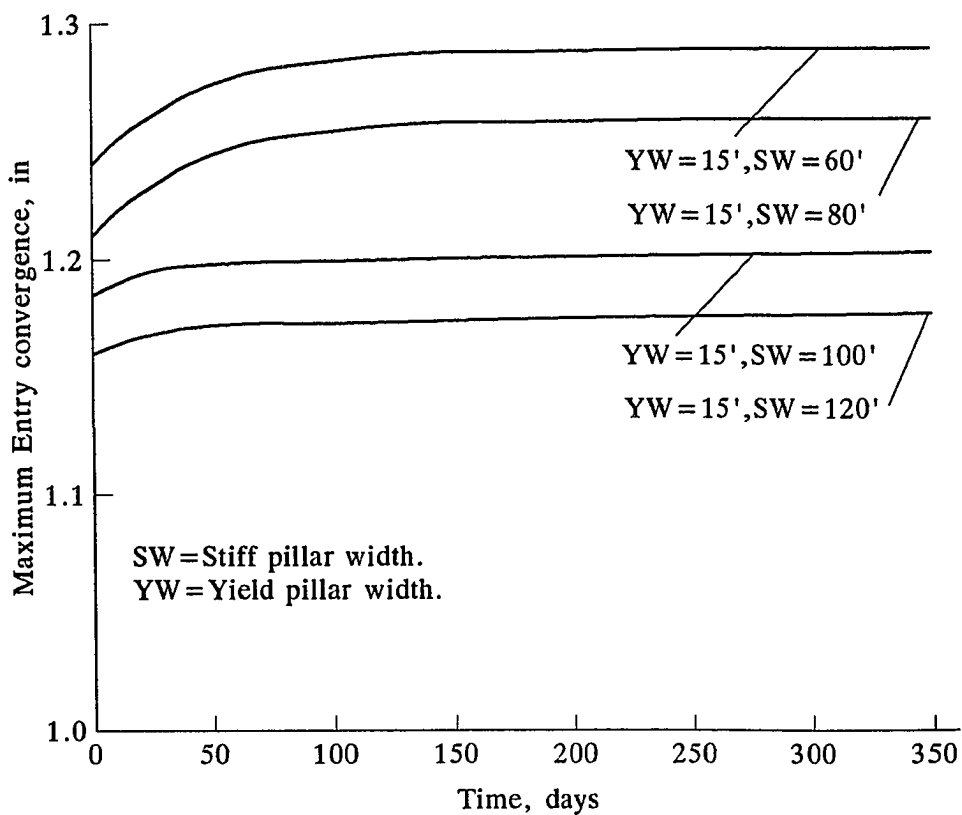


Figure 4.10. Maximum entry convergence in entry 2 changes with stiff pillar width before the 2nd panel mining.

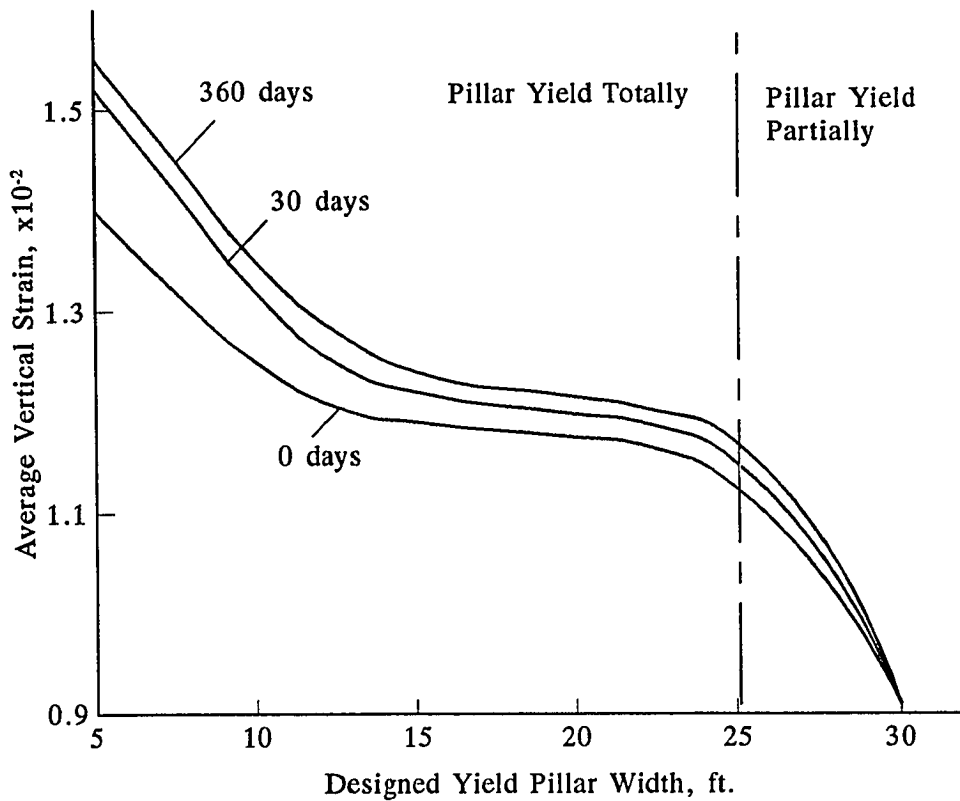


Figure 4.11. Average vertical strain in yield pillar before the 2nd panel mining while stiff pillar is 60 ft. wide.

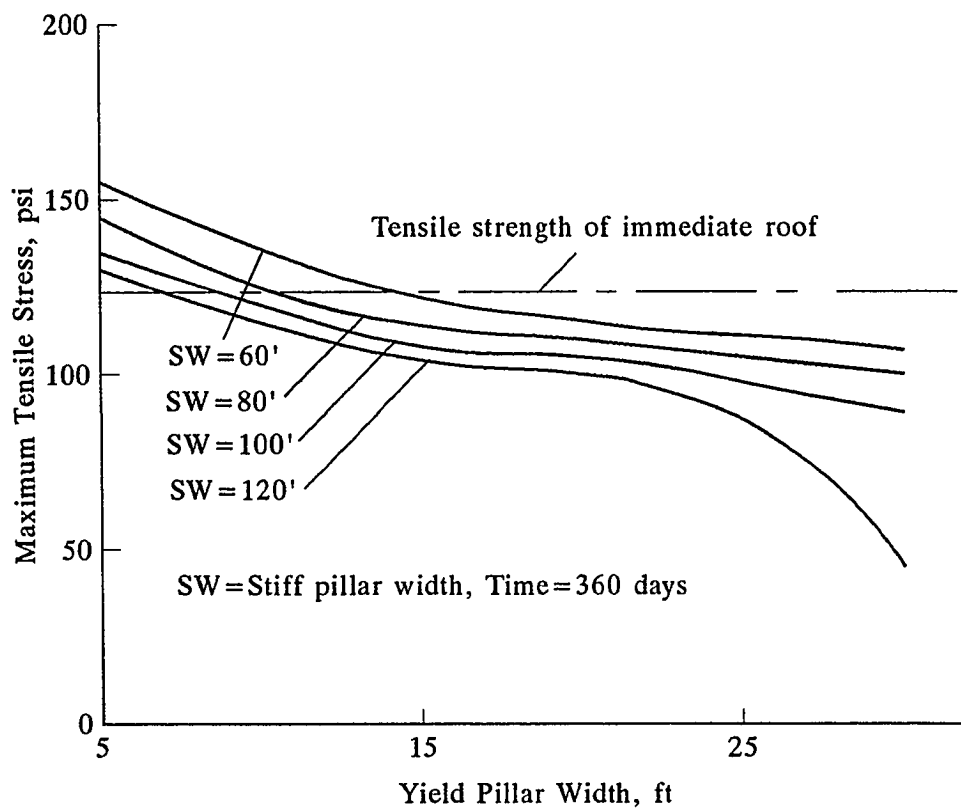


Figure 4.12. Maximum tensile stress in roof of entry 2 before the 2nd panel mining.

alone, it can not determine the lower limit of yield pillar size. So the maximum tensile stress in the roof is introduced. The relationship between pillar size and maximum tensile stress in the roof is represented in Fig. 4.12. Clearly, the maximum tensile stress in the roof will exceed its tensile strength if the yield pillar is too small and the roof will fail under tension regardless what the stiff pillar width is. By considering the maximum tensile stress in the roof and tensile strength of the roof, the lower limit of a yield pillar for a certain size of stiff pillar can be determined (Table. 4.3).

Table 4.3 Recommended Pillar Size for the Strong Roof and Strong Floor Condition

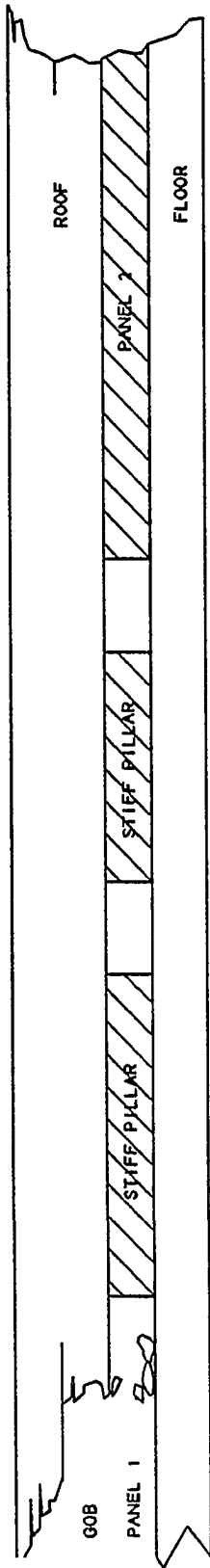
Recommended Pillar Size in Stiff-Yield Pillar System	
Stiff Pillar Width (ft)	Yield Pillar Width Range (ft.)
120	10-25
100	10-25
80	10-25
60	15-25

In conclusion, the yield pillar can be designed under the strong roof and strong floor conditions. Since both roof and floor are very strong in this case, S.F. factor of the roof and floor is all larger than 1.0. Shear failure of both roof and floor is very unlikely. The weakest element in the entry-pillar system is pillar itself. In addition, tensile stress in the roof may also cause the entry roof failure. Therefore, the yield pillar size can be determined by considering these two criteria only, i.e., the tensile stress in the roof and the average S.F. of the pillars.

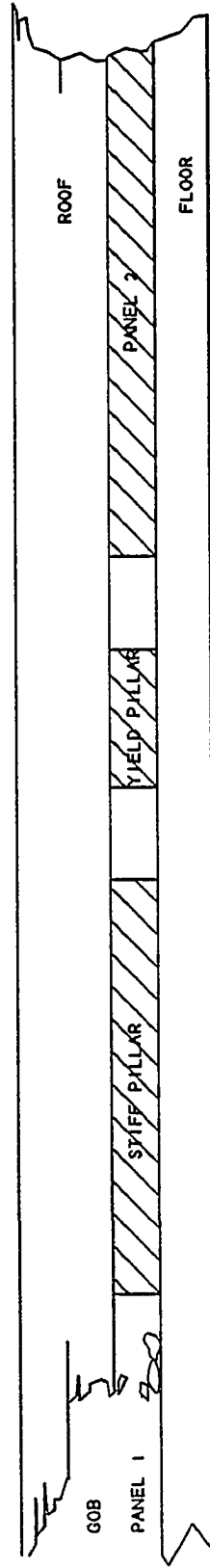
4.5.2 Strong Roof and Weak Floor Conditions

To evaluate the pillar performance under strong roof and weak floor conditions, i.e., Category 2, a total of 16 models was constructed, and 710 to 790 elements was used in each of the model. The overburden was 1000 ft. thick. The longwall panel width was 600 ft. wide, and entries were 20 ft wide. All material properties of rocks were the same as the previous case except the floor strata(see Fig. 4.4). Both conventional pillar design and yield pillar designs were analyzed under the same geological conditions. The conventional pillar design currently employed in the mine consisted of two stiff pillars and three entries on each side of the panels. The pillar widths were 70 ft. and 50 ft. with one large stiff pillar located on gob side(Fig. 4.13). In contrast, the yield pillar design had one stiff pillar, one yield pillar, and three entries in the entry-pillar system with the stiff pillar located on the gob side. The width of both stiff and yield pillars varied from 60 to 120 ft. and 10 to 40 ft. respectively, in order to determine the suitable yield pillar size.

Stress analysis on the yield zone development for both conventional and yield pillar designs are represented in Figs. 4.14, to 4.16. Fig. 4.14a shows the yield zones before the second panel was mined. Figure 4.14b, c and d shows the development of those yield zones immediately, 10 days and 160 days after 2nd panel has been mined, respectively. Large yield zones appear under both stiff pillars and propagate with time. Since both pillars do not yield properly, the overburden load is applied directly on the



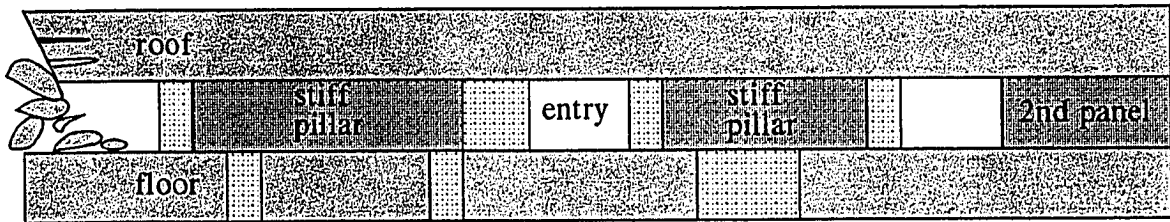
STIFF PILLAR DESIGN



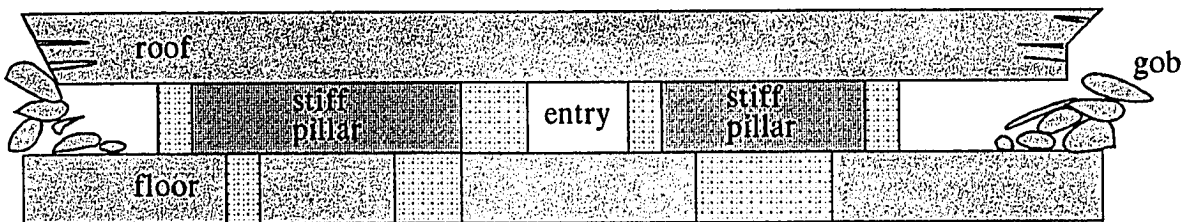
YIELD PILLAR DESIGN

Figure 4.13. Stiff and yield pillar designs under strong roof and weak floor condition.

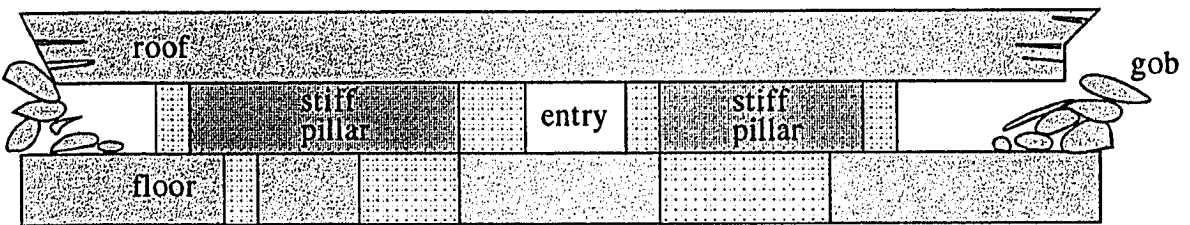
▣ -- yield zone



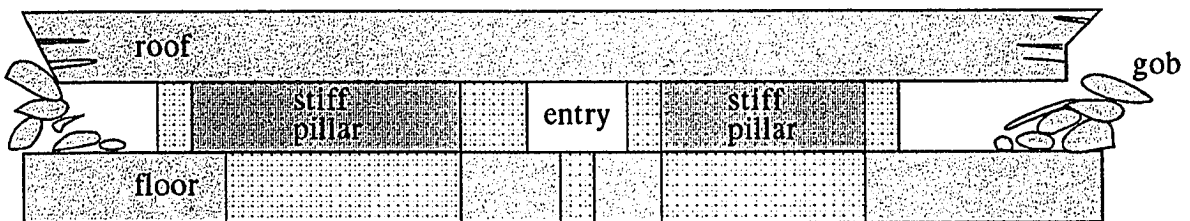
a) before mining the 2nd panel



b) 0 days after mining the 2nd panel



c) 10 days after mining the 2nd panel

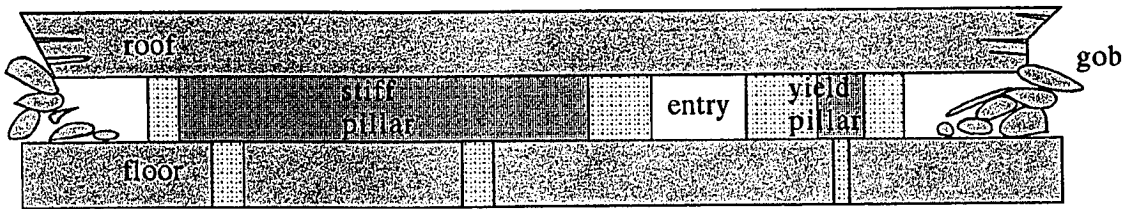


d) 160 days after mining the 2nd panel

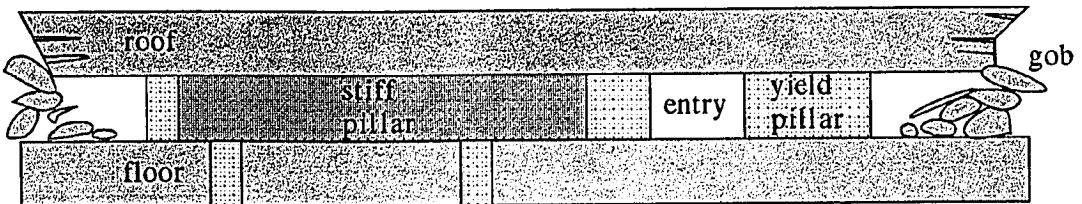
Figure 4.14. Yield zone development under the weak floor condition for conventional pillar design.

floor through the non-yielding stiff pillars and the yielded floor is easily squeezed out from the underneath of the stiff pillars and eventually creates floor heave problems in the entry. After 160 days of mining, the yield zone initiates in the entry (Fig. 4.14d). In order to eliminate the yield zone in the floor, both pillars should be increased to 120 ft. wide for the stiff pillar design based on the finite element model study. This design will result in a large loss of coal resources. So a possible alternative design, such as the yield pillar design, should be considered. In the yield pillar design (Fig. 4.15), the yield pillar is expected to yield substantially after development, while the stiff pillar yields only partially. The width of the stiff pillar was kept as constant, while the yield pillar width changed from 40 to 10 ft. There are small yield zones in the floor which is less than 8% of the total width of the pillars in these four designs that would not cause floor heave problems in the entries later. The yield zone in the floor under the yield pillar decreases with the width of the yield pillar (Fig. 4.15). Yield pillar will yield totally if its width is less than or equal to 30 ft. After the yield pillar yields, the load is transferred to the adjacent areas and a stress-released zone is created around the yield pillar to protect the entry-pillar system, and results in a slight increase of yield zone in the stiff pillar. In contrast, when the yield pillar yields partially (Fig. 4.15a), a small yield zone appears under its floor because the stress-released zone can not be fully formed. The stiff pillar size will also affect the yield zone distribution (Fig. 4.16). The yield zone in the stiff pillar and the floor under it increases with decreasing stiff pillar size. In

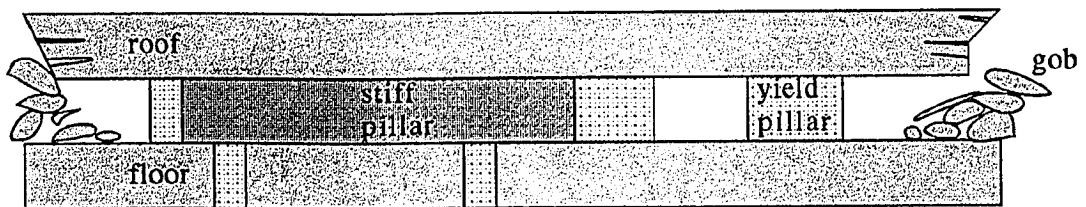
▣ -- yield zone



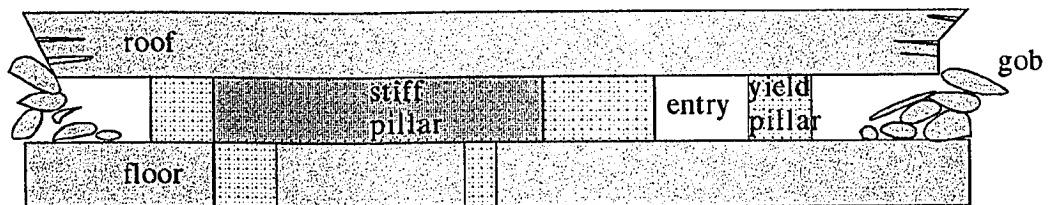
a) Stiff pillar is 120-ft wide, yield pillar is 40-ft wide.



b) Stiff pillar is 120-ft wide, yield pillar is 30-ft wide.

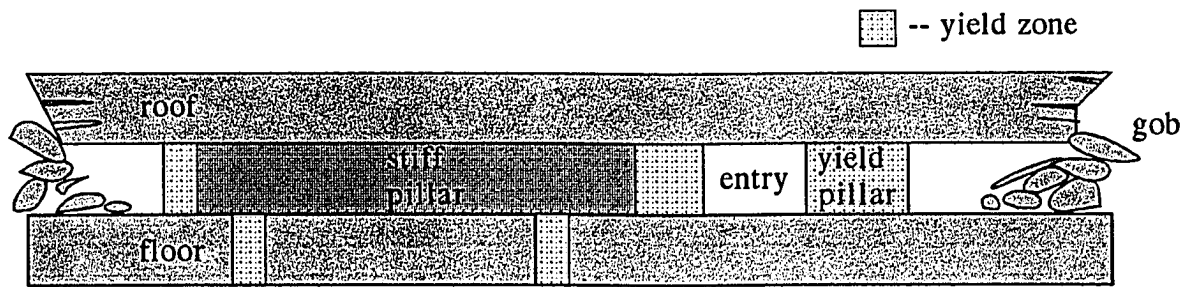


c) Stiff pillar is 120-ft wide, yield pillar is 20-ft wide.

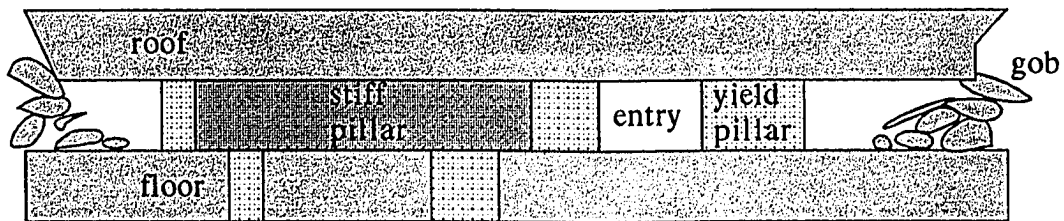


d) Stiff pillar is 120-ft wide, yield pillar is 10-ft wide.

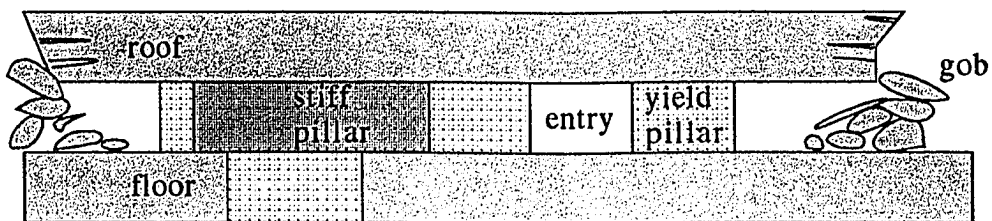
Figure 4.15. Yield zone changes with yield pillar size under the weak floor conditions.



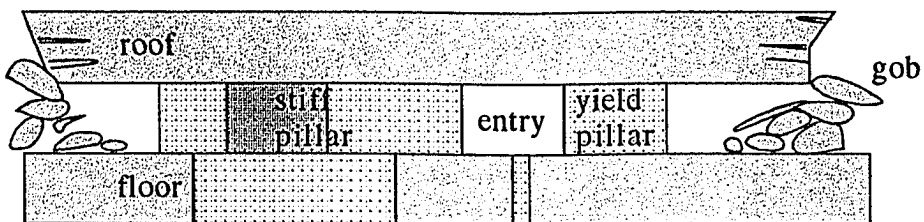
a) Stiff pillar is 120-ft wide, yield pillar is 20-ft wide.



b) Stiff pillar is 100-ft wide, yield pillar is 20-ft wide.



c) Stiff pillar is 80-ft wide, yield pillar is 20-ft wide.



d) Stiff pillar is 60-ft wide, yield pillar is 20-ft wide.

Figure 4.16. Yield zone changes with stiff pillar size under the weak floor conditions.

particular, when the stiff pillar size is 60 ft. wide, a large yield zone in the floor appears under the stiff pillar, and a small yield zone initiates in the entry. It will eventually cause the floor heave problems in the entry when the pillars punch into the floor. So for the weak floor condition, a stiff pillar has to be large enough in size to carry the load being transferred from an adjacent yield pillar and to prevent the development of a large yield zone under it. The design should be such that both stiff and yield pillars will not punch into the floor by creating low pillar stress acting on the floor, and thus the weak floor under both pillars will not be squeezed out easily. Therefore, the key to successful yield pillar design under weak floor condition is to reduce stresses acting on the floor.

Concerning the safety factor of the floor(Figs. 4.17 and 4.18), as the yield pillar size decreases, the safety factor of the floor under the yield pillar increases distinctly, while that under the stiff pillar decreases indicating load transformation from the yield to the stiff pillar. In this case, a 10 ft. wide yield pillar is still a functionable yield pillar since S.F. under both pillars is larger than 1 and chance of floor heave in the entry is very unlikely. When the yield pillar size is less than 10 ft. no convergence solution can be obtained because of large yield zone in the floor. When the stiff pillar changes from 120 to 60 ft.(Fig. 4.18), the safety factor of the floor under stiff pillar decreases continuously, and finally reaches 0.98 when stiff pillar is 60 ft. wide. So a 20 ft. wide yield pillar will not ensure the stability of the entry-pillar system when stiff pillar is 60

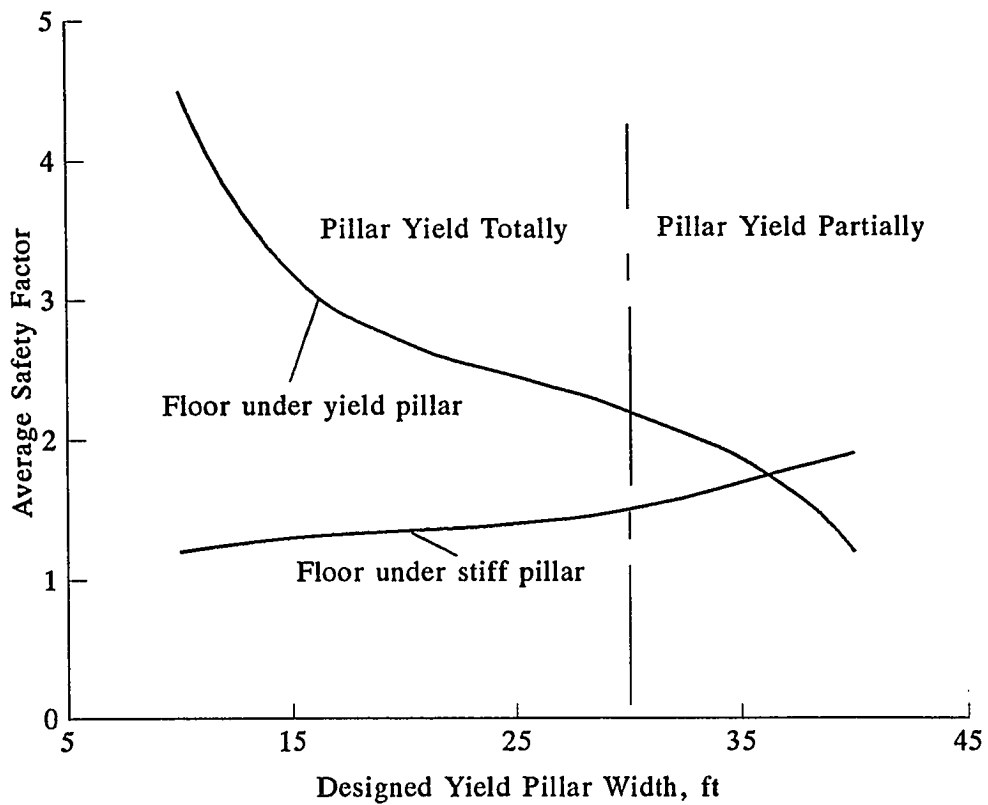


Figure 4.17. Floor safety factor changes with yield pillar width under weak floor condition when stiff pillar is 120 ft. wide.

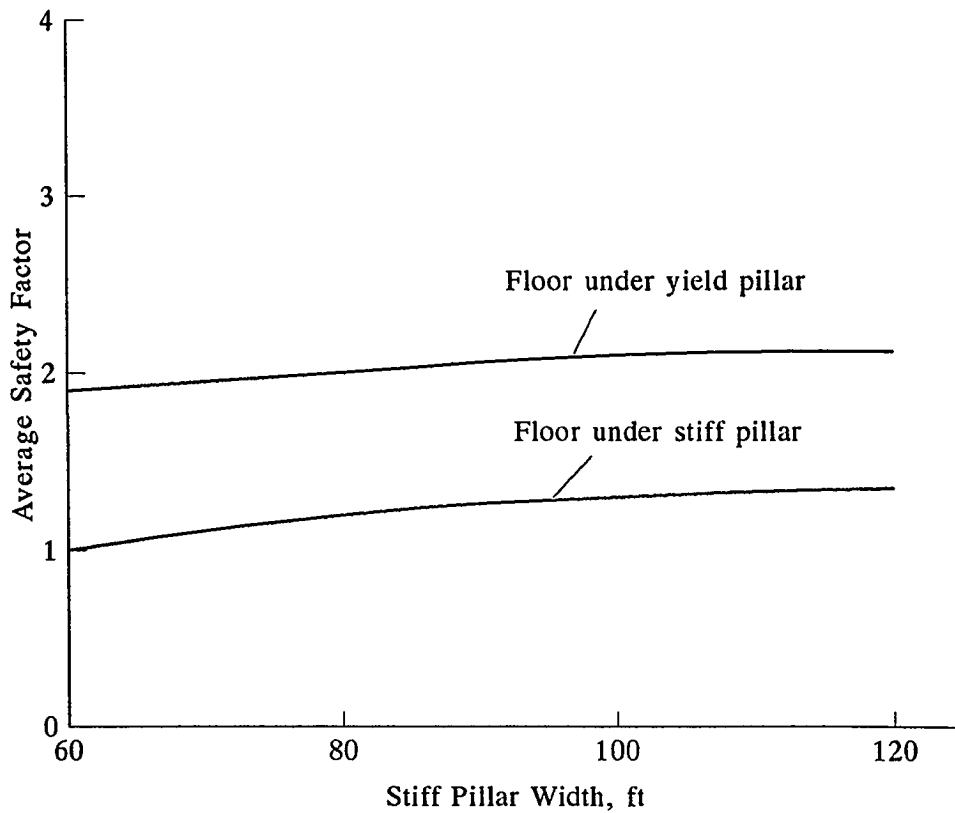


Figure 4.18. Floor safety factor changes with stiff pillar width under weak floor condition when yield pillar is 20 ft. wide.

ft. wide. By considering the effect of both pillars on the safety factor of the floor, the approximate yield pillar size can be determined.

Since the floor is weak, the maximum entry convergence in the system is also used to evaluate the system's stability(Figs. 4.19 and 4.20). It is obvious that maximum entry convergence increases with decreasing stiff and yield pillar sizes. When stiff pillar is 60 ft. wide and yield pillar is 20 ft. wide, entry convergence increases dramatically and no convergence solution can be obtained beyond 20 days after mining. So based on the convergence, a suitable yield pillar size can be determined also.

For stability analysis of pillars, the average vertical strain or S.F. of the yield pillar could be used here also. Figure 4.21 shows vertical strain change with the yield pillar width when the stiff pillar is 100-ft. wide. There are two curves in the figure, one represents the average vertical strain of yield pillar immediately after mining, and the other at 360 days after mining. The yield pillar is stable when its width ranges from 15 to 30 ft. because the increment of its average vertical strain is stable. But when yield pillar is less than 15 ft. wide, no convergence solution can be obtained due to massive failures in the roof and yield pillar. The average vertical strain in yield pillar increases with decreasing size of the yield pillar. So the smaller the yield pillar, the larger is the deformation.

Since the tensile stress in the roof is an important factor in roof stability, the maximum tensile stress in the system is analyzed(Fig. 4.22). The maximum tensile stress

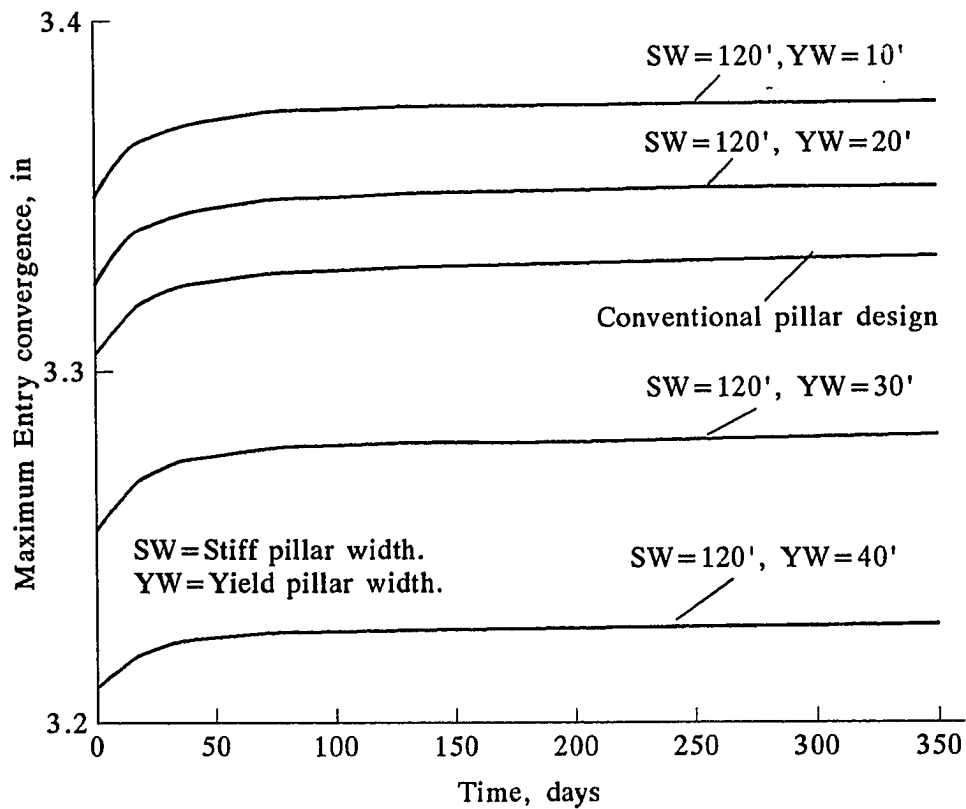


Figure 4.19. Maximum entry convergence changes with yield pillar width.

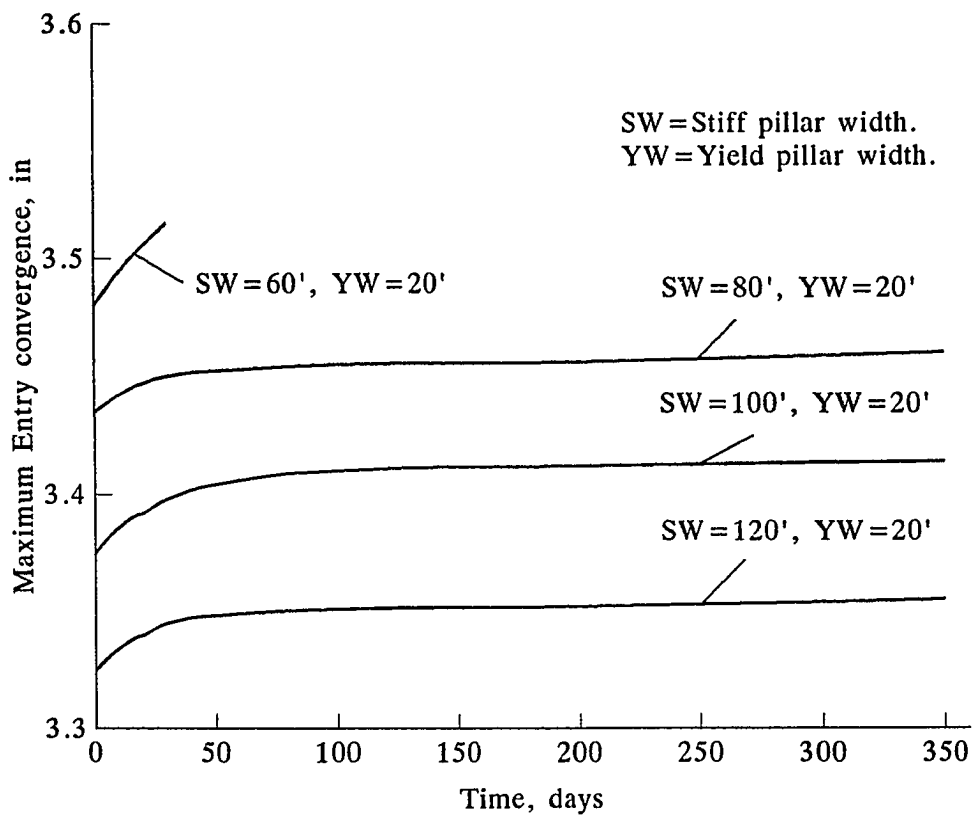


Figure 4.20. Maximum entry convergence changes with stiff pillar width.

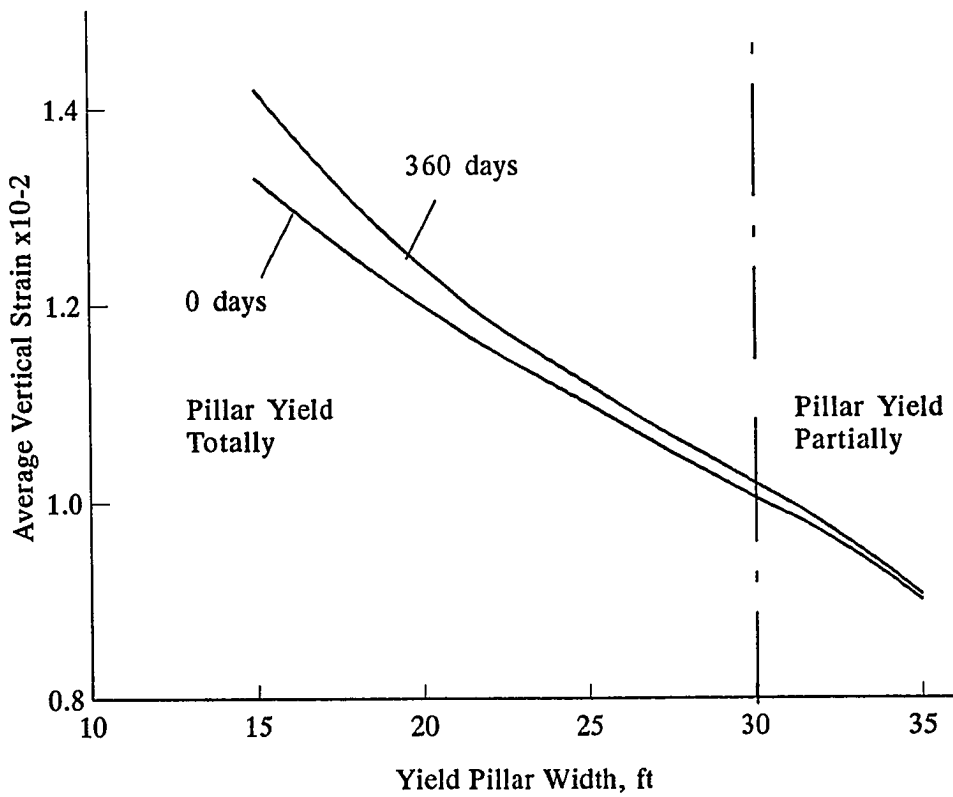


Figure 4.21. Pillar vertical strain changes with yield pillar width under weak floor condition when stiff pillar is 100 ft. wide.

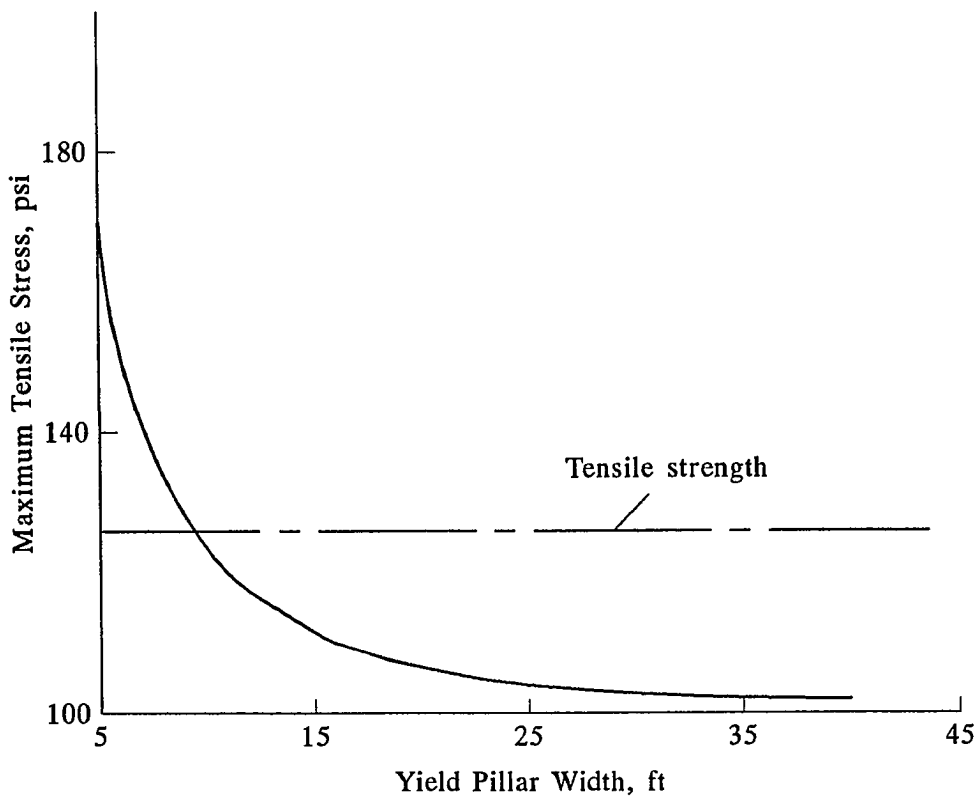


Figure 4.22. Maximum tensile stress in entry 2 when stiff pillar is 120 ft. wide.

in the entry increases with decreasing yield pillar size. The same thing is true for decreasing stiff pillar size. The broken line in Fig. 4.22 is the roof tensile strength. The maximum tensile stress finally exceeds the roof tensile strength when yield pillar size is less than 9.5 ft. wide. A possible roof tensile failure may occur in this design when yield pillar is too small. By considering S.F. of the floor, pillar strain or safety factor of pillar, and maximum tensile stress in the roof, a suitable yield pillar size can be determined (Table 4.4).

Table 4.4 Recommended Pillar Size for the Strong Roof and Weak Floor Condition

Recommended Pillar Size in Stiff-Yield Pillar System	
Stiff Pillar Width (ft)	Yield Pillar Width Range (ft.)
120	10-30
100	15-30
80	20-30

In summary, to ensure the stability of the entry-pillar system under the strong roof and weak floor condition, the yield pillar design should consider the stability problems of the roof, floor, and pillar simultaneously. According to this study, the safety factor of the floor and pillar are the governing factors for the stability of floor and pillar while the tensile stress in the roof is a main concern to roof stability.

4.6 Conclusions

Based on the study on the mechanism of yield pillar, the following conclusions

can be made:

The mechanisms and major functions of a yield pillar is to redistribute stress in the entry-pillar system. Since a yield pillar allows a large deformation in the pillar and its surroundings, it creates a stress release zone in the adjacent areas to balance the stability conditions of the whole entry-pillar system. In order to achieve this, a pillar has to be designed as a stable yield pillar which satisfies two basic requirements: (1) it yields properly and transfers the load to the adjacent areas, and (2) it has to sustain and maintain good working conditions in the adjacent entries during its service life periods.

The yield pillars can be applied to most geological conditions. It could be an optimum design in terms of safety and coal recovery. Especially, for weak floor conditions, it is a good alternative design to overcome the floor heave problem when the required stiff pillar is very large.

In most cases, a large entry convergence will be expected if a yield pillar is adopted. But as long as the entry convergence and pillar shortening are stable and satisfy the requirements of mining operation and safety during the service life period, a yield pillar can be applied safely.

As far as yield pillar design is concerned, the safety factor of pillars and maximum tensile stress in the roof are the determining factors under the strong roof and strong floor condition. But an additional factor, safety factor of the floor, should also be considered under the strong roof and weak floor condition.

CHAPTER 5

SIGNIFICANCE ANALYSIS ON VARIABLES AFFECTING

PERFORMANCE OF LONGWALL CHAIN PILLAR

5.1 Introduction

As mentioned earlier, the stability of entry-pillar system in underground coal mines depends not only on the mechanical properties of coal and surrounding rocks, (e.g. strength, Poisson's ratio, Young's modulus, etc.), but also on geological and mining conditions, including dimensions of longwall panel, mining height, entry width, overburden thickness, in-situ stress, etc. Each of these variables will affect the pillar performance to a different degree. Some of them may have significant effects on the stability of entry-pillar system while the others may have very little. To distinguish the effect of each variable is very important simply because it is impossible to consider all the variables in this study. On the other hand, the complexity of the geological environment in coal mines precludes consideration of every possible variable. In order to make this study possible and provide the most meaningful results at the same time, the most important variables that affect the stability of entry-pillar system have to be considered. Among these variables mentioned earlier, which of these have the significant effect? And how important are they? The answers to these questions will provide scientific bases for selecting important variables in this study, and help reduce

a large amount of work involved in finite element modeling. However, to examine the effects contributed by each variable can be a very difficult and complex task itself. In order to evaluate each variable's effect in the most efficient way, the theory of orthogonal experiment design was adopted in the study.

5.2 Variables Considered in Significance Analysis

Over the years, the stability of pillar has been studied by many investigators around the world. In their studies, different approaches and different variables have been considered. Table 5.1 summarizes the variables(or parameters) considered by the major investigators. All of the pillar design methods take pillar width (W), longwall panel width (W_2), coal strength(S_1), and overburden thickness (h) into their design considerations, and the most methods have also considered entry width (W_e), mining height (H), and angle of draw (β) for determining the pillar loadings. Clearly, the roof and floor conditions receive less attention. There are only two design methods among those listed in Table 5.1 that have considered the roof and floor conditions in their designs. One is Wilson method, and the other is Hsiung-Peng method. Wilson method deals with the roof and floor conditions by simply considering a strong roof and floor, and a weak roof and floor condition in two separated design categories, and provides no rules for quantifying the roof and floor conditions. While Hsiung-Peng method approaches the problem by introducing the Young's modulus of roof and floor

Table 5.1. Variables Considered in Different Pillar Design Methods

Method	Variables Considered											
	W	h	W	S ₁	β	W _e	H	L	φ	E _i /E _c	E _m /E _c	E _f /E _c
Bieniawski (1984)	✓	✓	✓	✓	✓	✓	✓					
ALPS(Mark, 1990)	✓	✓	✓	✓	✓	✓	✓					
Wilson(1973)	✓	✓	✓	✓	✓	✓	✓		✓			
Holland-Gaddy(1973)	✓	✓	✓	✓	✓	✓	✓					
Hsiung-Peng (1985)	✓	✓	✓	✓				✓		✓	✓	✓

Note

- | | |
|--|---|
| H = mining height, | W = pillar width, |
| h = overburden thickness, | L = longwall panel length, |
| W _p = longwall panel width, | S ₁ = strength of coal, |
| β = the angle of draw, | W _e = entry width, |
| φ = internal friction angle, | E _i = Young's modulus of immediate roof, |
| E _m = Young's modulus of main roof, | E _f = Young's modulus of floor, |
| E _c = Young's modulus of coal. | |

rock into their design formula. The reason for one method to consider one variable than another is mainly because of the limitations imposed on by the nature of the problem itself. A method that processes more variables usually becomes more complex and time consuming, and requires more in-depth knowledge. Such limitations are always there no matter how advanced the technologies are available. The study involved in this dissertation research is not an exception. Being limited by computer-

time and -resources and by the finite element program used, only those presumably important variables are considered in the significance analysis. For the variable significance analysis, the following commonly used variables are adopted in the finite element model analysis: mining height (H), panel width (W_2), entry width (W_e) and width of each pillar (W_1, W_2). $h\gamma/C$ (the ratio of mining depth multiplied by the average unit weight of the overburden to the cohesion strength of coal) and ϕ (internal friction angle of coal) are selected also. These two factors indicate the relative stress level in the coal and strength properties of the coal. In addition, the ratios of Young's modulus of roof to coal (E_r/E_c) and floor to coal (E_f/E_c), Poisson's ratio of coal (ν), horizontal stress (σ_h), and creep constants of floor (a_f, b_f , and d_f) are also chosen to be variables in the finite element models. The reason for considering the variation of the floor creep constants is to evaluate weak floor's effect in finite element models. A total of 14 variables were selected for significance analysis (Table 5.2). The rest of the necessary input data for finite element models were considered as constants during finite element modeling.

5.3 Orthogonal Experiment Design for Finite Element Modeling

As mentioned earlier, to completely evaluate the effect of all variables cited earlier is a very complex and time-consuming task. In this case, a complete factorial experiment investigating all possible combinations of all levels of the different variables

Table 5.2. Finite Element Models Designed by A 2-Level Orthogonal Experiment Plan

Variable	1	2	3	4	5	6	7	8	9	10	11	12	13	14
Model	E_r/E_c	E_r/E_c	W_c	W_1	W_2	ϕ	$h\gamma/C$	a_f	b_f	d_f	H	σ_h	v	W_p
1	1	1	1	1	1	1	1	1	1	1	1	1	1	1
2	1	1	1	1	1	1	1	2	2	2	2	2	2	2
3	1	1	1	2	2	2	2	1	1	1	1	1	1	1
4	1	1	1	2	2	2	2	1	1	1	1	1	1	1
5	1	2	2	1	1	1	1	2	2	2	2	2	2	2
6	1	2	2	1	1	1	1	2	2	2	2	2	2	2
7	1	2	2	1	1	1	1	2	2	2	2	2	2	2
8	1	2	2	2	2	2	2	1	1	1	1	1	1	1
9	2	1	2	1	2	2	2	1	2	2	2	2	2	2
10	2	1	2	1	2	2	2	1	2	2	2	2	2	2
11	2	1	2	2	1	1	1	2	2	2	2	2	2	2
12	2	1	2	2	1	1	1	2	2	2	2	2	2	2
13	2	2	1	1	2	2	2	1	2	2	2	2	2	2
14	2	2	1	1	2	2	2	1	2	2	2	2	2	2
15	2	2	1	1	2	2	2	1	2	2	2	2	2	2
16	2	2	1	1	2	2	2	1	2	2	2	2	2	2

will involve a large number of finite element models. Presumably, If each of the 14 variables varies twice(i.e., two levels), a complete factorial experiment would mean testing $2^{14} = 16384$ combinations(Kempthorne, 1952) or finite element models in just one simple replicate. Such a complete factorial experiment will enable us to evaluate both the lower and higher order effects of each variable. For example, if there are two variables, X_1 and X_2 , involved in a complete two-level factorial experiment, the experiment will require at least $2^2=4$ combinations. These four combinations will let us to evaluate not only the lower order effects due to X_1 and X_2 , but also the higher order effects due to X_1X_2 , X_1^2 and X_2^2 . Clearly, this type of experiment will only be possible to implement when the number of variables involved is small. But 16384 finite element models in this case is a huge number. Such a large experiment or finite element modeling analysis apart from being too expensive and impracticable in most situations, may not be at all necessary. Because the high order effects of each variable usually are insignificant and can be ignored(Dey, 1985). It is often true that if the lower order effect of one variable is insignificant, then the higher order effect due to the same variable can be neglected(Mukerjee, 1982). Therefore, to evaluate the lower order effects of each variable on an experiment will essentially explore all the possible effects of every variable, and will be far enough for the purpose of evaluating the significance of each variable that may have. Under this circumstance, only a subset of all possible

combination is needed in order to evaluate the lower order effect(Dey, 1985). Such a subset of all possible combination is called orthogonal experiment set(or design).

In order to find out the best experiment design or arrangement for finite element models to screen out the most important variables, a two level orthogonal factorial experiment design is used(Wang, 1977). For 14 variables selected for significance analysis, a 2-level 14 variable experiment design is shown in Table 5.2. In the table, 1 or 2 represents the number of levels that symbolizes the various values at which a variable is tested in the finite element model. In the design, the frequency of each level occurrence in any column is equal. In addition, there are all possible combinations in any two columns. Since the orthogonal experiment design has the above characteristics, the results from it are extremely simple to analyze, and can be directly used to determine which variable in the experiment has significant effect on the results. The 2-level orthogonal experiment is often used as variable selecting procedure because it requires the minimum experiment size or number of combinations. Based on this 2-level orthogonal experiment design(Table 5.2), a total of 16 finite element models are constructed for variable selecting purpose.

5.4 Finite Element Model

The models arranged by the orthogonal experiment design simulate a commonly used three-entry longwall layout(Fig.5.1) A typical 2-D finite element model is shown

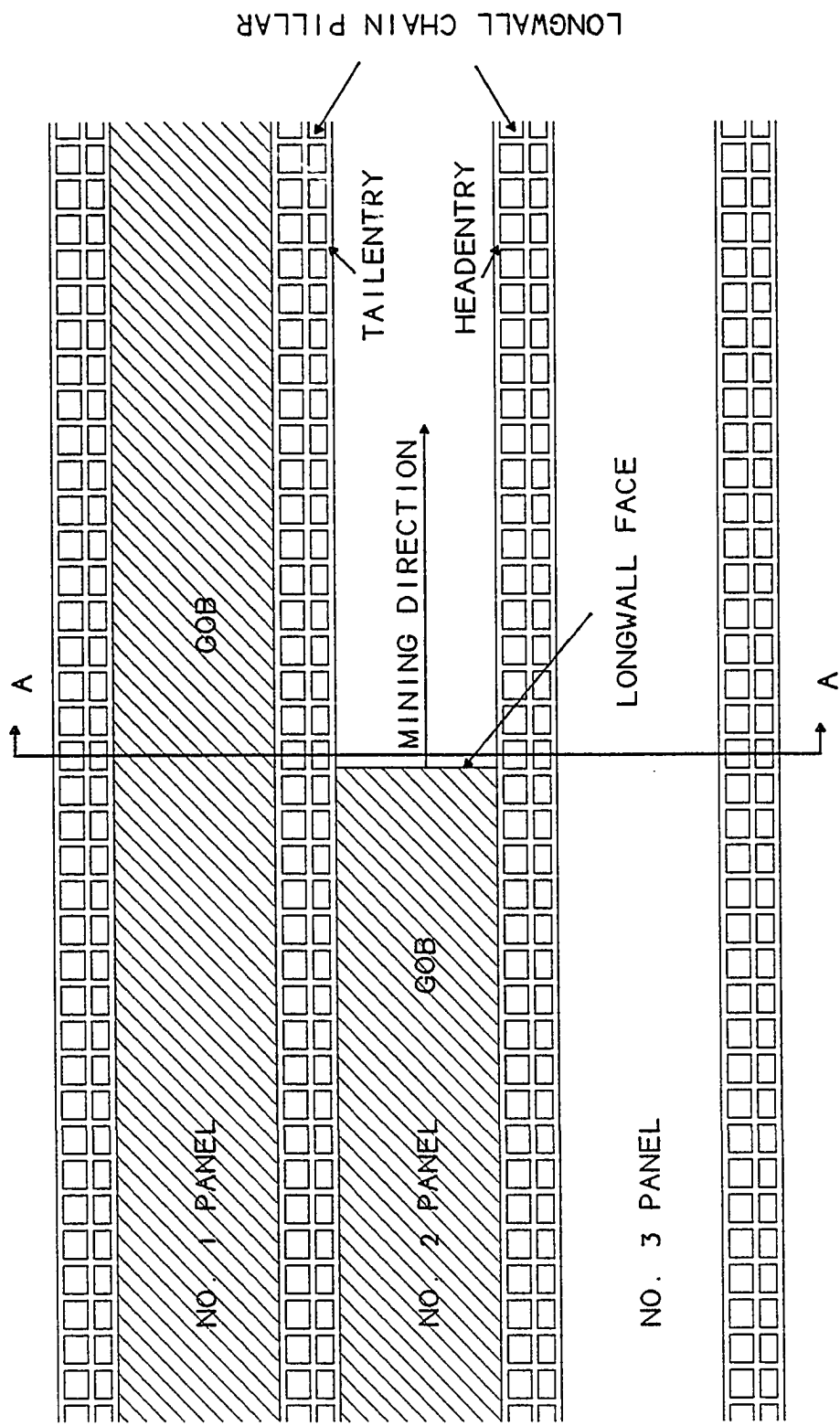


Figure 5.1. A typical longwall layout.

in Fig. 5.2. It simulates a geological cross-section A-A which is perpendicular to the mining direction and 10 to 20 ft. outby the second panel longwall face(Fig.5.1). In this cross-section, the tailentry pillars are under the most critical loading condition before the second panel passage. The pillars are subjected to the overburden load, the side abutment load due to the presence of the gob area in the first panel, and the front abutment load caused by longwall mining the second panel. Both the overburden load and side abutment load are automatically accommodated by the finite element model used in the study. To consider the front abutment load effect, a 3-D finite element model would be ideal. But due to the limitations imposed by the computer resources and the computing time, it is ineffective to do so. According to the empirical approach proposed by Mark(1990), the front abutment load can be represented in terms of the side abutment load, and is also indirectly related to overburden thickness. Assuming the pillar width equals to 0.08 times of overburden thickness and the front abutment factor is 0.7, then the front abutment load would cause about 1.3 times of overburden load increase in the pillars. In order to consider the front abutment load effect, an additional load which equals to one-half of overburden load was imposed on the top of the models for simulating the front abutment load effect in 2-D finite element models. The horizontal stress is also distributed at the right side nodal points as shown in Fig. 5.2. The gob effect has been considered by using the similar approaches described in previous chapter. A typical geological column used in finite element model analysis is

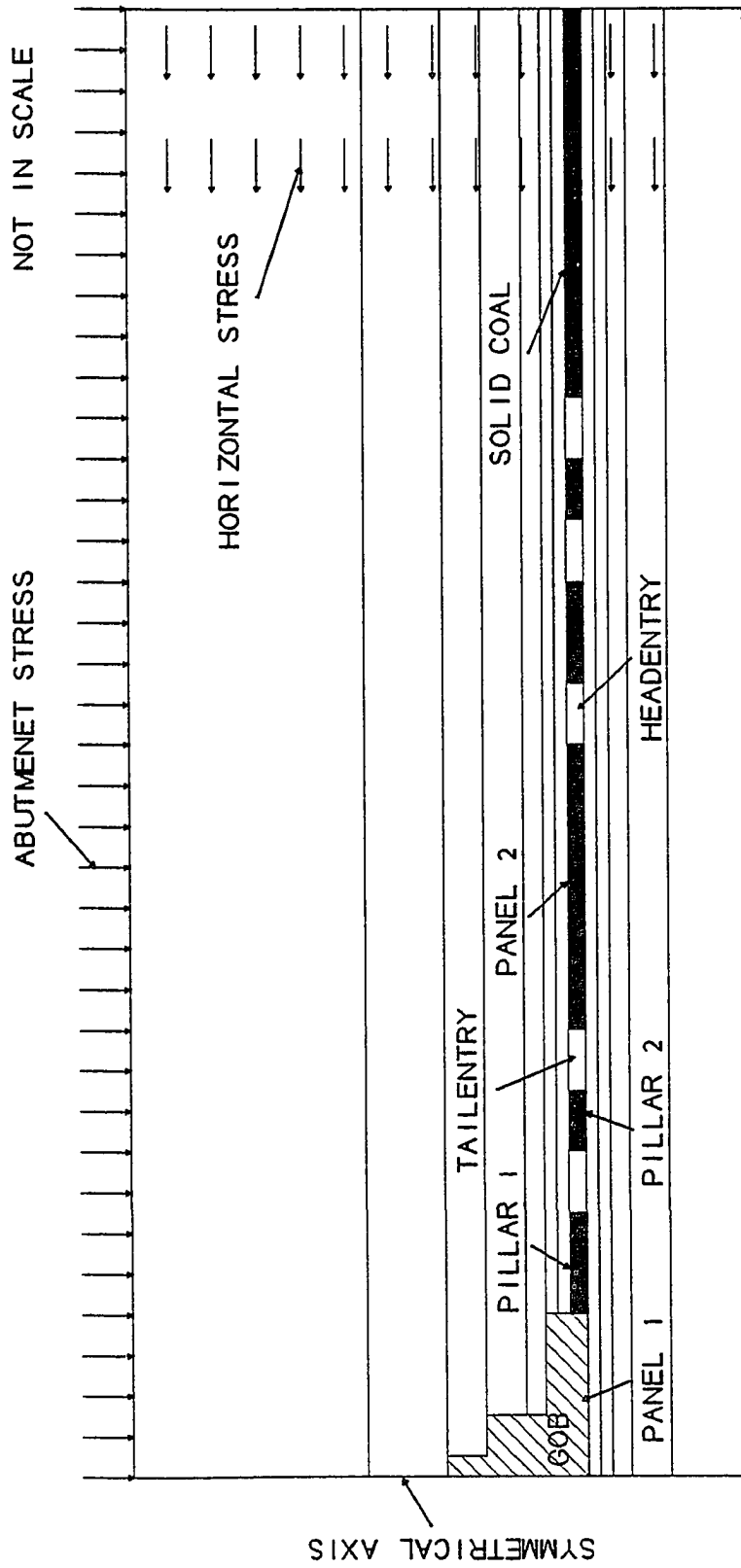


Figure 5.2. Cross-section A-A used in finite element analysis.

presented in Fig. 5.3. The roof strata in the model consist of 7 different layers with layer 3 and 4 representing the immediate roof, and 5 and 6 for the main roof. The floor also consists of 5 different layers. Layer 1 and 2 are the immediate floor. The material properties for each layer used in this study are listed in Table 5.3.

Table 5.3. Rock Mechanical Properties

Type of Rock	Young's Modulus (10 ⁶ psi)	Poisson's Ratio	Unit Weight (pcf)
Sandstone	3.0	0.228	170
Sandy Shale	2.5	0.300	165
Shale	2.0	0.158	160
Layer 4	varied	0.200	160
Layer 3	varied	0.200	160
Coal	varied	varied	80
Layer 2	varied	0.200	160
Layer 1	varied	0.200	160

In the models, the 14 variables were varied from Level 1 to Level 2 according to the orthogonal experiment design (Table 5.2). And the value of Level 1 and 2 for each variable was obtained from the data base established in Chapter 3, and listed in Table 5.4. They are the maximum and minimum values of each variable. Therefore, the variables were tested in their full range. The models have also considered the material nonlinearity and time dependent behavior. The same yield criteria and

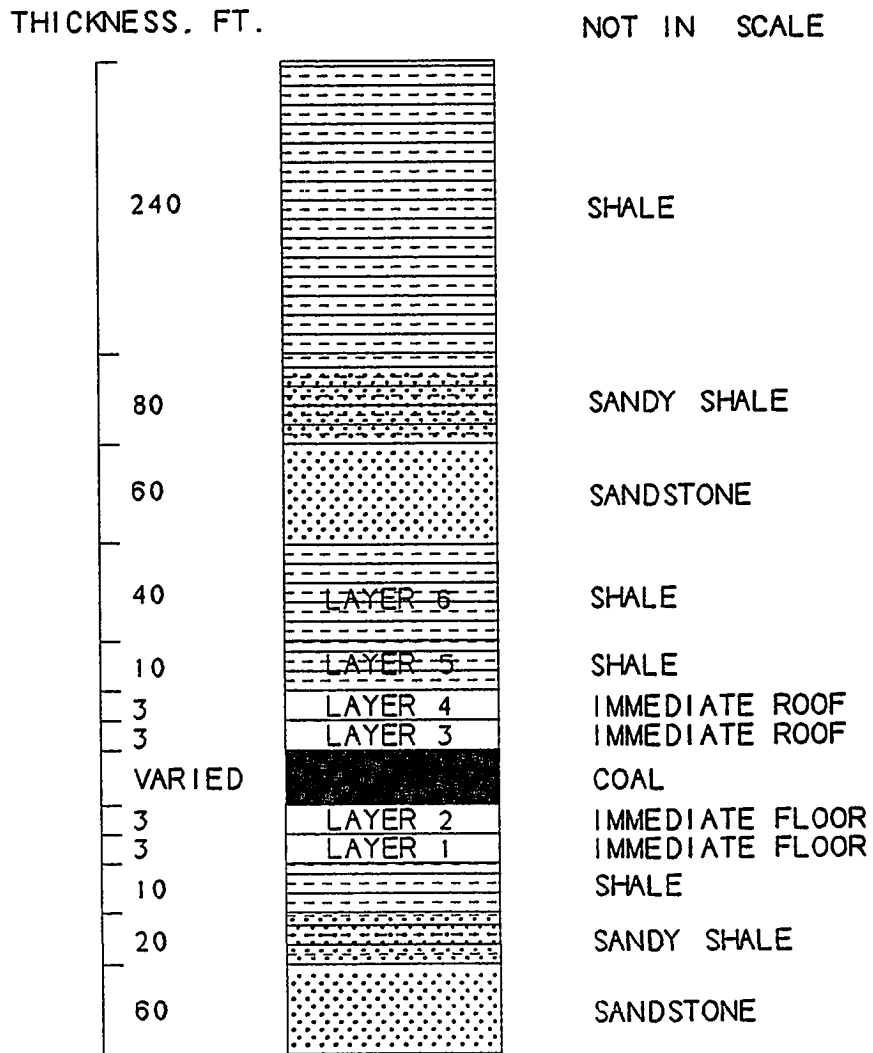


Figure 5.3. A typical geological column.

Table 5.4. Database for Finite Element Model Analysis

Variable	Unit	Level 2	Level 1	Average
E_f/E_c		10	0.5	5.25
E_f/E_c		10	0.5	5.25
W_e	ft	25	15	20
W_1	ft	150	10	80
W_2	ft	150	10	80
W_p	ft	1000	500	750
ϕ	degree	33	17	25.0
$h\gamma/C$		3.5	0.5	2.0
a_f		$3.291 \cdot 10^{-3}$	$2.736 \cdot 10^{-9}$	$1.646 \cdot 10^{-3}$
b_f		3.400096	1.867024	2.63356
d_f		1.867	0.050	0.959
H	ft	10	4.5	7.25
σ_b	psi	2000	500	1250
ν		0.44	0.2	0.2975

empirical creep Law as in the previous chapter are also used here.

5.5 Results and Discussion

5.5.1 Stability Indexes

In underground longwall mining, a stable entry-pillar system should ensure the stability of both entries and pillars in its system. Therefore, in order to evaluate the stability of an entry-pillar system the performances of both entries and pillars should be considered simultaneously. For this reason, yield zone in Pillar 1 and 2, and average safety factor of pillars were chosen as stability indices for evaluating the performance of pillars. While maximum entry convergence, maximum tensile stress in the entry roof and minimum safety factors of the immediate roof and floor are selected as the stability indices for examining stability conditions of the roof and floor in each of the model. A total of 7 indices were selected for significance analysis of the chosen variables. Hence, the results of the finite element modeling, in general, can be presented by a stability index matrix $[Y]$,

$$[Y] = \begin{bmatrix} y_{1,1} & y_{1,2} & \cdot & \cdot & \cdot & y_{1,m} \\ y_{2,1} & y_{2,2} & \cdot & \cdot & \cdot & y_{2,m} \\ \cdot & \cdot & \cdot & \cdot & \cdot & \cdot \\ \cdot & \cdot & \cdot & y_{i,k} & \cdot & \cdot \\ \cdot & \cdot & \cdot & \cdot & \cdot & \cdot \\ y_{n,1} & y_{n,2} & \cdot & \cdot & \cdot & y_{n,m} \end{bmatrix} \quad \begin{matrix} i=1,\dots,n \\ k=1,\dots,m \end{matrix} \quad (5.1)$$

where $y_{i,k}$ is the value of the k th stability index obtain from the i th finite element model. n is the number of models, m is the number of index. In this case, n and m are equal to 16 and 7, respectively. For example, when i is 1, then $y_{1,1}, y_{1,2}, \dots, y_{1,7}$ are the stability indices of Model 1. They are the finite element results on the yielded width of Pillar 1 and 2, maximum convergence, maximum tensile stress in the roof, minimum safety factor of roof and floor and average safety factor of pillars obtained from Model 1, respectively. Therefore, $[Y]$ represents the complete results of the 16 finite element model analysis. These indexes will be used to evaluate the effects of each variable.

5.5.2 Maximum Variance Analysis

To evaluate the effect of each of the 14 variables on the stability of the entry-pillar system in the 16 models, the directive evaluation method was selected. Table 5.5 summarizes the procedures of maximum variance analysis. In the table, $K_{l,k}^j$ denotes the summation of k th stability index at l th level due to j th variable.

$$K_{l,k}^j = \sum_{i=1}^n y_{i,k} \times p(o_{i,j}) \quad \begin{array}{l} p(o_{i,j}) = 1, \text{ if } o_{i,j} = l \\ p(o_{i,j}) = 0, \text{ if } o_{i,j} \neq l \end{array} \quad (5.2)$$

Where $o_{i,j}$ is the number of level at which the j th variable in the i th model is tested.

For example, $K_{1,1}^2 = y_{1,1} + y_{2,1} + y_{3,1} + y_{4,1} + y_{9,1} + y_{10,1} + y_{11,1} + y_{12,1}$. $G_{l,k}^j$

Table 5.5. Maximum Variance Analysis on the 2-Level Orthogonal Experiment Design with 14 Variables

Variable	1	2	3	4	5	6	7	8	9	10	11	12	13	14	Index
Model	E_r/E_c	E_r/E_c	W_c	W_1	W_2	ϕ	h ν /C	a_r	b_r	d_r	H	σ_h	ν	W_p	Y_{ij}
1	1	1	1	1	1	1	1	1	1	1	1	1	1	1	Y_{1j}
2	1	1	1	1	1	1	1	2	2	2	2	2	2	2	Y_{2j}
3	1	1	1	2	2	2	2	1	1	1	1	1	1	1	Y_{3j}
4	1	1	1	2	2	2	2	2	2	2	2	2	2	2	Y_{4j}
5	1	2	2	1	1	2	2	1	1	1	1	1	1	1	Y_{5j}
6	1	2	2	1	1	2	2	2	2	2	2	2	2	2	Y_{6j}
7	1	2	2	2	2	1	1	1	1	1	1	1	1	1	Y_{7j}
8	1	2	2	2	2	1	1	2	2	2	2	2	2	2	Y_{8j}
9	2	1	2	1	2	1	2	1	2	1	2	1	2	1	Y_{9j}
10	2	1	2	1	2	1	2	2	1	2	1	2	1	2	Y_{10j}
11	2	1	2	2	1	2	1	1	2	1	2	1	2	1	Y_{11j}
12	2	1	2	2	1	2	1	2	1	2	1	2	1	2	Y_{12j}
13	2	2	1	1	2	2	1	1	2	1	2	1	2	1	Y_{13j}
14	2	2	1	1	2	2	1	2	1	2	1	2	1	2	Y_{14j}
15	2	2	1	2	1	1	2	1	2	1	2	1	2	1	Y_{15j}
16	2	2	1	2	1	1	2	2	1	2	1	2	1	2	Y_{16j}
K_{1k}^{1k}	K_{1k}^{1k}	K_{1k}^{1k}	K_{1k}^{1k}	K_{1k}^{1k}	K_{1k}^{1k}	K_{1k}^{1k}	K_{1k}^{1k}	K_{1k}^{1k}	K_{1k}^{1k}	K_{1k}^{1k}	K_{1k}^{1k}	K_{1k}^{1k}	K_{1k}^{1k}	K_{1k}^{1k}	K_{1k}^{1k}
K_{2k}^{1k}	K_{2k}^{1k}	K_{2k}^{1k}	K_{2k}^{1k}	K_{2k}^{1k}	K_{2k}^{1k}	K_{2k}^{1k}	K_{2k}^{1k}	K_{2k}^{1k}	K_{2k}^{1k}	K_{2k}^{1k}	K_{2k}^{1k}	K_{2k}^{1k}	K_{2k}^{1k}	K_{2k}^{1k}	K_{2k}^{1k}
G_{1k}^{1k}	G_{1k}^{1k}	G_{1k}^{1k}	G_{1k}^{1k}	G_{1k}^{1k}	G_{1k}^{1k}	G_{1k}^{1k}	G_{1k}^{1k}	G_{1k}^{1k}	G_{1k}^{1k}	G_{1k}^{1k}	G_{1k}^{1k}	G_{1k}^{1k}	G_{1k}^{1k}	G_{1k}^{1k}	G_{1k}^{1k}
G_{2k}^{1k}	G_{2k}^{1k}	G_{2k}^{1k}	G_{2k}^{1k}	G_{2k}^{1k}	G_{2k}^{1k}	G_{2k}^{1k}	G_{2k}^{1k}	G_{2k}^{1k}	G_{2k}^{1k}	G_{2k}^{1k}	G_{2k}^{1k}	G_{2k}^{1k}	G_{2k}^{1k}	G_{2k}^{1k}	G_{2k}^{1k}
R_k^{1k}	R_k^{1k}	R_k^{1k}	R_k^{1k}	R_k^{1k}	R_k^{1k}	R_k^{1k}	R_k^{1k}	R_k^{1k}	R_k^{1k}	R_k^{1k}	R_k^{1k}	R_k^{1k}	R_k^{1k}	R_k^{1k}	R_k^{1k}

denotes the mean of the k th index at the l th level due to the j th variable.

$$G_{l,k}^j = \frac{2 \times K_{l,k}^j}{n} \quad (5.3)$$

Therefore, the effect of the j th variable on the k th index is estimated by the maximum variance between $G_{1,k}^j$ and $G_{2,k}^j$, and is defined by the following equation;

$$R_k^j = \max(G_{1,k}^j, G_{2,k}^j) - \min(G_{1,k}^j, G_{2,k}^j) \quad (5.4)$$

where R_k^j is the maximum variance of the k th index caused by variation of the j th variable. The larger the value of R_k^j , the more significant the effect of the j th variable on the k th index is. Since the indices have different units the maximum variance of each index is normalized for comparison:

$$SR_k^j = \frac{R_k^j}{\sum_{j=1}^{14} R_k^j} \quad (5.5)$$

Where SR_k^j is standardized maximum variance. Therefore, the effect of each variable on each index can be evaluated by the standardized maximum variance. According to the standardized maximum variance analysis, the yield zone in Pillar 1 is mainly affected by $h\gamma/C$, the width of Pillar 1 and entry (Fig. 5.4). In contrast, the yield zone in Pillar 2 is mainly affected by the width of Pillar 2, $h\gamma/C$, and E_t/E_c (Fig. 5.5). Considering the maximum entry convergence, it is mainly affected by $h\gamma/C$, entry width and widths of

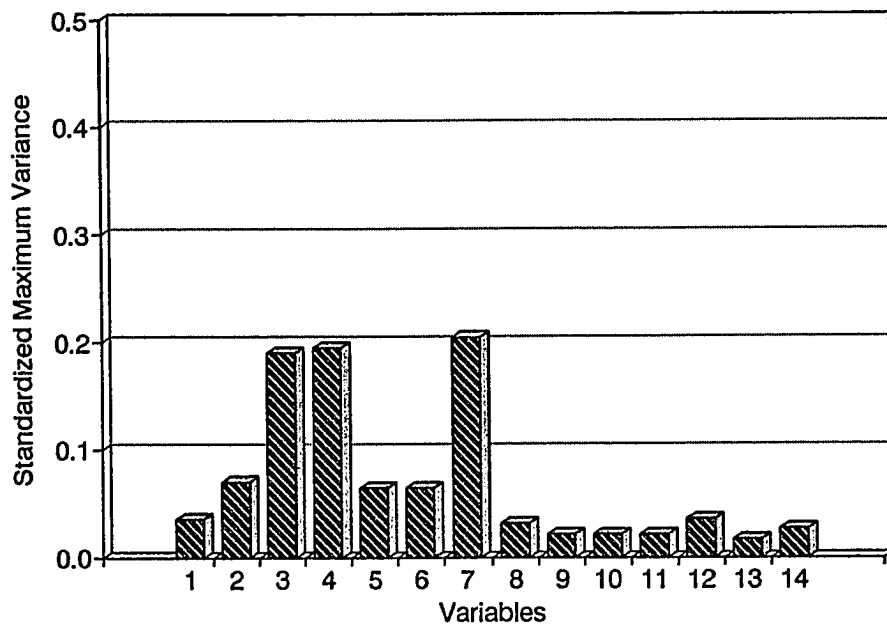


Figure 5.4. Effect of variable on yield zone in Pillar 1.

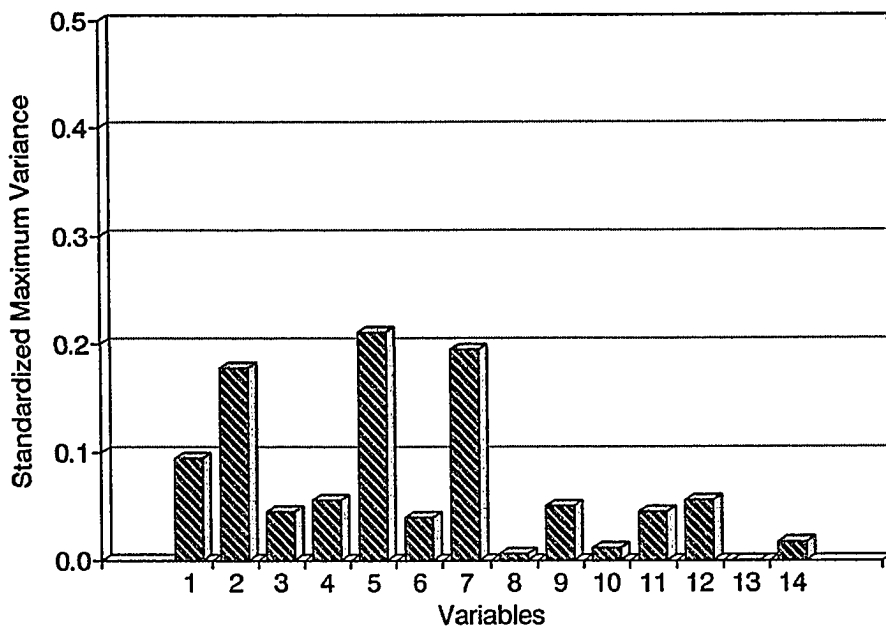


Figure 5.5. Effect of variable on yield zone in Pillar 2.

both pillars(Fig. 5.6) while the maximum tensile stress in entry roof is mainly controlled by $h\gamma/C$, E_r/E_c , the widths of the pillars and entry(Fig. 5.7). The minimum safety factors of roof and floor and average safety factor of pillar are mainly governed by $h\gamma/C$, E_r/E_c , E_r/E_c and pillar width(Figs. 5.8 to 5.10).

The overall effect of each variable on the stability of the entry-pillar system is evaluated by an overall standardized maximum variance which is defined as the summation of the standardized maximum variances of each variable on seven stability indices.

$$R^j = \sum_{k=1}^7 SR_k^j \quad (5.6)$$

R^j represents the effect of the j th variable on all seven stability indices. The overall maximum variance is presented in Fig.5.11. The significance of each variable on the stability of the entry-pillar system is in the following order.

$$\frac{h\gamma/C \quad E_r/E_c \quad W_1 \quad W_2 \quad E_r/E_c \quad W_c \quad \phi \quad \sigma_h \quad W_p \quad H \quad b_r \quad a_r \quad v_c \quad d_r}{\text{Significance Decreasing} \rightarrow}$$

If the overall effect on the entry-pillar system by these 14 variables is equal to 100%, then the former seven variables contribute 85.9%, the next three variables contribute 9%, and the last 4 variables contribute only has 5.1%. Up to this point, it can be concluded that the stability condition of the entry-pillar system is mainly controlled by $h\gamma/C$, E_r/E_c , W_1 , W_2 , W_c , E_r/E_c and ϕ . The horizontal stress(σ_h), panel width(W_p) and mining height(H) also have significant effect on the stability of the entry-

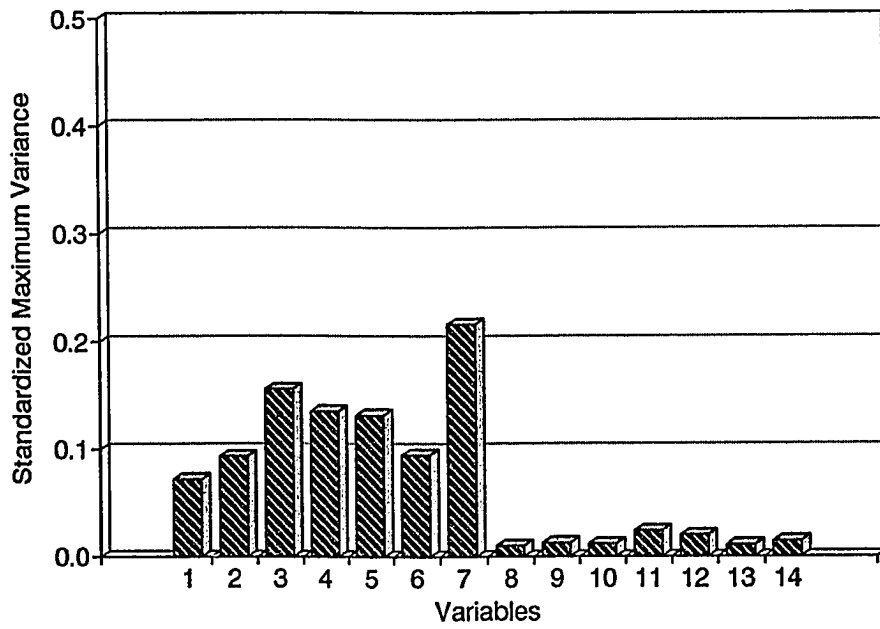


Figure 5.6. Effect of variable on the maximum entry convergence in the entry-pillar system.

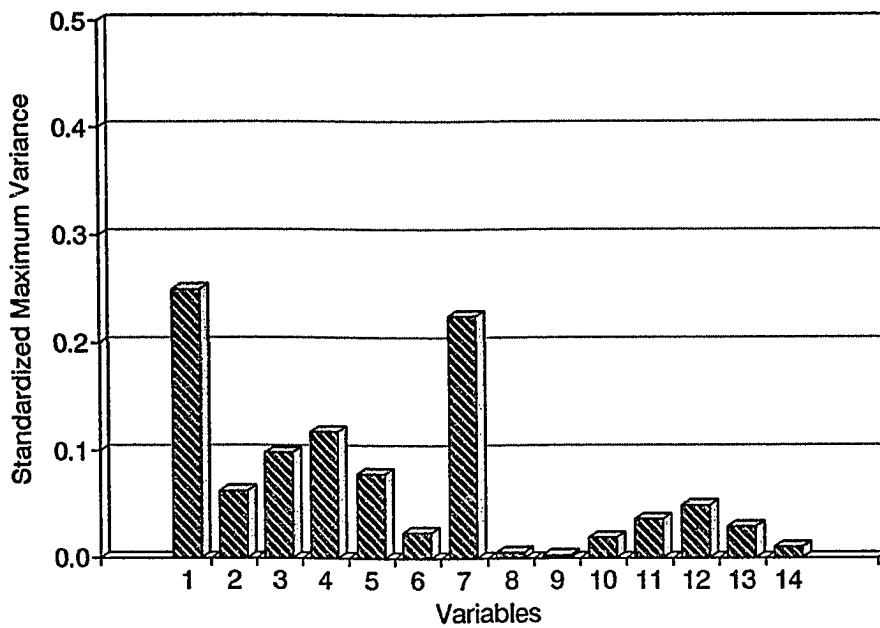


Figure 5.7. Effect of variable on the maximum roof tensile stress in the entry-pillar system.

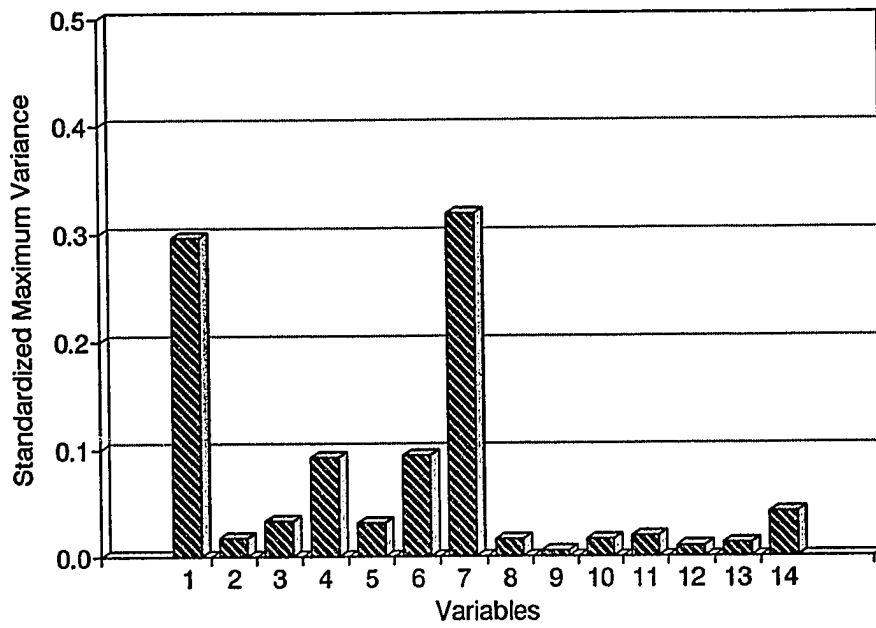


Figure 5.8. Effect of variable on the minimum safety factor of the roof.

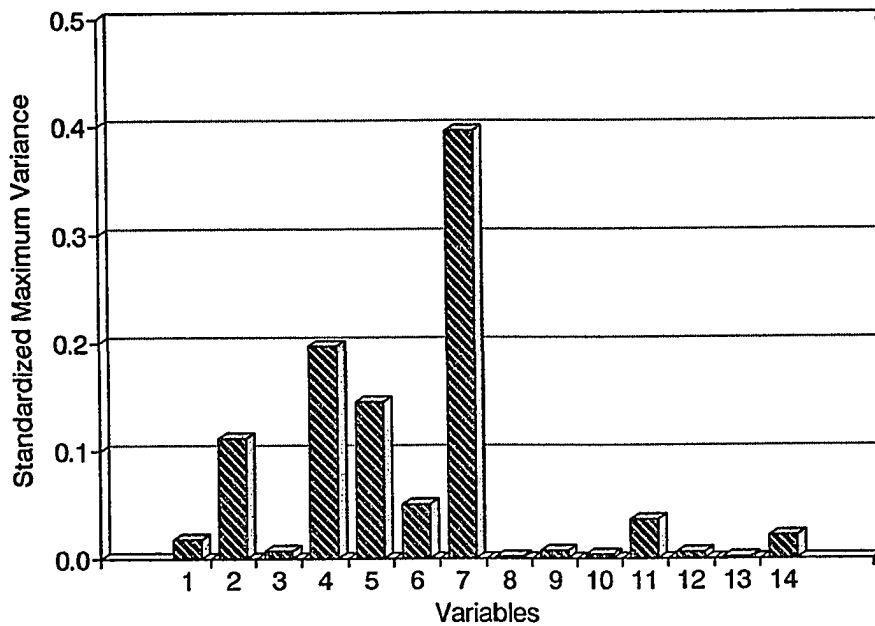


Figure 5.9. Effect of variable on the minimum safety factor of the floor.

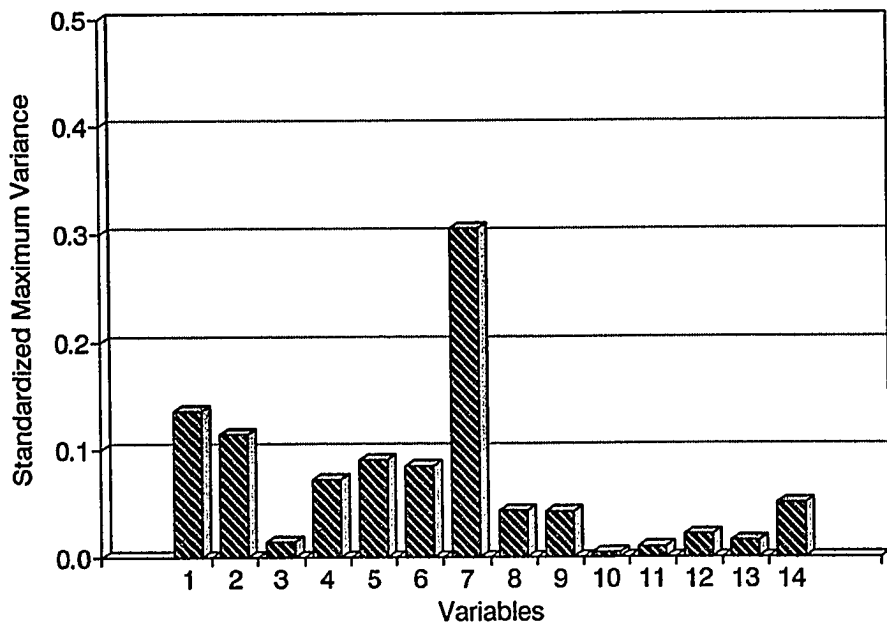


Figure 5.10. Effect of variable on average safety factor of pillars.

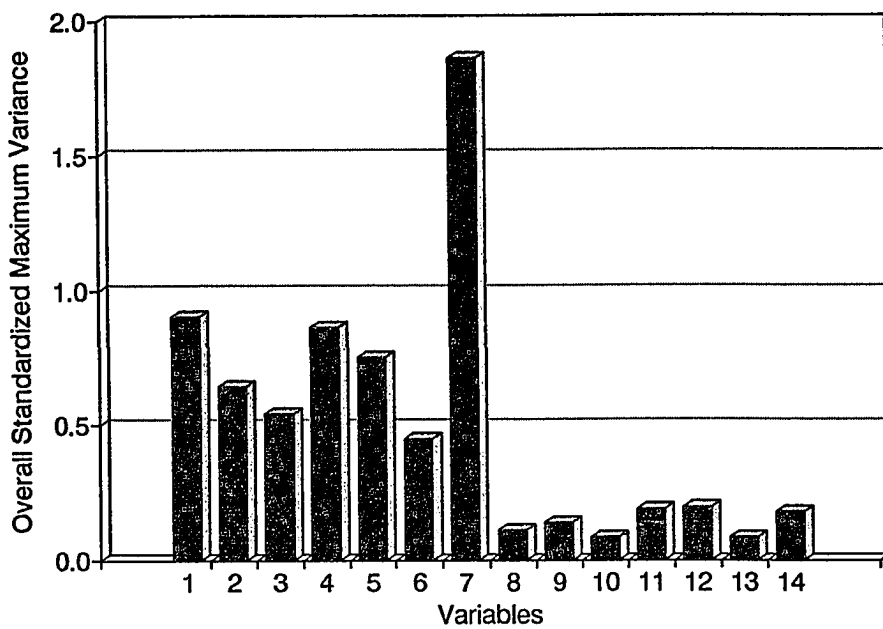


Figure 5.11. Effect of variable on overall stability of the entry-pillar system

pillar system while the effects due to the creep constants of the floor rock(a_f , b_f , and d_f) and Poisson's ratio of coal(ν) are insignificant. Therefore, a_f , b_f , d_f , and ν can be ignored in the later finite element modeling. These results provide the scientific bases for screening and selection of variable and also confirm previous investigations by others(Table 5.1). Based on this result, the following 10 variables, $h\gamma/C$, E_f/E_c , W_1 , W_2 , W_c , E_f/E_c , ϕ , σ_h , W_p and H are selected as the most important variables that will dictate the performance of longwall entry-pillar system. Therefore, the consideration of these variables in the later FEM modeling is essential. By reducing the four insignificant variables from the variables initially selected, it cuts down tremendously the number of finite element models needed for the development of pillar design formula later.

CHAPTER 6

DEVELOPMENT OF NEW PILLAR DESIGN METHOD

6.1 Introduction

A number of pillar design formulae derived from both numerical modeling and empirical study(Chapter 2) are available. Based on the conventional pillar design concept, the design formulae were developed for stiff pillar design only. Moreover, most of the formulae consider the stability of pillar only. Therefore, those formulae can not be used to design a yield pillar for longwall entry-pillar system without further modification.

As demonstrated earlier(Chapter 5), the stability of a longwall entry-pillar system is mainly affected by pillar loading and pillar strength(i.e., $h\gamma/C$, σ_b , ϕ_c , and W_p), the geometry of the entry-pillar system(W_1 , W_2 , and W_c) and the roof and floor conditions encountered in the mine(E_r/E_c , and E_f/E_c). The design of an entry-pillar system should consider these important variables in order to ensure the stability of entries and pillars in the system, especially when a yield pillar is adopted in the system. The design criteria for an entry-pillar system can also vary with the roof and floor conditions based on the discussion of the mechanisms of yield pillar(Chapter 4). In this chapter, new pillar design formulae are proposed by considering each type of roof and floor conditions categorized in Chapter 3.

6.2 3-Level Orthogonal Experimental Design for Finite Element Modeling

The discussion in the previous chapters demonstrates that the stability of an entry-pillar system is affected by both geological and mining conditions, mainly the following ten variables: the ratio of overburden load to coal strength($h\gamma/C$), the ratios of Young's modulus of roof to coal(E_r/E_c) and floor to coal(E_f/E_c), the widths of pillar and entry(W_1 , W_2 and W_c), the internal friction angle of coal(ϕ_c), horizontal stress(σ_h), panel width(W_p) and mining height(H). From the mechanics point of view, failure of an entry-pillar system is always initiated at the most critically stressed region, the location of which also varies with different roof and floor conditions. For example, under the strong roof and strong floor condition, i.e., Category 1, pillars are usually under the critical compressive stress, while entry roof is often under critical tensile stress. In contrast, under the strong roof and weak floor condition, besides the pillar and roof, the floor may also be under critically stressed condition. Therefore, to develop the design formulae for yield pillar, it is necessary to analyze the stability condition of an entry-pillar system under each type of roof and floor condition. This will simplify the stability analysis involved in this study. Based on the stability analysis, the design formulae can be established for each type of roof and floor condition.

According to the classification scheme developed in Chapter 3, there are four types of roof and floor conditions; 1) strong roof and strong floor condition, 2) strong roof and weak floor condition, 3) weak roof and strong floor condition, and 4) weak

roof and weak floor condition. To analyze the stability condition of an entry-pillar system, the ten variables have been considered in each category although the effects of each variable on the stability of an entry-pillar system may vary under different roof and floor conditions. In order to establish the design formulae, each variable has to be evaluated at least at three levels or values, e.g., the maximum, mean and minimum values. A complete factorial experiment design for such study would mean testing $3^{10} = 59049$ combinations of these ten variables, or finite element models in just one simple replicate. Such a huge number of experiment is simply impossible to implement. In order to find out the best experiment design or arrangement of the finite element models for these ten variables, the orthogonal experiment design method was chosen once again. According to the theory, a total of 27 finite element models is need for an orthogonal experimental design with 10 variables at 3 levels(Wang, 1977). Table 6.1 illustrates the detailed experimental plan. In the table, 1, 2 or 3 is the number of level that symbolizes the various value at which a variable is tested in a finite element model. In this case, 1, 2 and 3 represent the minimum, the average and the maximum value of each variable, respectively. For the four types of roof and floor conditions, a total of $27 \times 4 = 108$ finite element models are required for implementation of stability analysis. Within each type of roof and floor condition, each variable is evaluated in full range using the data base established earlier(Chapter 3).

The finite element models used in this part of the study are similar to those used

Table 6.1. 3-level Orthogonal Experiment Design for 10 Variables

Variable	1	2	3	4	5	6	7	8	9	10
Model	E_r/E_c	E_t/E_c	W_c	W_1	W_2	ϕ	$h\gamma/C$	H	σ_b	W_p
1	1	1	1	1	1	1	1	1	1	1
2	1	1	1	1	2	2	2	2	2	2
3	1	1	1	1	3	3	3	3	3	3
4	1	2	2	2	1	1	1	2	2	2
5	1	2	2	2	2	2	2	3	3	3
6	1	2	2	2	3	3	3	1	1	1
7	1	3	3	3	1	1	1	3	3	3
8	1	3	3	3	2	2	2	1	1	1
9	1	3	3	3	3	3	3	2	2	2
10	2	1	2	3	1	2	3	1	2	3
11	2	1	2	3	2	3	1	2	3	1
12	2	1	2	3	3	1	2	3	1	2
13	2	2	3	1	1	2	3	2	3	1
14	2	2	3	1	2	3	1	3	1	2
15	2	2	3	1	3	1	2	1	2	3
16	2	3	1	2	1	2	3	3	1	2
17	2	3	1	2	2	3	1	1	2	3
18	2	3	1	2	3	1	2	2	3	1
19	3	1	3	2	1	3	2	1	3	2
20	3	1	3	2	2	1	3	2	1	3
21	3	1	3	2	3	2	1	3	2	1
22	3	2	1	3	1	3	2	2	1	3
23	3	2	1	3	2	1	3	3	2	1
24	3	2	1	3	3	2	1	1	3	2
25	3	3	2	1	1	3	2	3	2	1
26	3	3	2	1	2	1	3	1	3	2
27	3	3	2	1	3	2	1	2	1	3

in Chapter 5(Fig. 5-2). The models simulate a commonly used three-entry longwall system. Entry cross-cut is 100 ft-wide. To consider the most critical loading condition for the tail-entries and pillars an additional load is imposed on top of the models to simulate the front abutment load effect. The additional load equals to one-half of the overburden load. The boundary conditions and the reduction factors for gob materials are the same as those used in Chapter 5.

The models have also taken the material nonlinearity behavior into considerations. The yield criterion is the same as those in previous chapters. The time-dependent behavior of material was not considered in this part of the study mainly because they have limited effects on the stability of entry-pillar system(Chapter 5), and there is only a very small database available. The stability analysis is performed under each type of roof and floor condition. Based on the results of the stability analysis, yield pillar design formulae are proposed for each type of roof and floor condition.

6.3 The Strong Roof and Strong Floor Condition

6.3.1 Introduction

The strong roof and strong floor condition are encountered mostly by coal producers in U. S. underground coal mines. According to the 3-level orthogonal experiment design(Table 6.1), a total of 27 finite element models was planned. The input data are listed in Table 6.2. The material properties of roof and floor were

Table 6.2. Database for Finite Element Modeling under Strong Roof and Strong Floor Condition

Variable	Unit	Data Range		
		Level 1	Level 2	Level 3
E_f/E_c		2	6	10
E_f/E_c		2	6	10
W_c	ft	15	20	25
W_1	ft	10	80	150
W_2	ft	10	80	150
ϕ	degree	20	25	30
$h\gamma/C$		1	2	3
H	ft	4.5	7.25	10
σ_h	psi	500	1250	2000
W_p	ft	500	750	1000

selected from a database that consists of material properties of strong rocks as defined by the classification system proposed in Chapter 4.

6.3.2 Regression Model

Based on the variable arrangement defined in Table 6.1, the finite element model analysis was performed on WVNET mainframe computer by using MSC NASTRAN program. According to the stability analysis, entry roof and pillars are very often under the most critically stressed condition. The stability of the entry-pillar system under strong roof and floor condition essentially depends on the stability conditions of the entry roof and pillars in the system. From pillar design point of view, the key to ensure the stability of an entry-pillar system under strong roof and strong floor condition is to examine whether the tensile stress in the roof will exceed the tensile strength of the roof and if pillars in the system will be stable. Therefore, if relationships between the entry stability conditions and control variables can be established under strong roof and strong floor condition, a stable entry-pillar system can be designed. In order to establish such relationships, nonlinear regression analysis was performed on the WVNET mainframe computer by using SAS software(SAS Institute, 1985). Throughout the regression analysis, the following regression equations are obtained.

$$W_1 = \left(\frac{C}{h}\right)^{-0.4048} (52.7884SF_1 - 15.4181SF_2 + 0.0005HW_p) \quad (6.1)$$

$$W_2 = \left(\frac{C}{h}\right)^{-0.5581} (44.9214SF_2 - 23.1242SF_1 + 0.0005HW_p) \quad (6.2)$$

$$T_r = h^{0.7454} \left(\frac{2.9877}{\sqrt{W_1}} + \frac{1.0168}{\sqrt{W_2}} + 2.8 \times 10^{-9} W_e E_r \right) \quad (6.3)$$

Where W_1 and W_2 are pillar widths for pillar 1 and 2, respectively, T_r is the maximum tensile stress in the roof, SF_1 and SF_2 are the safety factors for pillar 1 and pillar 2 in the entry-pillar system, respectively, C is the cohesion strength of the coal, h is the depth of cover, W_e is entry width, W_p is panel width, E_r is Young's modulus of the immediate roof, H is mining height, and all numerical constants in the equations are regression constants. The R-square is 0.968, 0.979 and 0.991 for Eqs.6.1, 6.2 and 6.3, respectively. Equations 6.1 and 6.2 describe the relationships between pillar width, safety factor and other important control variables, while Equation 6.3 relates the maximum tensile stress in the roof to pillar width, entry width and Young's modulus of the roof. For the design of a three-entry pillar system, one can use known material properties and select safety factors of pillars to determine the pillar width according to Equations 6.1 and 6.2. After determining the initial pillar widths the maximum tensile stress in the roof can be calculated by Eq. 6.3 and compared with the tensile strength of the roof. If the stress in the roof is less than its strength, the pillar widths are

suitable. If not, roof tensile failure is very likely to occur in the entries. To ensure the stability of roof, the pillar widths have to be enlarged by adjusting safety factors of the pillars until the tensile stress in the roof is less than its strength. Sometimes, several iterations are needed in order to determine the most suitable pillar size.

6.3.3 Design of Three-Entry system under Strong Roof and Strong Floor Condition

Obviously, there is no unique solution to the entry-pillar system design for underground longwall panel. Rather there are several solutions or options to the problems. For a three-entry longwall system, there are three types of design based on the pillars used in the system; 1) stiff-stiff pillar design(Figure 6.1), 2) yield-yield pillar design(Figure 6.2), and 3) combination of a stiff and a yield pillar design(Figure 6.3). For the combination of a stiff and a yield pillar design, it can be divided further into stiff-yield(Fig. 6.3a) or yield-stiff(Fig. 6.3b) pillar design by changing the location of the yield pillar. According to the finite element results, when the average safety factor of a pillar was less than 1.0, but larger than 0.85, the pillar yielded substantially, but still sustained the loading and could survive after the longwall mining. When the average safety factor of a pillar was less than and equal to 0.85, the pillar became unstable. It could not provide adequate support to the roof and eventually failed during the longwall mining. If a pillar had an average safety factor larger than 1.0, the pillar would provide adequate support to the roof and could be considered as a stiff pillar. By considering

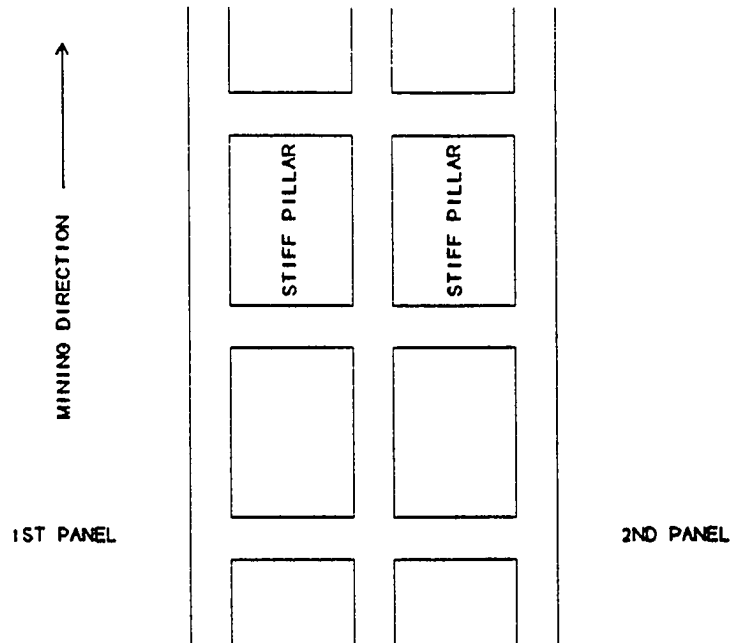


Figure 6.1. Stiff-stiff pillar design.

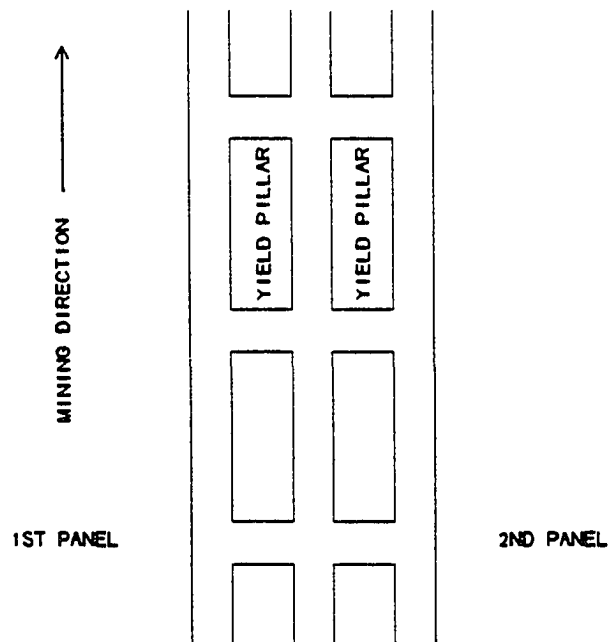
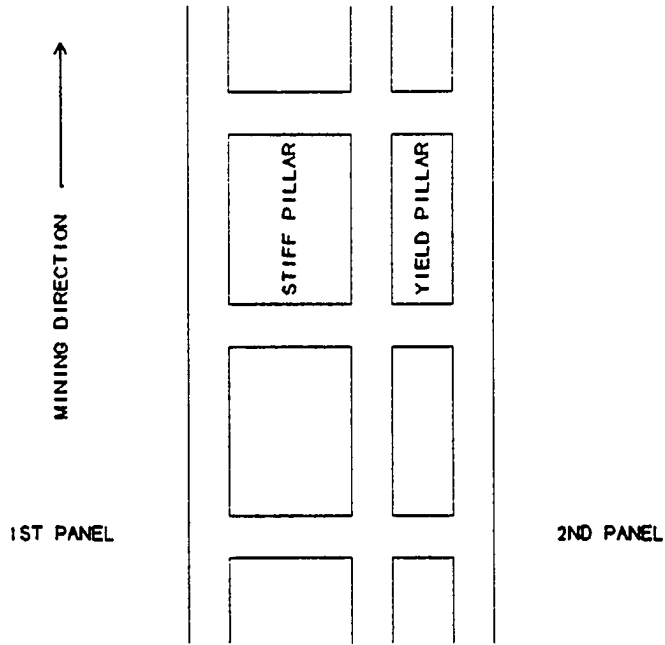
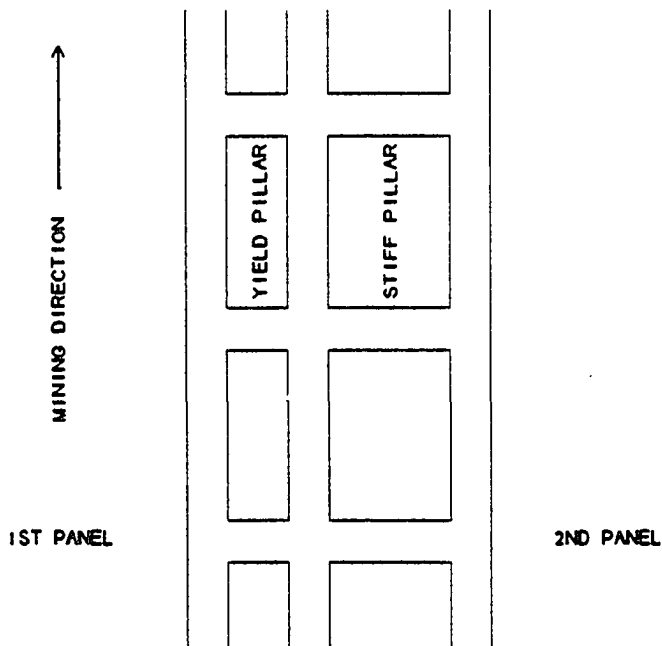


Figure 6.2. Yield-yield pillar design.



(a) Stiff-yield pillar design.



(b) Yield-stiff pillar design.

Figure 6.3. Combinations of a stiff and a yield pillar design.

the stability of pillars alone, a safety factor of 1.5 and 0.9 is recommended for stiff and yield pillar, respectively, in both the stiff-yield and yield-stiff pillar designs. For the stiff-stiff pillar design, a safety factor of 1.3 is suggested for both pillars. A safety factor of 0.9 is recommended for both yield pillars in the yield-yield pillar design. On the other hand, whether the designed pillars are suitable for an entry-pillar system will depend on the stability of entry roof also. After determining the pillar widths, the maximum tensile stress in the roof can be calculated by Eq. 6.3. If the maximum tensile stress in the roof is less than the tensile strength of the roof, the pillar widths determined from Eqs. 6.1 and 6.2 can be recommended. Based on these criteria, different pillar size can be recommended according to different type of design of entry-pillar system. The question is then which is the best type of design? To answer this question, the total pillar width and the maximum tensile stress in the roof from the four types of pillar designs are compared with each other. Table 6.3 shows the input data for comparison study.

A 900 psi uniaxial coal strength and 30° degree internal friction angle were used in the calculation. In addition, the entry width was 20 ft. and Young's modulus of the roof was equal to 4.5×10^6 psi. The longwall panel was 800-ft wide, seam height was 6 ft. A safety factor of 1.5 and 0.9 was assigned to stiff and yield pillar, respectively. In general, the stiff-yield pillar design has a smaller total pillar width than the yield-stiff pillar design(Fig. 6.4). The maximum tensile stress in the roof is also lower for the stiff-yield pillar design than the yield-stiff pillar design(Fig. 6.5). Therefore, the stiff-yield

pillar design has more advantages than the yield-stiff pillar design in terms of roof stability and maximizing coal recovery.

Table 6.3. Input Data for Comparison Study under Strong Roof and Strong Floor Condition

Variable	Level Used (Unit)
Mining height, H	6 (ft)
Uniaxial Compressive Strength of Coal, S_1	900 (psi)
Internal friction angle of coal, ϕ	30°
Cohesion strength of coal, C	260 (psi)
Young's modulus of roof, E_r	4.5 x 10 ⁶ (psi)
Young's modulus of floor, E_f	4.5 x 10 ⁶ (psi)
Horizontal stress, σ_h	500 (psi)
Entry width, W_e	20 (ft)
Longwall panel width, W_p	800 (ft)
Safety factors of pillars	according to recommendation

Figures 6.6 and 6.7 show total pillar width and maximum tensile stress in the roof in the stiff-stiff, the yield-yield and the stiff-yield pillar designs. The safety factor of pillar used in the calculations was the same as recommended previously. The total pillar width of the stiff-stiff design is the largest in all three types of design, while the maximum tensile stress in the roof is the smallest. Usually, the stiff-stiff pillar design has a higher safety factor for its pillar and provides the best protection to the entry roof. On the other hand, both the stiff-yield and the yield-yield pillar designs have a narrower

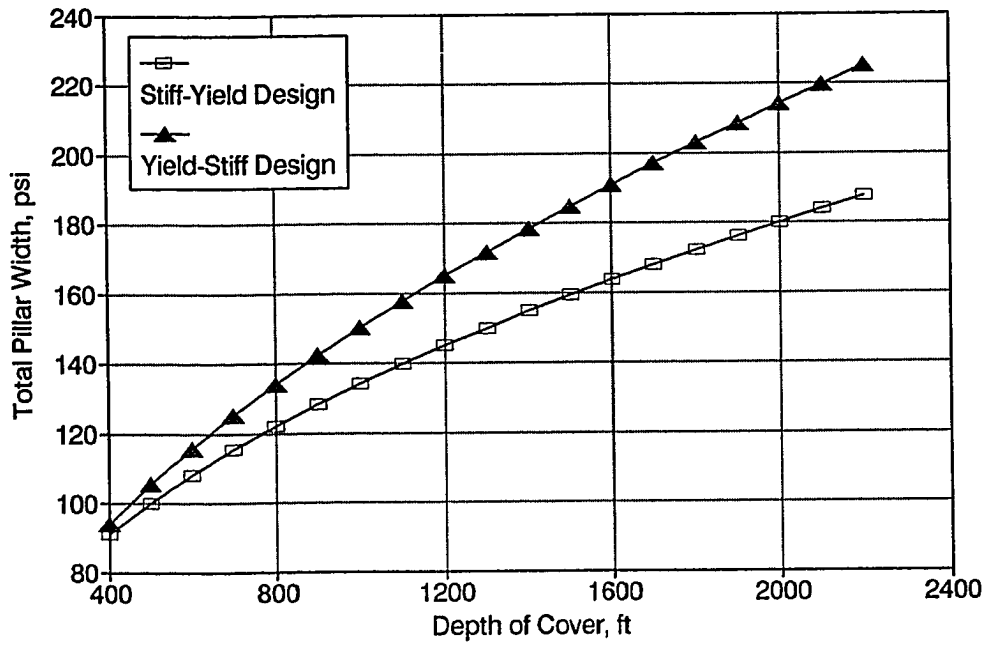


Figure 6.4. Total pillar width vs depth of cover for both stiff-yield and yield-stiff pillar designs under strong roof and strong floor condition.

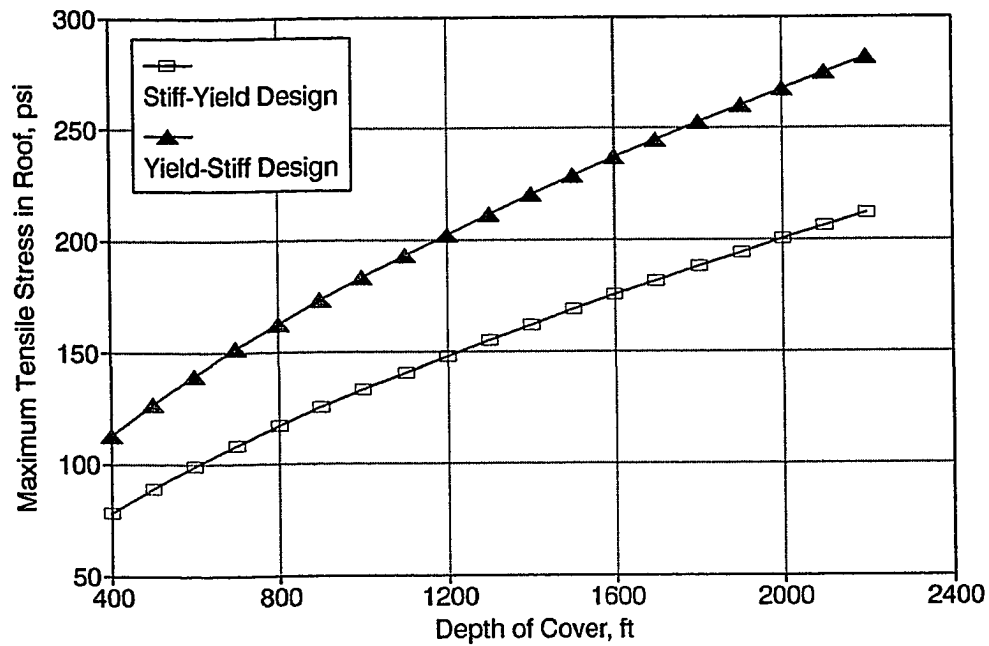


Figure 6.5. Maximum tensile stress in roof vs depth of cover for both stiff-yield and yield-stiff pillar designs under strong roof and strong floor condition.

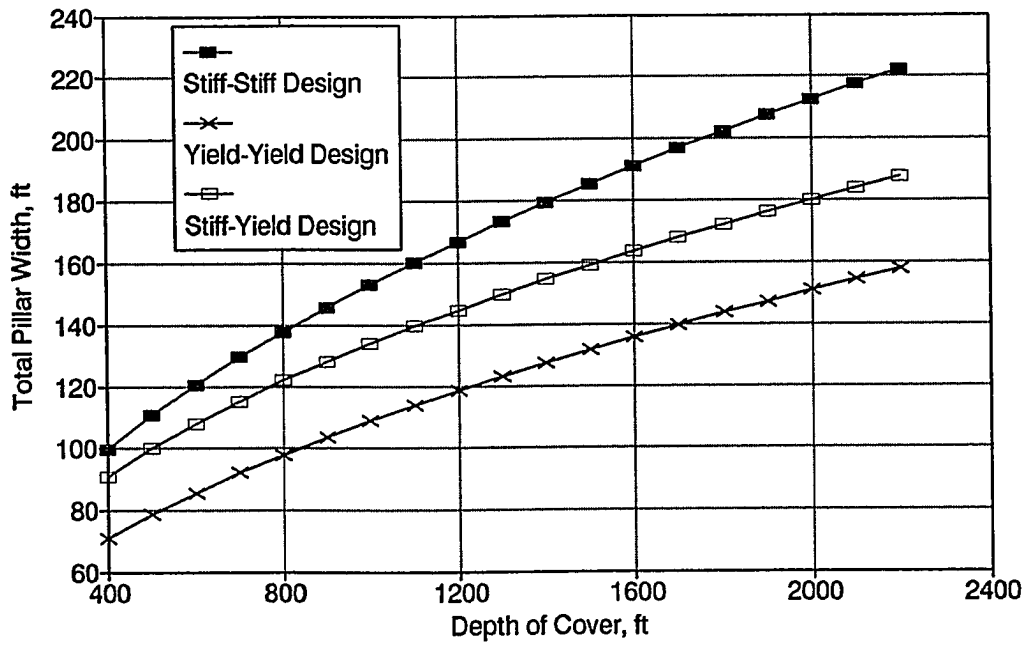


Figure 6.6. Total pillar width vs depth of cover for stiff-stiff, yield-yield and stiff-yield pillar designs under strong roof and strong floor condition.

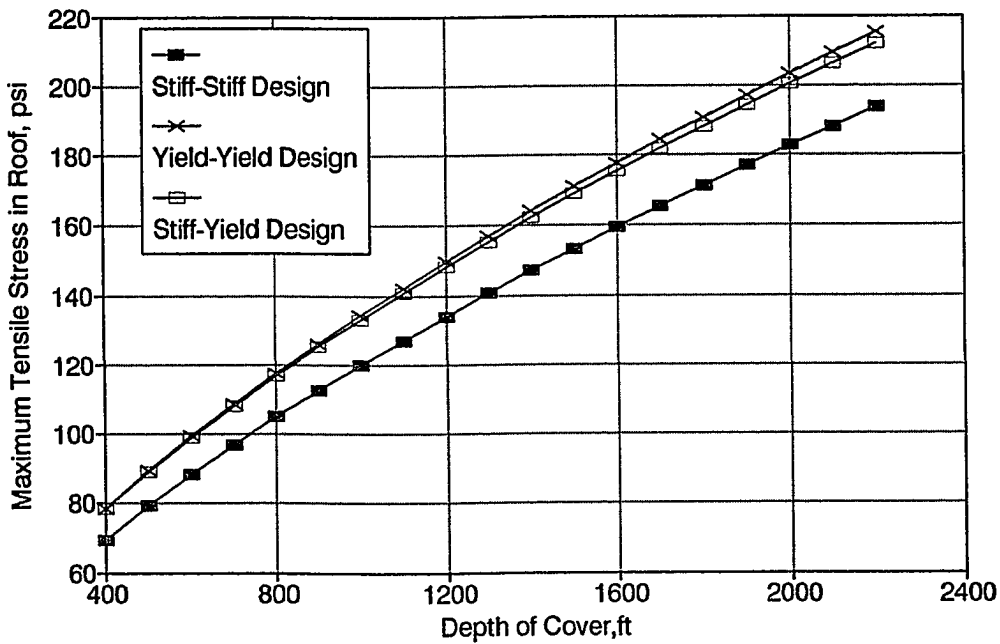


Figure 6.7. Maximum tensile stress in roof vs depth of cover for stiff-stiff, yield-yield and stiff-yield pillar designs under strong roof and strong floor condition.

total pillar width. The yield-yield pillar design has the smallest total pillar width but the highest tensile stress in the roof. Under strong roof and strong floor condition, the stiff-yield pillar design appears to be a little more conservative than yield-yield pillar design in terms of the maximum tensile stress in the roof and the total pillar width. There is a possibility that all three designs are suitable under the strong roof and strong floor condition. But the selection of a particular design over the others will depend on the roof condition, i.e., the maximum tensile stress should be less than its tensile strength. An optimum design, therefore, should ensure roof stability and maximize coal recovery at the same time.

6.4 The Strong Roof and Weak Floor Condition

6.4.1 Introduction

The strong roof and weak floor condition is very often encountered in the U. S. underground coal mines. Based on the same principle used in the strong roof and strong floor condition, a total of 27 finite element models were planned according to the Table 6.1. The only thing which is different from the strong roof and strong floor condition is input data for weak floor strata (Table 6.4), and the material properties of the weak floor strata were much lower than the strong roof strata.

Table 6.4. Database for Finite Element Modeling under Strong Roof and Weak Floor Condition

Variable	Unit	Data Range		
		Level 1	Level 2	Level 3
E_f/E_c		2	6	10
E_f/E_c		0.5	1	1.5
W_e	ft	15	20	25
W_1	ft	10	80	150
W_2	ft	10	80	150
ϕ	degree	20	25	30
$h\gamma/C$		1	2	3
H	ft	4.5	7.25	10
σ_h	psi	500	1250	2000
W_p	ft	500	750	1000

6.4.2 Regression Model

Once again the finite element model analysis was performed on WVNET mainframe computer by using MSC NASTRAN program. The stability analysis indicates that the stabilities of floor and pillar are crucial to the stability of the entry-pillar system under strong roof and weak floor condition. In addition, the roof tensile stress may cause roof tensile failure. Therefore, the regression equations were established to evaluate stability conditions of the roof, pillars and floor. Nonlinear regression were performed on the mainframe computer by using SAS software package. The following regression equations were obtained.

$$W_1 = \left(\frac{C}{h}\right)^{-0.4162} (57.1280SF_1 - 24.9814SF_2 + 1.03 \times 10^3 \frac{HW_p}{E_f}) \quad (6.4)$$

$$W_2 = \left(\frac{C}{h}\right)^{-0.4931} (52.9712SF_2 - 30.3162 + 1.01 \times 10^3 \frac{HW_p}{E_f}) \quad (6.5)$$

$$SF_f = 2.162 \times 10^{-3} \left(\frac{E_f}{h}\right)^{0.4442} (0.2548W_1 + 0.1403W_2 + 6.4 \frac{\sigma_h}{W_p}) \quad (6.6)$$

$$T_r = h^{0.6775} \left(\frac{3.7869}{\sqrt{W_1}} + \frac{1.2029}{\sqrt{W_2}} + 9.7 \times 10^{-9} W_e E_r \right) \quad (6.7)$$

Where W_1 and W_2 are pillar widths for pillar 1 and 2, respectively, SF_f is the minimum safety factor of the floor, T_r is the maximum tensile stress in the roof, σ_h is the horizontal stress and E_f is the Young's modulus of the floor. The R-squares for Eqs.

6.4 to 6.7 are 0.974, 0.915, 0.977, and 0.995, respectively. The regression equations represent the relationships between the safety factors of pillars and floor, and the maximum tensile stress in the roof and control variables, such as pillar width, entry width and panel width. These equations can be used for the design of all types of three-entry systems. After initial pillar sizes have been determined by selecting the safety factors of pillars, whether or not the design can be used under certain strong roof and weak floor conditions will be dependent on both the minimum safety factor of the floor and the maximum tensile stress in the roof.

6.4.3 Design of Three-Entry System under Strong Roof and Weak Floor Condition

Just like the three-entry system design under strong roof and strong floor condition, the four types of design are also available to strong roof and weak floor condition. Figures 6.8 to 6.10 compare the stiff-yield with the yield-stiff pillar design under the same conditions. The input data are listed in Table 6.5.

Table 6.5 Input Data for Comparison Study under Strong Roof and Weak Floor Condition

Variable	Level Used (Unit)
Mining height, H	6 (ft)
Uniaxial Compressive Strength of Coal, S_1	900 (psi)
Internal friction angle of coal, ϕ	30°
Cohesion strength of coal, C	260 (psi)
Young's modulus of roof, E_r	4.5 x 10 ⁶ (psi)
Young's modulus of floor, E_f	0.5 x 10 ⁶ (psi)
Horizontal stress, σ_h	500 (psi)
Entry width, W_e	20 (ft)
Longwall panel width, W_p	800 (ft)
Safety factors of pillars	according to recommendation

Overall, the stiff-yield pillar design appears to be better than the yield-stiff pillar design because of its smaller pillar size(Fig. 6.8), a higher safety factor of the floor(Fig. 6.9) and lower tensile stress in the roof(Fig. 6.10). Therefore, the stiff-yield pillar design is prefer to a yield-stiff pillar design under the same geological and mining conditions.

Both stiff-stiff and yield-yield pillar designs are also compared with the stiff-yield pillar design. The results are presented in Figs. 6.11 to 6.13. The stiff-stiff pillar design requires the largest total pillar width while the total pillar width is the lowest for the yield-yield pillar design(Fig. 6.11). The stiff-stiff and stiff-yield pillar designs provide a much better control of the floor than the yield-yield pillar design by promising a higher

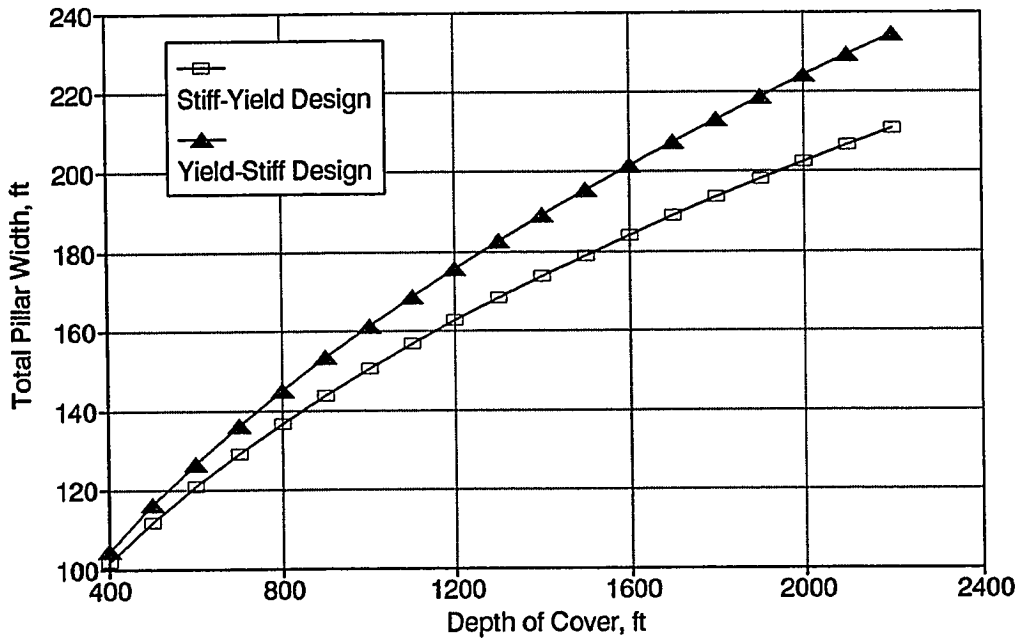


Figure 6.8. Total pillar width vs depth of cover for both stiff-yield and yield-stiff pillar designs under strong roof and weak floor condition.

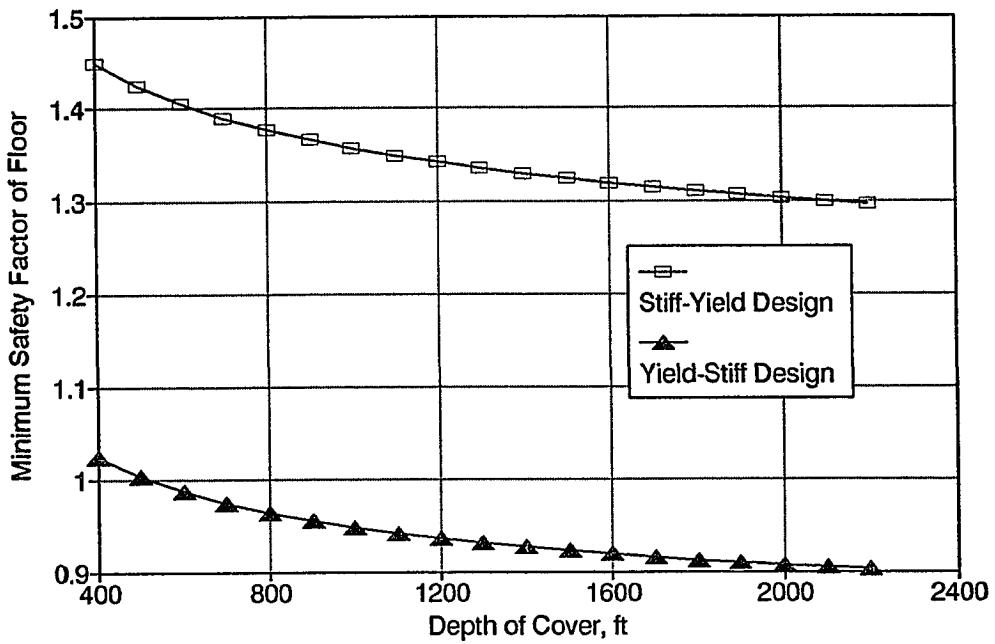


Figure 6.9. Minimum safety factor of floor vs depth of cover for both stiff-yield and yield-stiff pillar designs under strong roof and weak floor condition.

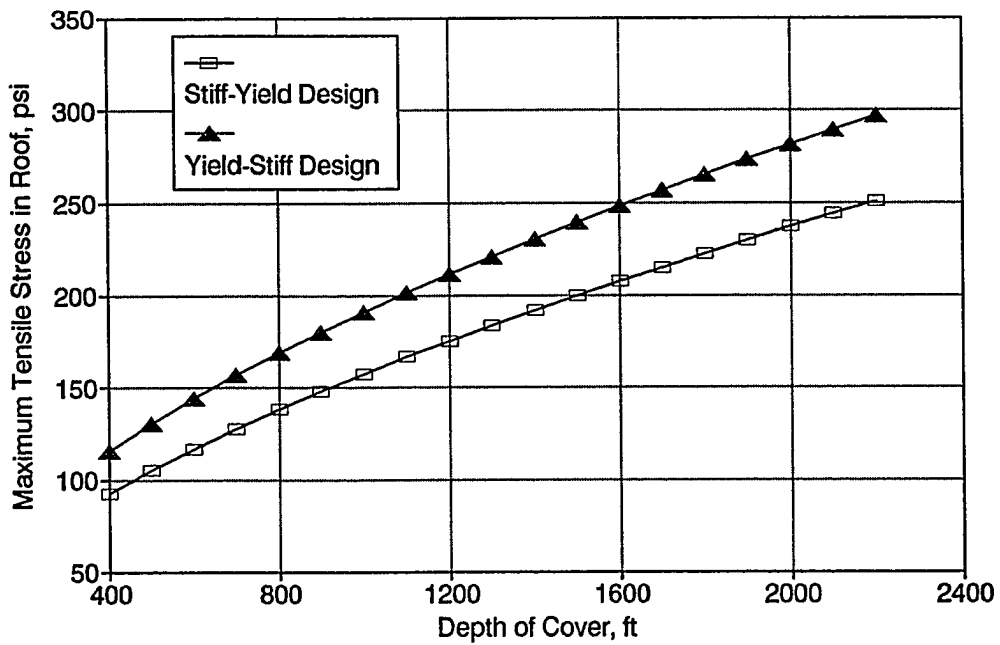


Figure 6.10. Maximum tensile stress in roof vs depth of cover for both stiff-yield and yield-stiff pillar designs under strong roof and weak floor condition.

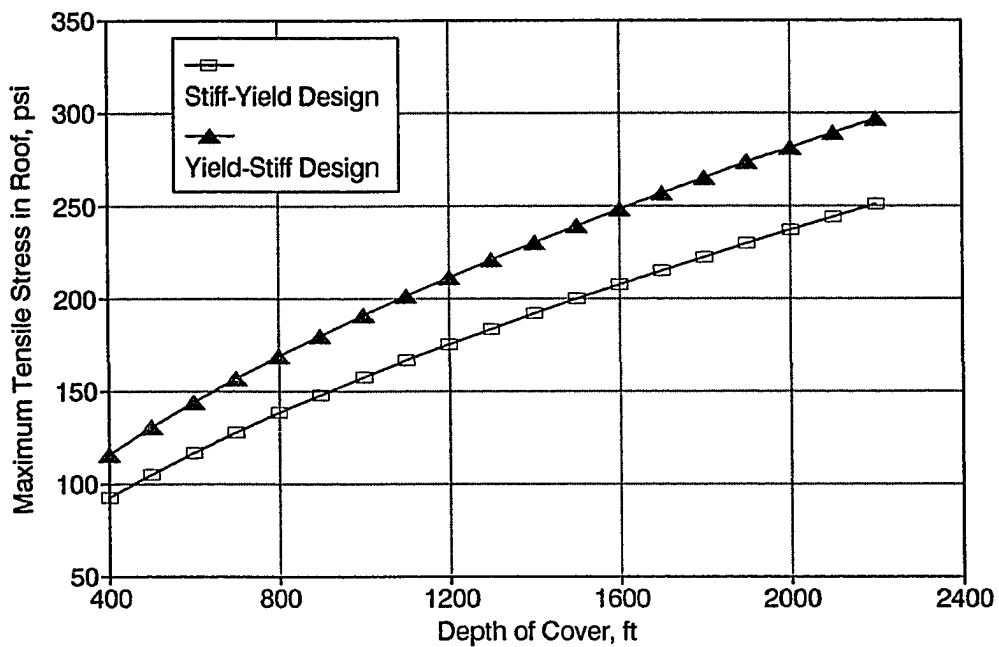


Figure 6.11. Total pillar width vs depth of cover for stiff-stiff, yield-yield and stiff-yield pillar designs under strong roof and weak floor condition.

safety factor of the floor(Fig. 6.12). On the other hand, the yield-yield pillar design usually causes a high tensile stress in the roof(Fig. 6.13). Therefore the stiff-stiff and stiff-yield pillar designs are more preferable than the others.

In the design of a stable three-entry system, the stability of pillars has to be ensured first, followed by the stability conditions of the floor and roof. If a safety factor of 1.3 is recommended for the floor, then the yield-yield pillar design will not be applicable under strong roof and weak floor condition(Fig. 6.12). Therefore, the design of a stable three-entry system must consider the stability conditions of pillar, floor and roof simultaneously.

6.5 The Weak Roof and Strong Floor Conditions

6.5.1 Introduction

The weak roof and strong floor condition is encountered more often than the strong roof and weak floor conditions. Traditionally, the coal producers pay more attentions to roof control problems because of the high potential for serious injury by roof falls in the underground. According to Table 6.1, 27 finite element models were constructed, and the input data are presented in Table 6.6. The material properties of the weak roof strata are the same as those used for the weak floor strata in the strong roof and weak floor condition.

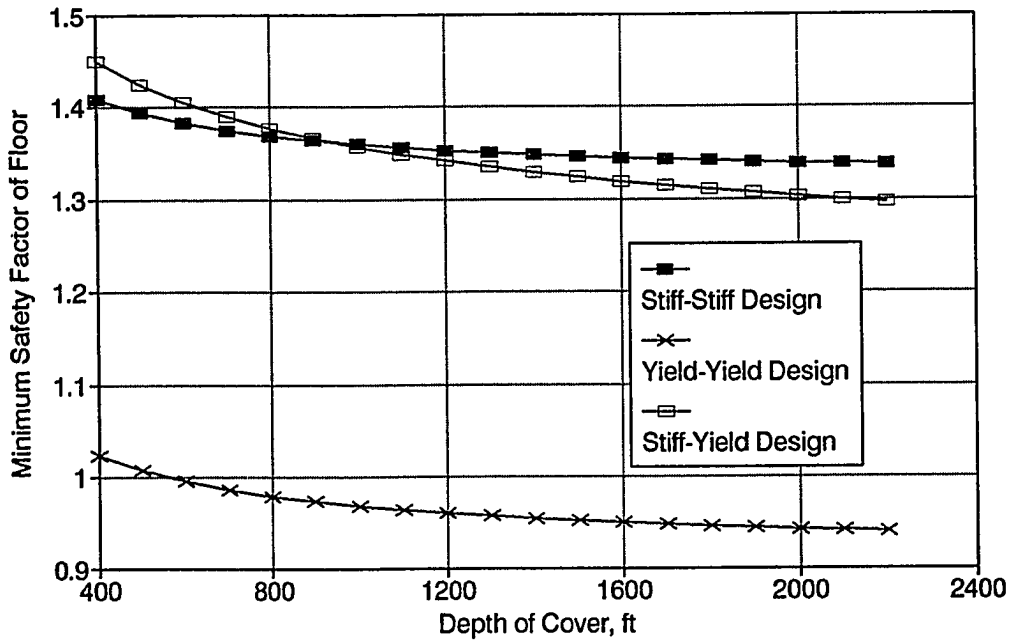


Figure 6.12. Minimum safety factor of floor vs depth of cover for stiff-stiff, yield-yield and stiff-yield pillar designs under strong roof and weak floor condition.

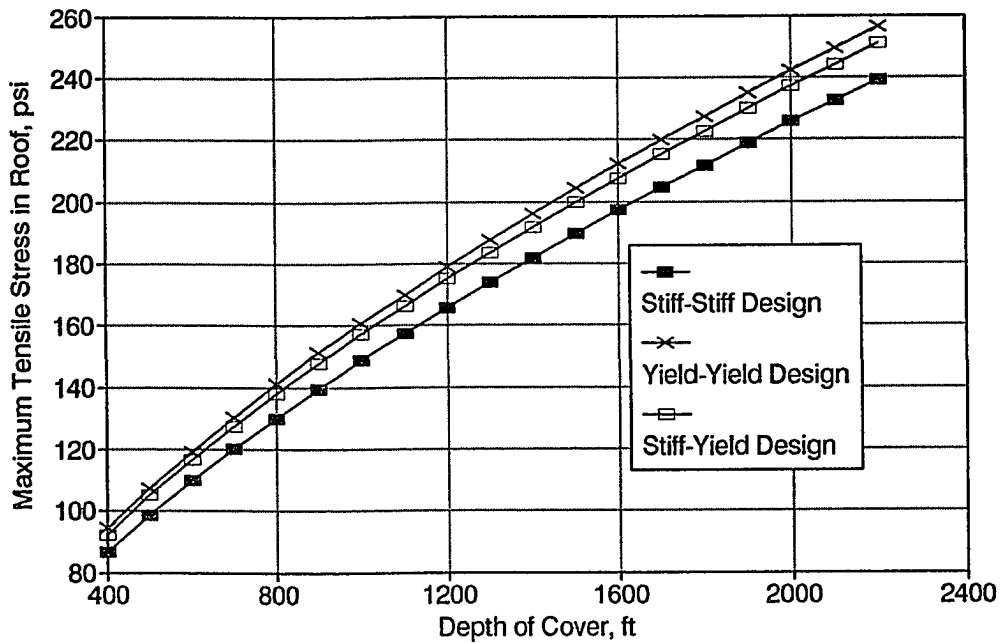


Figure 6.13. Maximum tensile stress in roof vs depth of cover for stiff-stiff, yield-yield and stiff-yield pillar designs under strong roof and weak floor condition.

Table 6.6. Database for Finite Element Modeling under Weak Roof and Strong Floor Condition

Variable	Unit	Data Range		
		Level 1	Level 2	Level 3
E_r/E_c		0.5	1	1.5
E_r/E_c		2	6	10
W_e	ft	15	20	25
W_1	ft	10	80	150
W_2	ft	10	80	150
ϕ	degree	20	25	30
$h\gamma/C$		1	2	3
H	ft	4.5	7.25	10
σ_h	psi	500	1250	2000
W_p	ft	500	750	1000

6.5.2 Regression Model

The model simulations were performed on WVNET mainframe computer. The results indicated that besides possible pillar failures, both roof shear failure and floor tensile failure are likely to happen under weak roof and strong floor condition. The nonlinear regression analysis leads to the establishment of the following relationships between the control variables and pillar width, safety factor of roof and tensile stress in floor.

$$W_1 = \left(\frac{C}{h}\right)^{-0.4135} (62.7666SF_1 - 22.8459SF_2 + 8.15\frac{HW_p}{E_r}) \quad (6.8)$$

$$W_2 = \left(\frac{C}{h}\right)^{-0.4616} (62.8519SF_2 - 29.7170SF_1 + 1.8 \times 10^2 \frac{HW_p}{E_r}) \quad (6.9)$$

$$SF_r = 2.398 \times 10^{-3} \left(\frac{E_r}{h}\right)^{0.4367} (0.2384W_1 + 0.1217W_2 + 4.5\frac{\sigma_h}{W_p}) \quad (6.10)$$

$$T_f = h^{0.8759} \left(\frac{1.3043}{\sqrt{W_1}} + \frac{0.4907}{\sqrt{W_2}} + 3.4 \times 10^{-4} W_e E_r + \frac{0.9236}{\sigma_h} \right) \quad (6.11)$$

Where W_1 and W_2 are the pillar widths for pillar 1 and 2, respectively, SF_r is the minimum safety factor of the roof, T_f is the maximum tensile stress in the floor. The R-square is 0.922, 0.973, 0.948 and 0.873 for Eqs. 6.8 to 6.11, respectively. Just like the previous two types of roof and floor conditions, the equations developed under weak roof and strong floor condition can also be used to design various types of three-entry

system by selecting a proper safety factor for each pillar.

6.5.3 Design of Three-Entry System under Weak Roof and Strong Floor Condition

To discuss the difference among the four types of design, each design is evaluated under the same geological and mining conditions. The input data are listed in Table 6.7.

Table 6.7 Input Data for Comparison Study under Weak Roof and Strong Floor Condition

Variable	Level Used (Unit)
Mining height, H	6 (ft)
Uniaxial Compressive Strength of Coal, S_1	900 (psi)
Internal friction angle of coal, ϕ	30°
Cohesion strength of coal, C	260 (psi)
Young's modulus of roof, E_r	0.75×10^6 (psi)
Young's modulus of floor, E_f	5×10^6 (psi)
Horizontal stress, σ_h	500 (psi)
Entry width, W_e	20 (ft)
Longwall panel width, W_p	800 (ft)
Safety factors of pillars	according to recommendation

Figures 6.14 to 6.16 present the total pillar width, the minimum safety factor of roof and the maximum tensile stress in the floor under various depth of cover for both the stiff-yield and the yield-stiff pillar designs. By comparing the stiff-yield with the

yield-stiff pillar designs a conclusion similar to the one drawn for strong roof and weak floor condition can be reached: the stiff-yield pillar design is more favorable in total pillar width, minimum safety factor of roof and maximum tensile stress in the floor. In addition, the stiff-stiff, the yield-yield and the stiff-yield pillar designs are also compared with each other(Figs. 6.17 to 6.19). Clearly, the stiff-stiff pillar design is the most conservative design in the safety factor of floor(Fig. 6.18) and the maximum tensile stress in the floor(Fig. 6.19), but yields the lowest coal recovery because of the largest total pillar width(Fig. 6.17). On the other hand, the yield-yield pillar design will lead to the lowest safety factor of the roof and the highest maximum tensile stress in the floor and can not be used under weak floor and strong roof condition. Conversely, the stiff-yield pillar design, considering the maximum tensile stress in the floor and the minimum safety factor of the roof, is a good alternative between stiff-stiff and yield-yield design, and may find a wide range of using this type of design under weak roof and strong floor condition.

6.6 The Weak Roof and Weak Floor Condition

6.6.1 Introduction

The weak roof and weak floor condition is much less likely to be encountered in the U. S. underground coal mines. In practices, it is rare to see both mine roof and floor to fail at the same place and at the same time. This may be attributed to the

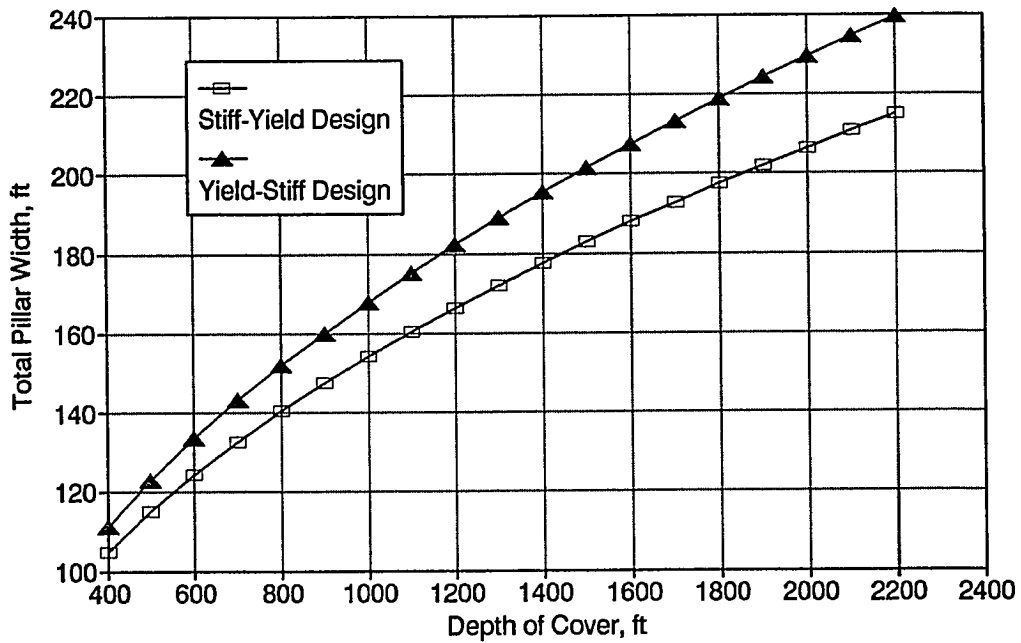


Figure 6.14. Total pillar width vs depth of cover for both stiff-yield and yield-stiff pillar designs under weak roof and strong floor condition.

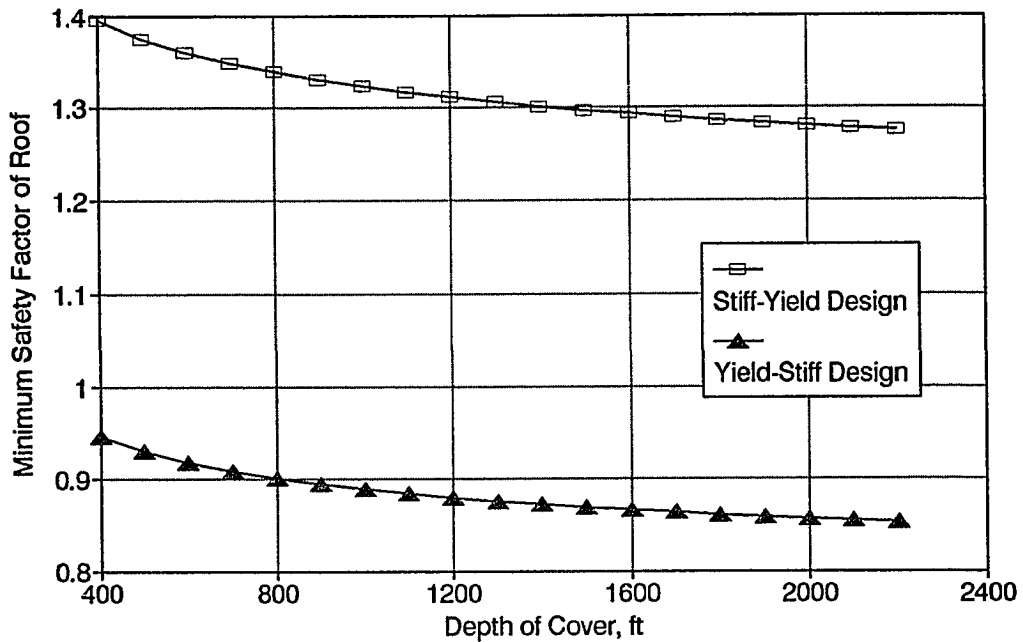


Figure 6.15. Minimum safety factor of roof vs depth of cover for both stiff-yield and yield-stiff pillar designs under weak roof and strong floor condition.

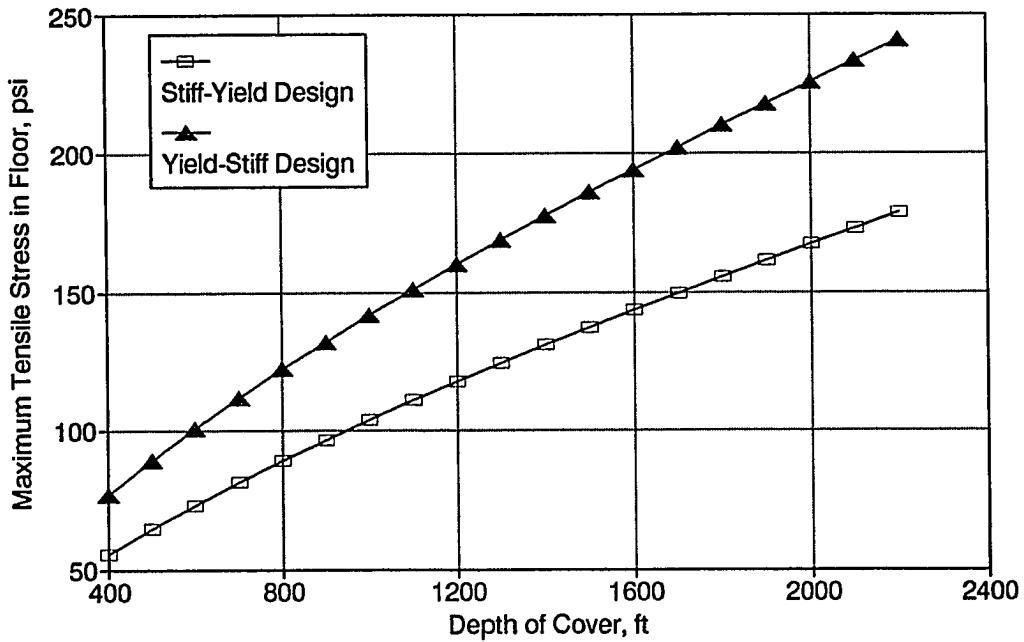


Figure 6.16. Maximum tensile stress in floor vs depth of cover for both stiff-yield and yield-stiff pillar designs under weak roof and strong floor condition.

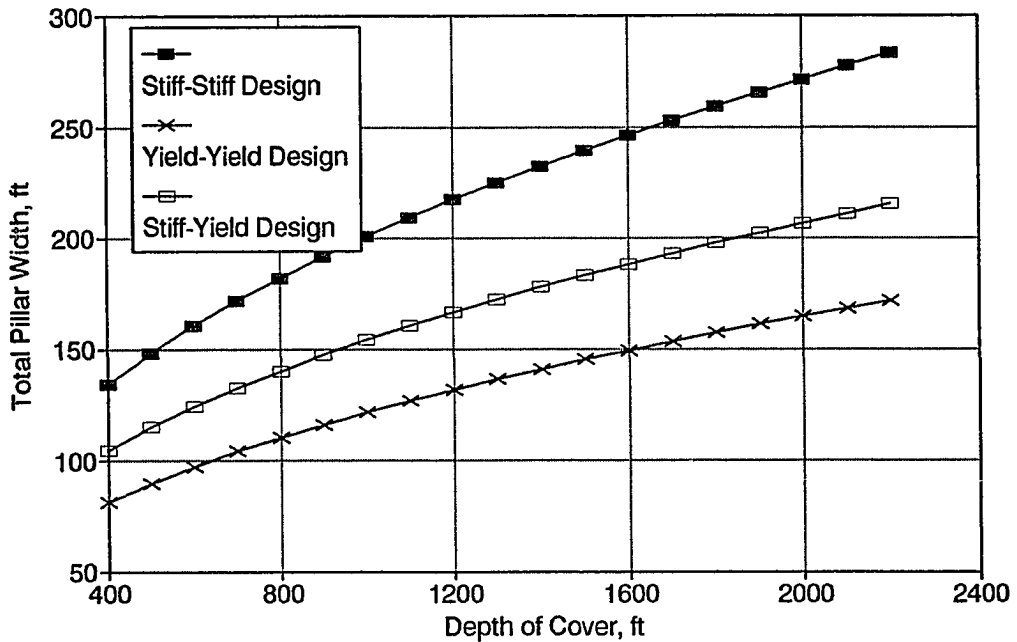


Figure 6.17. Total pillar width vs depth of cover for stiff-stiff, yield-yield and stiff-yield pillar designs under weak roof and strong floor condition.

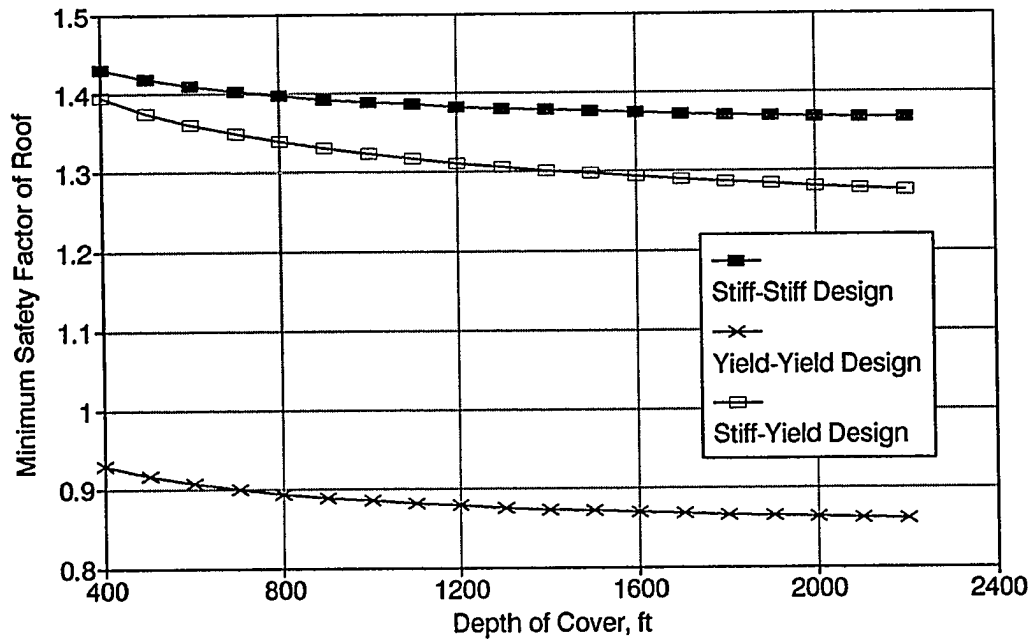


Figure 6.18. Minimum safety factor of roof vs depth of cover for stiff-stiff, yield-yield and stiff-yield pillar designs under weak roof and strong floor condition.

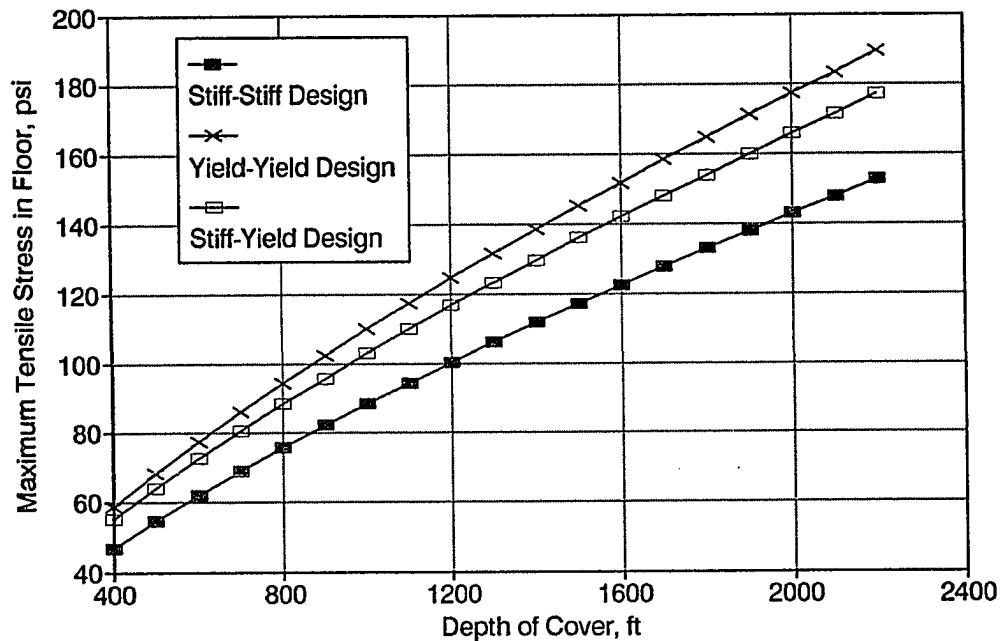


Figure 6.19. Maximum tensile stress in floor vs depth of cover for stiff-stiff, yield-yield and stiff-yield pillar designs under weak roof and strong floor condition.

stress release caused by either roof or floor failure, whichever comes first, so the remaining intact roof or floor can survive in the stress released zone. For the purpose of theoretical analysis, 27 finite element models were assembled as defined in Table 6.1. The input data are listed in Table 6.8.

6.6.2 Regression Model

Again the finite element model analysis was performed on WVNET mainframe computer. According to the results, tensile stresses in the roof and floor are extremely small, therefore, tensile failures of the roof and floor are less likely to happen. On the contrary, shear failures in the roof and floor are highly possible under weak roof and weak floor condition. To consider the stability of an entry-pillar system, the following relationships are established based on the nonlinear regression analysis.

$$W_1 = \left(\frac{C}{h}\right)^{-0.5235} (52.7862 SF_1 - 15.2109 SF_2 + 1.17 \times 10^7 \frac{HW_p}{E_r E_f}) \quad (6.12)$$

$$W_2 = \left(\frac{C}{h}\right)^{-0.5341} (53.7009 SF_2 - 23.4415 SF_1 + 2.02 \times 10^7 \frac{HW_p}{E_r E_f}) \quad (6.13)$$

$$SF_r = 4.521 \times 10^{-3} \left(\frac{E_r}{h}\right)^{0.3908} (0.1339 W_1 + 0.1532 W_2 + 6.5989 \frac{\sigma_h}{W_p}) \quad (6.14)$$

Table 6.8. Database for Finite Element Modeling under Weak Roof and Weak Floor Condition

Variable	Unit	Data Range		
		Level 1	Level 2	Level 3
E_r/E_c		0.5	1	1.5
E_f/E_c		0.5	1	1.5
W_c	ft	15	20	25
W_1	ft	10	80	150
W_2	ft	10	80	150
ϕ	degree	20	25	30
$h\gamma/C$		1	2	3
H	ft	4.5	7.25	10
σ_h	psi	500	1250	2000
W_p	ft	500	750	1000

$$SF_f = 2.4 \times 10^{-4} \left(\frac{E_f}{h} \right)^{0.6032} (0.5568 W_1 + 0.8454 W_2 + 53.8824 \frac{\sigma_h}{W_p}) \quad (6.15)$$

Where W_1 and W_2 are the pillar widths for pillar 1 and 2, respectively, SF_f and SF_t are the minimum safety factors of the floor and floor, respectively. The R-square is 0.912, 0.862, 0.942 and 0.961 for Eqs. 6.12 to 6.15, respectively.

6.6.3 Design of Three-Entry System under Weak Roof and Weak Floor Condition

To consider the possibility of using various types of three-entry system, the previous four types of design were examined by using the following set of input data.

Table 6.9 Input Data for Comparison Study under Weak Roof and Weak Floor Condition

Variable	Level Used (Unit)
Mining height, H	6 (ft)
Uniaxial Compressive Strength of Coal, S_t	900 (psi)
Internal friction angle of coal, ϕ	30°
Cohesion strength of coal, C	260 (psi)
Young's modulus of roof, E_r	0.5 x 10 ⁶ (psi)
Young's modulus of floor, E_f	0.5 x 10 ⁶ (psi)
Horizontal stress, σ_h	500 (psi)
Entry width, W_e	20 (ft)
Longwall panel width, W_p	800 (ft)
Safety factors of pillars	according to recommendation

Figures 6.20 to 6.22 show the results from both the stiff-yield and the yield-stiff pillar designs. In general, the yield-stiff pillar design requires a larger total pillar width(Fig. 6.20) and higher safety factor of roof(Fig. 6.21) and floor(Fig. 6.22). The stiff-yield pillar design requires less total pillar width in the three-entry system. But the safety factors of the roof and floor are also lower than the yield-stiff pillar design. If both designs can ensure the stabilities of the roof and floor, then the stiff-yield pillar design will be a better choice because of its higher recovery. Comparisons are also made among the stiff-stiff, yield-yield and stiff-yield pillar designs(Figs. 6.23 to 6.25). Considering the total pillar width and the minimum safety factors of the roof and floor for the three designs, the stiff-stiff pillar design is the most conservative design and gives a much better control of the roof and floor. The yield-yield pillar design is the worst design in term of safety factor of the roof and floor, and can not be used because the safety factor of the roof is all less than 1.3. While the stiff-yield pillar design is somewhere between the stiff-stiff and the yield-yield pillar designs. If a safety factor of 1.3 is recommended for roof and floor for each design under weak roof and weak floor condition, then both the stiff-yield, and yield-yield pillar design can only be used under shallow depth(<1500 ft). After having determined the initial pillar width, it must depend on the safety factors of the roof and the floor to determine whether or not the chosen design can be used under the weak roof and weak floor condition.

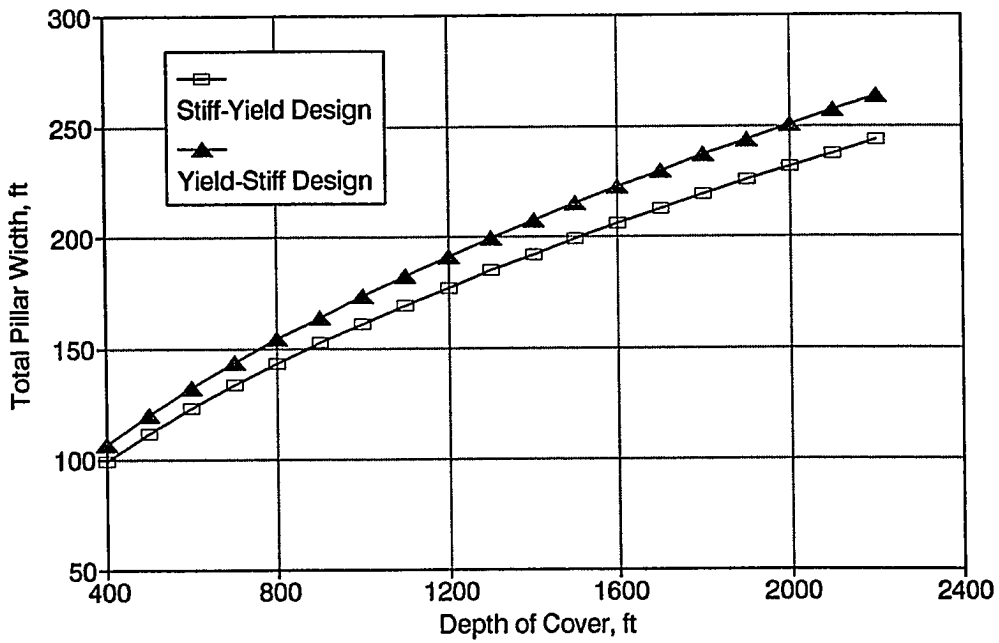


Figure 6.20. Total pillar width vs depth of cover for both stiff-yield and yield-stiff pillar designs under weak roof and weak floor condition.

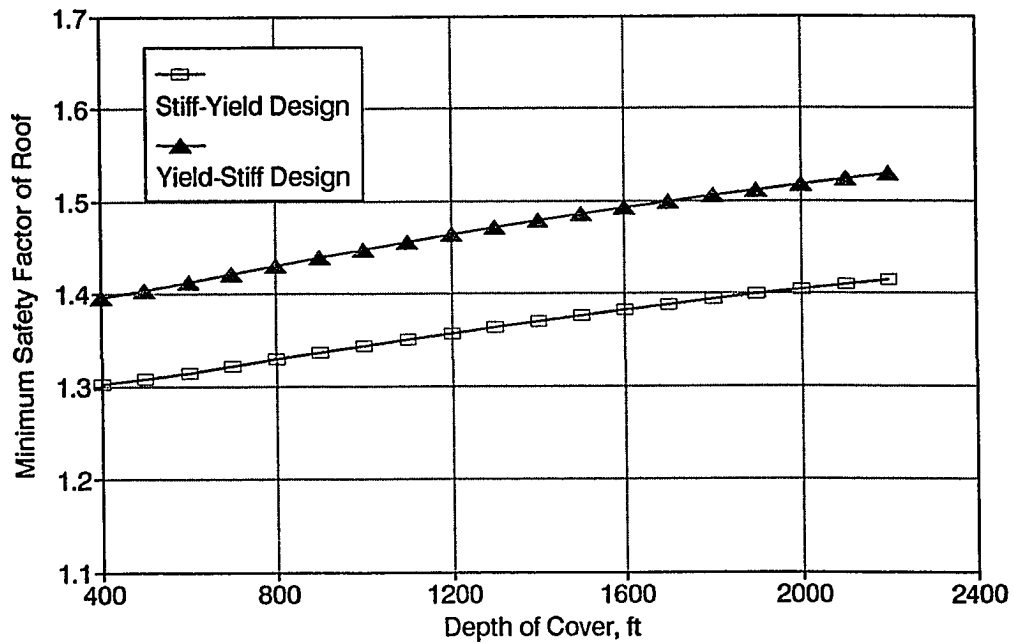


Figure 6.21. Minimum safety factor of roof vs depth of cover for both stiff-yield and yield-stiff pillar designs under weak roof and weak floor condition.

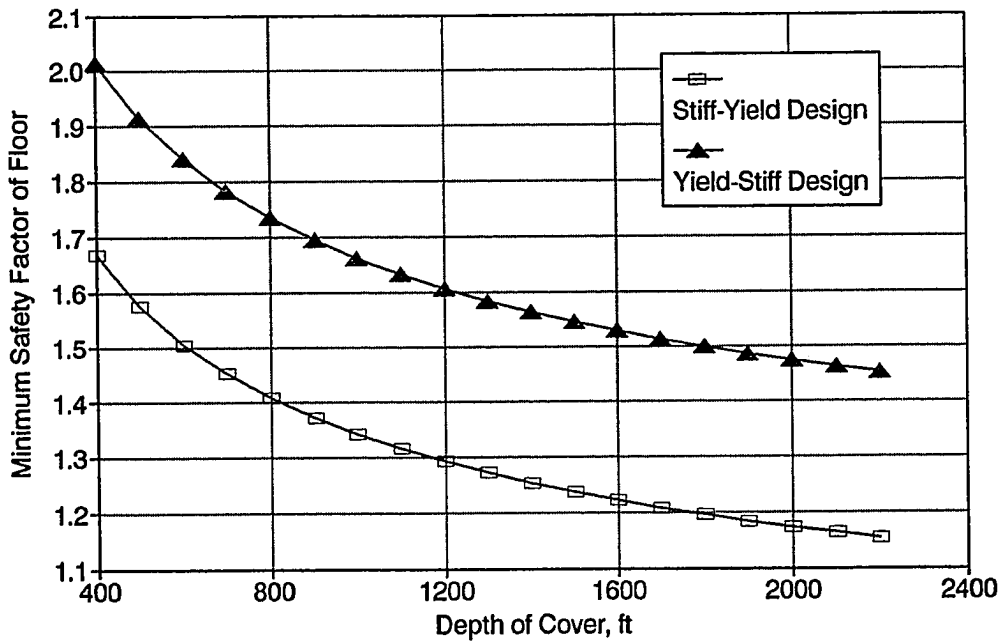


Figure 6.22. Minimum safety factor of floor vs depth of cover for both stiff-yield and yield-stiff pillar designs under weak roof and weak floor condition.

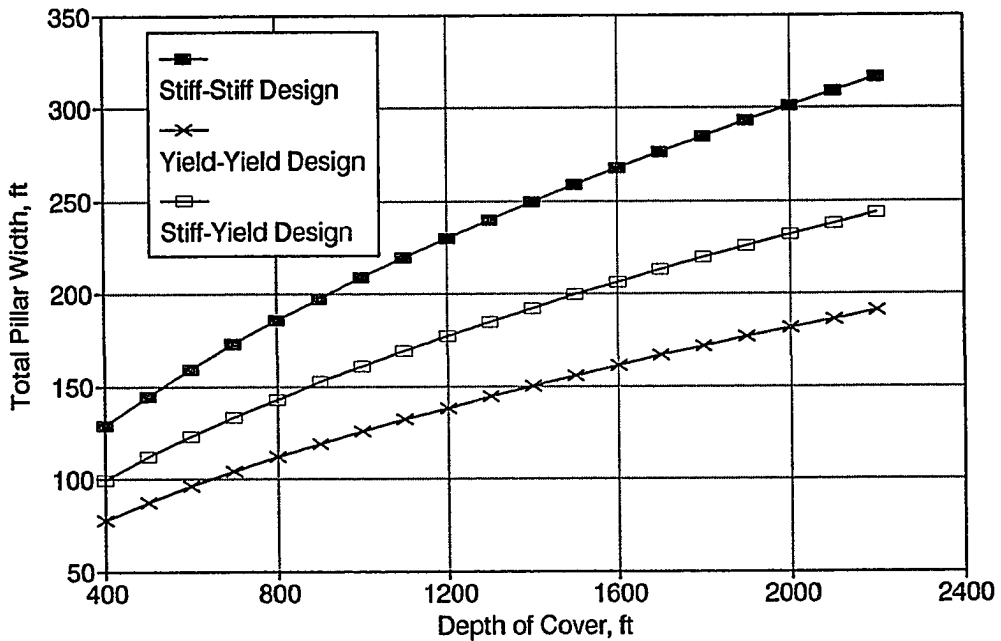


Figure 6.23. Total pillar width vs depth of cover for stiff-stiff, yield-yield and stiff-yield pillar designs under weak roof and weak floor condition.

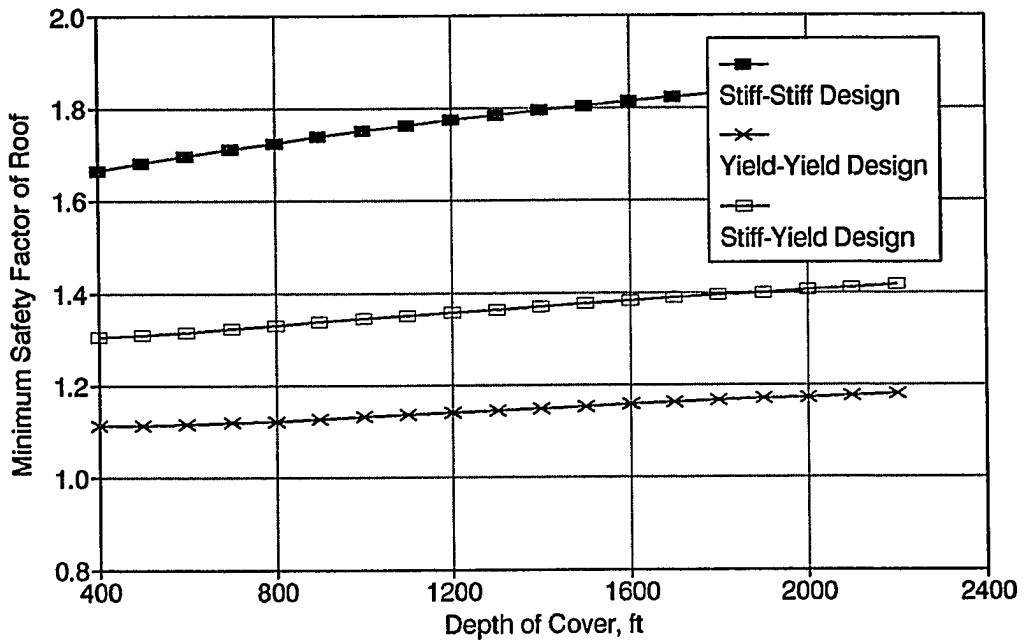


Figure 6.24. Minimum safety factor of roof vs depth of cover for stiff-stiff, yield-yield and stiff-yield pillar designs under weak roof and weak floor condition.

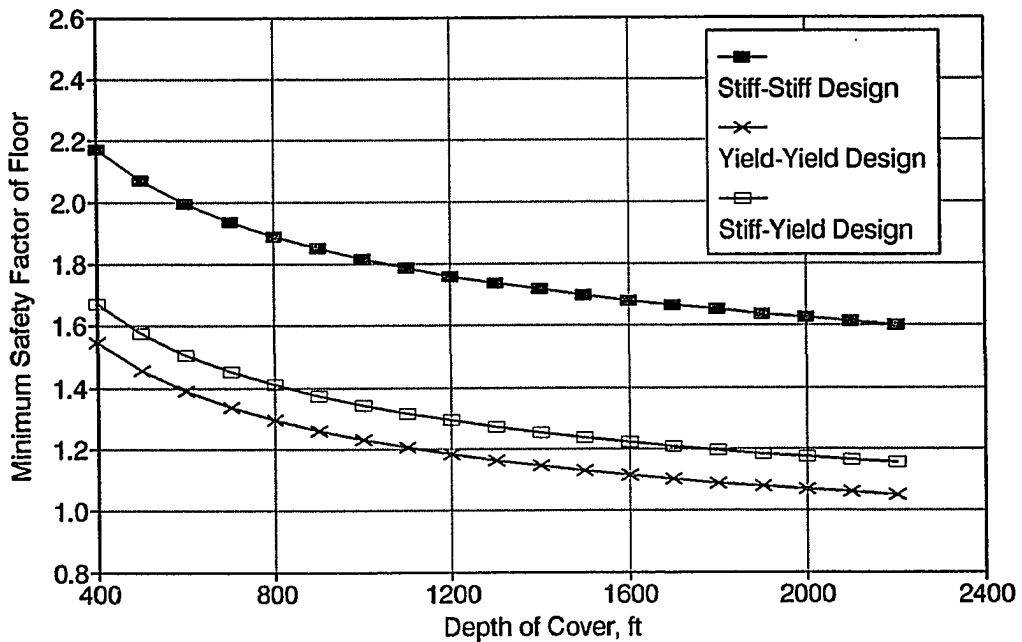


Figure 6.25. Minimum safety factor of floor vs depth of cover for stiff-stiff, yield-yield and stiff-yield pillar designs under weak roof and weak floor condition.

6.7 Summary

Several conclusions can be reached at this point. First of all, the regression equations derived in this study present precisely the relationships between the stability conditions of the entry-pillar system and the most important variables under different roof and floor conditions. By using these regression equations, different types of three-entry system can be designed to satisfy the stability requirement of the roof, pillar and floor. Sometimes, several tries on the safety factors may be needed in order to find a workable three-entry system.

Based on the comparison studies, it can be concluded that the combinations of a stiff and a yield pillar designs are the designs between the stiff-stiff and the yield-yield pillar designs considering the stability conditions of roof, pillar and floor. If the stability conditions of the roof and floor can be satisfied by the stiff-yield and the yield-stiff pillar designs, they can be used as alternatives especially for deeper underground coal mines.

In general, the stiff-yield pillar design is more favorable than the yield-stiff pillar design except under weak roof and weak floor condition. The stiff-stiff pillar design is the most conservative design, thus the recovery of this design is the lowest. It may result in uneconomical mining under deep cover. On the other hand, the yield-yield pillar design is less likely to be used because it can not ensure the stability of roof or floor except under strong roof and strong floor condition.

Overall, the best design should be the one which can ensures the stabilities of

CHAPTER 7

COMPARISON STUDY AND APPLICATION

7.1 Introduction

There are two types of pillar currently used in the U.S. underground coal mines based on its design mechanism and function; one is called "stiff pillar," and the other is known as "yield pillar." The decision to use either a stiff or a yield pillar or a combination of stiff and yield pillars depends mainly on geological and mining conditions. The new design method developed in the previous chapters can handle both the stiff and yield pillar designs based on in-situ geological and mining conditions. How can one use the new method to design a longwall entry system under various geological and mining conditions? How much does the new method differ from the existing longwall pillar design methods? In this chapter, standard design procedures and an application example are illustrated. A comparison study of the new method with the other available methods is performed also.

7.2 Design Procedures

Since the design equations vary with the different geological and mining conditions, use of the new pillar design method developed in this study involves the following two major steps(Fig. 7.1); 1) to classify the in-situ roof and floor conditions,

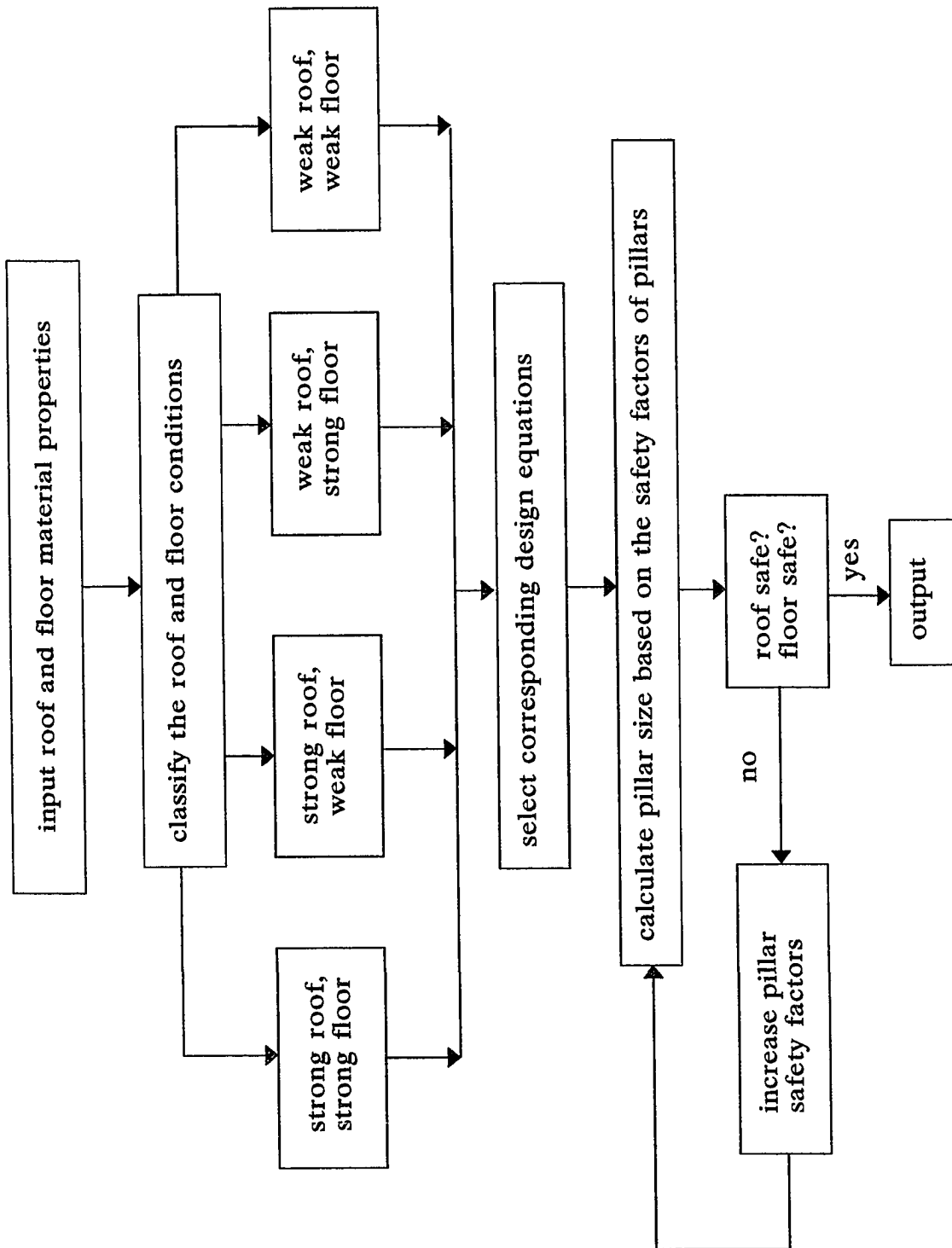


Figure 7.1. Design procedures.

and 2) to use the corresponding equations for determining the pillar size.

7.2.1 Classification of In-situ Roof and Floor Conditions

In the first step of using the new design method, the five classification variables and weighting factors of in-situ roof and floor strata (Table 3.2) are needed. The classification method used is essentially a cluster analysis method. Based on the Euclidean distance between the new samples and the centers of the predefined groups, the classification system categorizes the in-situ roof and floor conditions into one of the two predefined groups, i.e., either strong or weak rock groups defined in Chapter 3. For cluster analysis purpose, the classification variables of a new sample are converted into the standardized data using Eq.7.1.

$$S_{nj} = \frac{X_{nj} - X_{jmin}}{X_{jmax} - X_{jmin}} \quad (7.1)$$

Where S_{nj} is the j th variable of the new sample after standardizing, n denotes the new sample, which can be either roof and floor rock. X_{nj} is the raw value of the j th variable of the new sample. X_{jmin} and X_{jmax} are the minimum and maximum values of the j th variable of the original database, respectively (Table 3.3). The Euclidean distance between the new sample and the predefined group can be defined by the following equation.

$$D_{nk} = \sqrt{\sum_{j=1}^n (S_{nj} - C_{kj})^2 W_j} \quad (7.2)$$

Where D_{nk} denotes the distance between the new sample and the center of the k th predefined group, C_{kj} is the center of the k th group and j th variable (Table 3.4). Based on the Euclidean distances between the new samples and the predefined groups, the new samples will be classified into either a strong or a weak rock group according to the nearest neighbor rule. After classification of the roof and floor rocks, the in-situ roof and floor condition can be categorized into one of the following four roof and floor conditions; 1) strong roof and strong floor condition, 2) strong roof and weak floor condition, 3) weak roof and strong floor condition, 4) weak roof and weak floor condition.

7.2.2 Use of Corresponding Equations for Determining Suitable Pillar Size

After the in-situ roof and floor conditions have been determined, the corresponding equations can be selected from Chapter 6 for pillar design purpose. Since the stiff-yield pillar design is the most favorable design under most roof and floor conditions, the stiff-yield pillar design is recommended for the new design method. A safety factor of 1.5 and 0.9 is recommended for determining the initial pillar width of the stiff and yield pillar, respectively. Using the equations selected, the initial pillar widths of the stiff and yield pillars, tensile stress in the roof or floor as well as safety

factor of the roof or floor can be determined. If tensile stress of the roof or floor is less than their tensile strength, and safety factors of the roof and floor are larger than or equal to the recommended value(1.3), then the pillar size is adopted. Otherwise, the safety factor of stiff or yield pillar or both has/have to be increased until both the roof and floor are safe and stable.

7.3. Application Example

In a hypothetical situation, a coal company is to develop a new longwall panel within its properties. The new longwall panel is 800-ft. wide, and 8000-ft. long under 1200-ft. cover. Average seam height is 6 ft. A three-entry system is adopted, and the entry width is 20 ft. with 100-ft. crosscuts center to center. The company wants to use the stiff-yield pillar design for its new longwall panel. After conducting laboratory rock tests, mechanic properties of roof, coal and floor are obtained(Table 7.1).

Table 7.1 Mechanical Properties of Related Rocks

Type of Rock	Young's Modulus (x10 ⁶) psi	Uniaxial Compressive Strength (psi)	Internal Friction Angle (degree)	Poisson's Ratio	Cohesion Strength (psi)	Tensile Strength (psi)
roof	2.0	6000	35	0.15	1562	130
coal	0.5	1500	30	0.25	433	
floor	2.5	10300	35	0.15	2681	200

1. Classify in-situ roof and floor condition

For classification of the roof and floor conditions, the classification variables of the in-situ roof and floor are calculated (Table 7.2).

Table 7.2. Classification Variables of New Samples

Type of Rock	Classification Indices				
	$h\gamma/C$	E (10^6 psi)	ν	ϕ (degree)	T (psi)
Roof	0.845	2.00	0.15	35°	130
Floor	0.492	2.50	0.15	35°	200

After using equation 7.1 to normalize the classification variables, the Euclidean distances between the new samples and the predefined groups (sample groups) are calculated by equation 7.2 (Table 7.3). According to the results, the roof and floor conditions of the mine belong to Group 1 as defined in Chapter 3, i.e., strong roof and floor condition.

Table 7.3 Euclidean Distances between New Samples and Centers of the Predefined Groups

Type of Rock	Distance from New Sample to		Classification Results (nearest neighbor rule)
	Center of Strong Rock Group	Center of Weak Rock Group	
Roof	0.5283	1.6686	strong
Floor	0.5999	1.3566	strong

2) Determining the pillar size

Step 2 is to use the corresponding equations for determining the pillar size. Since the geological condition of the mine belongs to Group 1, Equations 6.1 to 6.3 are selected for pillar design. To design a stiff-yield pillar system, a safety factor of 1.5 and 0.90 is recommended for stiff and yield pillar, respectively. By substituting the input data into Eqs. 6.1 and 6.2, the initial pillar widths can be determined;

$$\begin{aligned}W_1 &= \left(\frac{433}{1200}\right)^{-0.4048} (52.7884 \times 1.5 - 15.4181 \times 0.9 + 0.0005 \times 6 \times 800) \\ &= 102.3 \text{ (ft)}\end{aligned}$$

$$\begin{aligned}W_2 &= \left(\frac{433}{1200}\right)^{-0.5581} (44.9214 \times 0.9 - 23.1242 \times 1.5 + 0.0005 \times 6 \times 800) \\ &= 14.4 \text{ (ft)}\end{aligned}$$

After determining the initial pillar widths, the maximum tensile stress in the entry-pillar system is calculated by Eq.6.3 and compared with the tensile strength of the immediate roof. If the stress in the immediate roof is less than its strength, then the pillar size is suitable. If not, roof tensile failure will be very likely to occur in the entry. To ensure the stability of the roof, the pillar widths have to be enlarged by adjusting the safety factors of both pillars until the tensile stress in the roof becomes less than or equal to its strength. Sometimes, several iterations are needed to determine the most suitable pillar size. Based on the first try, the tensile stress in the case example is, which is larger than its strength(>130 psi), therefore, roof tensile failure is expected.

$$T_r = 1200^{0.7454} \left(\frac{2.9877}{\sqrt{102.3}} + \frac{1.0168}{\sqrt{14.4}} + 2.8 \times 10^{-9} \times 20 \times 2 \times 10^6 \right)$$

$$= 133.3 \text{ (psi)}$$

In order to ensure roof stability, the safety factors have to be increased. In this case the safety factors for the second try are 1.55 and 0.95 for stiff and yield pillar, respectively.

$$W_1 = \left(\frac{433}{1200} \right)^{-0.4048} (52.7884 \times 1.55 - 15.4181 \times 0.95 + 0.0005 \times 6 \times 800)$$

$$= 105.1 \text{ (ft)}$$

$$W_2 = \left(\frac{433}{1200} \right)^{-0.5581} (44.9214 \times 0.95 - 23.1242 \times 1.55 + 0.0005 \times 6 \times 800)$$

$$= 16.3 \text{ (ft)}$$

$$T_r = 1200^{0.7454} \left(\frac{2.9877}{\sqrt{105.1}} + \frac{1.0168}{\sqrt{16.3}} + 2.8 \times 10^{-9} \times 20 \times 2 \times 10^6 \right)$$

$$= 129.3 \text{ (psi)}$$

Since this time the tensile stress in the roof is less than its strength, no further iteration is needed. Therefore a 105-ft wide stiff pillar and a 16.5-ft wide yield pillar are recommended for the three-entry system for the longwall development in the mine. The suitable pillar size so chosen is not unique. Depend on the safety factors chosen, there may be different pairs of pillars which satisfy the stability requirements of the roof and the floor. The best choice is the one which ensure roof and floor stability and maximizes coal recovery.

7.4 Comparison Study

Currently, there are a number of longwall pillar design methods available. Among those available design methods, ALPS, Wilson, Hsiung-Peng and Choi-McCain methods are more popular, and reportedly have been used in the real mining practice. Although, these four design methods are based on different assumptions and use different design criteria as well, they all have one thing in common, which is to consider the stability of the pillars only. On the contrary, the new pillar design method developed in this study is more flexible and can be used to design stiff and yield pillars for a three-entry longwall system. Besides considering the stability of pillars, the new design method estimates the stability of the roof and floor also. The purpose of a comparison study in this section is to identify the differences between the new method and the four other methods mentioned above. Since the other methods do not consider tensile stress and safety factor of the roof and floor, comparison is only made between the total pillar width of the three-entry system designed by each method. For the new method, total pillar width is predicted for the stiff-stiff and stiff-yield pillar designs, respectively. Predictions are made under both the best and the worst geological conditions, i.e., a) strong roof and strong floor and b) weak roof and weak floor conditions. Since Hsiung-Peng method considers roof and floor condition in their design, the method is used to estimate total pillar width under the best and the worst roof and floor conditions also. ALPS and Wilson methods are used to design two

equal-sized stiff pillars and a combination of a stiff and a yield pillar for the three-entry system. The yield pillar is assumed to be 20-ft. wide in both ALPS and Wilson methods. In order to see the variation of ALPS's prediction, a stability factor of 0.6 and 1.3 was used for the stiff pillar in ALPS method. On the contrary, Choi-McCain method is only used to design a stiff pillar and a 32-ft wide yield pillar. A 900 psi of uniaxial compressive coal strength is used in the prediction. The internal friction angle is assumed 30 degree. The panel width and length are assumed to be 800 and 8000 ft respectively. Coal seam height is 6 ft, and the entry is 20 ft wide. Both the stiff-stiff and stiff-yield pillar designs by the different method are compared with each other separately. Figures 7.2 and 7.3 show the total pillar width predicted by each method. For the stiff-stiff pillar design(Fig. 7.2), the new method predicts the smallest pillar size under deep cover(>750 ft.). If a safety factor of 1.3 is required for stiff pillar in the stiff-yield pillar design, the new method also predicts the smallest pillar size when the depth of cover is larger than 1000 ft.(Fig. 7.3). When the depth of cover is less than 1300 ft., the total pillar width predicted by the new method is very close to both Wilson's and ALPS's prediction. Over all, the new method predicts a smaller total pillar width under deep cover except when overburden is less than 1000 ft. ALPS, Wilson and Choi-McCain methods predict a smaller pillar than the new method under shallow cover. On the other hand, the total pillar width is directly related to the safety factor of pillar in all pillar design methods. By reducing the safety factor of pillar in the stiff-

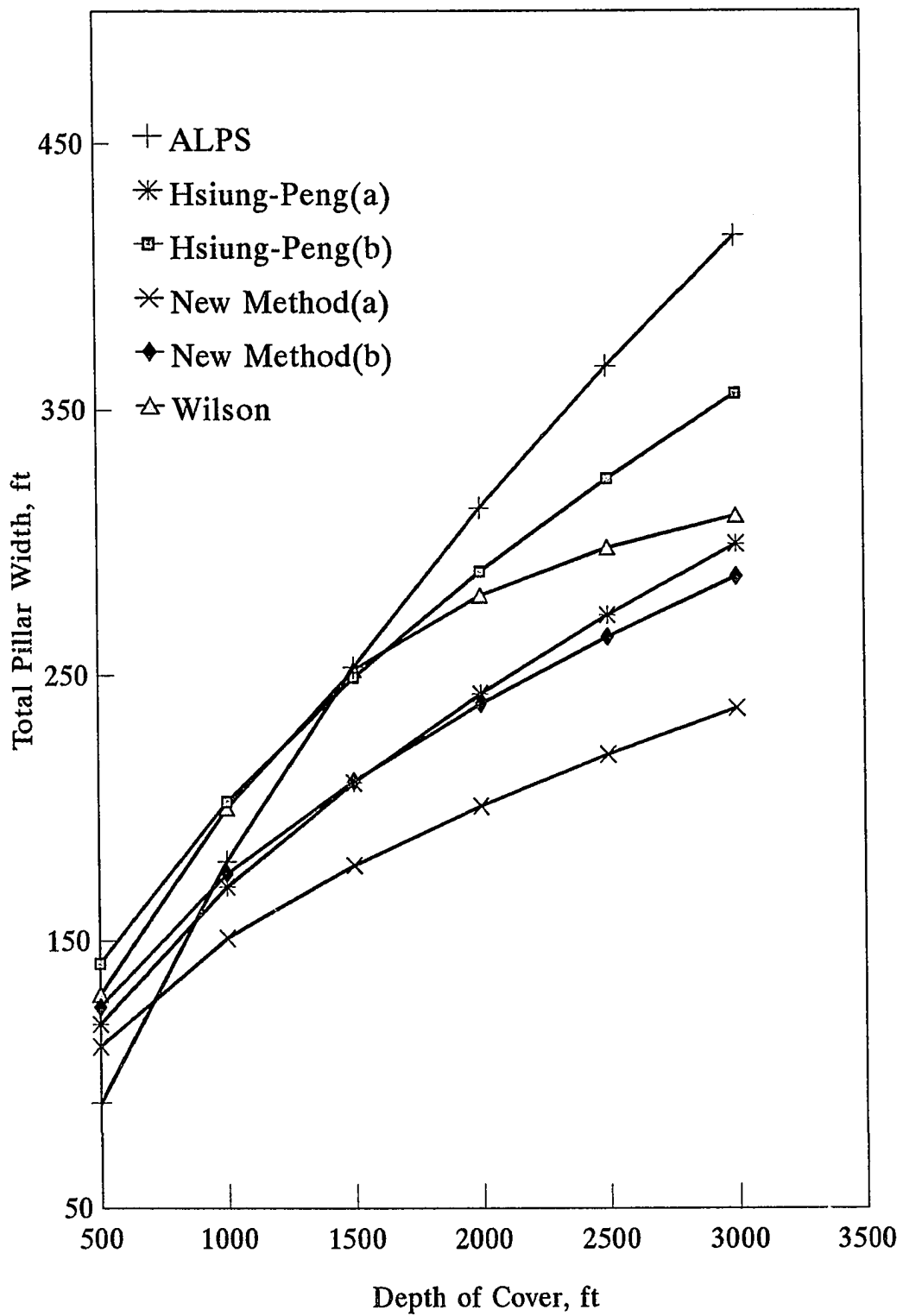


Figure 7.2. Total pillar width of stiff-stiff pillar design predicted by the different design methods for a three-entry system.

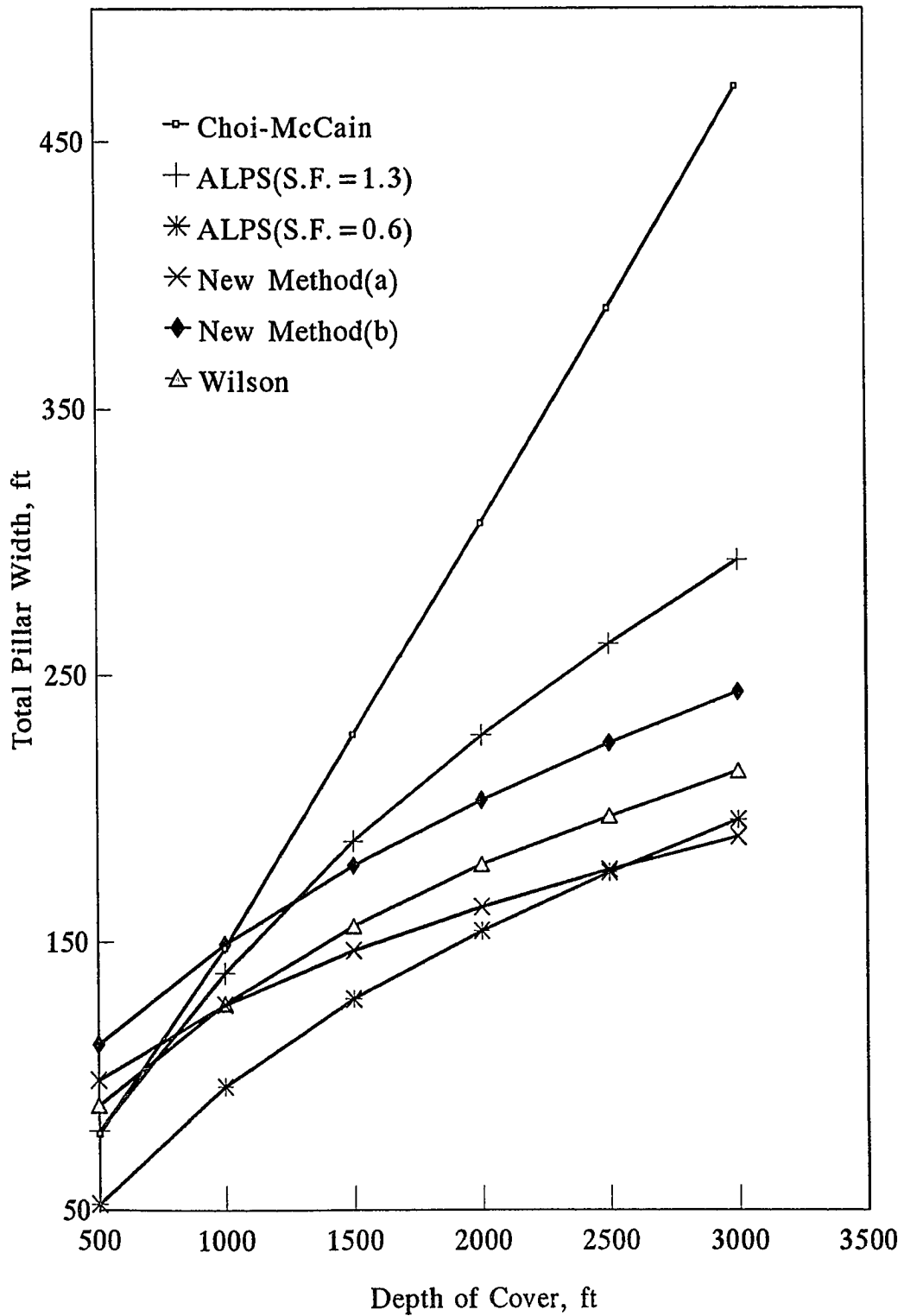


Figure 7.3. Total pillar width of stiff-yield pillar design predicted by the different design methods for a three-entry system.

yield pillar design, the total pillar width will also be reduced. The ALPS method is a very good example. According to the new method, the predicted total pillar width will vary with different roof and floor conditions. The prediction is not unique. Under a given roof and floor condition, the suitable pillar size will fall into the range predicted based on the best and the worst roof and floor conditions.

7.5 Summary

As demonstrated, the new pillar design method is a simple design method. It mainly involves two major steps during pillar design process, 1) to classify the in-situ roof and floor condition, and 2) to use the corresponding equation for determining pillar size. The prediction is not unique depends on the safety factors chosen. The best prediction will ensure the stability of roof and floor and maximize coal recovery. The new method considers the stabilities of roof, pillar and floor. Therefore, the design should be more reliable and realistic. It can be used to design different types of entry-pillar system as well. Usually, the new method predicts a smaller total pillar width under deep cover.

CHAPTER 8

CONCLUSIONS

Current success in longwall mining can be attributed to the continuous improvement on mining technology and mining equipment, and better mining conditions. As longwall mining goes deeper both geological and mining conditions become more complicated. An improper longwall panel design may lead to an unstable entry-pillar system and results in serious ground control problems, such as roof fall, floor heave and pillar bump under. Moreover, with the conventional pillar design concept, these ground control problems sometimes can not be overcome due to economic and environmental constraints. Based on the numerical model simulation and stability analysis, this study has demonstrated that the new pillar design method, which is developed based on the yield pillar design concept, can be used as an alternative for longwall chain pillar design, especially for deep longwall mining if the stability conditions of roof and floor can be satisfied. The study has also illustrated the importance of considering the stabilities of roof, pillar and floor for an entry-pillar system design. Because the stability of an entry-pillar system in underground mines can only be guaranteed when the stability of each basic element, such as roof, pillars and floor is ensured. Failure of any one of these elements would lead to total failure of the whole entry-pillar system.

The study on the yield pillar performance has also revealed the major functions

and mechanisms of yield pillar. Since a yield pillar allows a large deformation in the pillar and the surroundings, it redistributes stress in the entry-pillar system, and creates a stress release zone in the adjacent area to balance the stability conditions of the whole system. From the pillar design point of views, to achieve this goal, a pillar has to be designed as a stable yield pillar which satisfies two basic requirements: 1) it yields properly and transfers the loads to the adjacent area, and 2) it has to be self sustain and maintain good working conditions in the adjacent entries. Usually, a large entry convergence and a high tensile stress in the roof and floor are expected if a yield pillar is adopted in the entry-pillar system.

A new pillar method has been developed based on the stability analysis of the entry-pillar system under various roof and floor conditions in this study. The study shows the new design method can be used to design different types of three-entry system. Over all, the combination of a stiff and a yield pillar is the most preferable design in terms of coal recovery and roof and floor control. On the other hand, a stiff-stiff pillar design is the most conservative design and gives a better control on roof and floor in comparison with a yield-yield or a stiff-yield or a yield-stiff pillar design. But coal recovery in the stiff-stiff pillar design is also the lowest. On the contrary, a yield-yield pillar design is less likely to be used for three-entry longwall system except under strong roof and strong floor condition. In comparison with other design methods, the new design method predicts a smaller pillar size at deep cover, and a larger pillar size

than Choi and McCain and ALPS at shallow depth.

The study has demonstrated that the use of yield pillar design is also confined by the roof and floor conditions. It is possible that under certain roof and floor conditions a yield pillar can not be used as an alternative because it can not ensure the stability of roof and floor unless the roof and floor are reinforced by other artificial supports.

In addition, the study has identified the most important variables that affect the stability of an entry-pillar system in longwall mining. Since the new method consider the stability of roof, pillar and floor in the design, it should be more reliable and realistic.

Finally, the results from this study proved that the finite element method combining with orthogonal experiment design method is a very effective tool for underground structure analysis. It may be used to solve a variety of problems involved in underground coal mining.

REFERENCES

- Adler, L. and Sun, M., 1968, Ground Control in Bedded Formations, Bull. 20, VPI & SU, pp. 94-103.
- Barton, N., 1976, Recent Experiences with the Q-system for Tunnel Support, Proc. Symp. on Exploration for Rock Engineering, ed. Z. T. Bieniawski, A. A. Balkema, Rotterdam, Vol.1, p. 107-114.
- Barton, T. M., 1989, "Field Evaluation of Three Longwall Pillar Systems in a Kentucky Coal Mine," U. S. Bureau of Mines, RI 9283, pp. 1-13.
- Bieniawski, Z. T., 1976, Rock Mass Classifications in Rock Engineering, Proc. Symp. on Exploration for Rock Engineering, ed. Z. T. Bieniawski, A. A. Balkema, Rotterdam, pp. 97-106.
- Bieniawski, Z. T., 1979, The Geomechanics Classification in Rock Engineering Applications. Proc. 4th Int. Congress Rock Mechanics, ISRM, Montreux, A. A. Balkema, Rotterdam, Vol.2, p. 51-58.
- Bieniawski, Z. T., 1984, Rock Mechanics Design in Mining and Tunneling, A. A. Balkema, Boston, 272 pp.
- Britton, S., 1986, "Designing Deep-Seam Ground Control," Coal Mining & Processing, May, pp. 60-62.
- Carr, F., and Wilson, A. H., 1982, "A New Approach to the Design of Multi-Entry Developments for Retreat Longwall Mining," Proceedings of the 2nd Conference on Ground Control in Mining, West Virginia University, Morgantown, WV., pp. 1-21.
- Carr, F., Martin, E. and Gardner, B., 1984-85, "How to Eliminate Roof and Floor Failures with Yield Pillars," Coal Age, December 1984, p.62 and January, 1985, pp. 44-51.
- Choi, D. S. and McCain, D. L., 1979, "Design of Longwall Systems," Proceedings Mini-Symposium on Underground Coal Mine Design and Planning, SME-AIME Annual Meeting, Atlanta, GA, pp. 15-26.

- Combs, Trigg H., 1990, "Longwall Productivity Jumps 24% in Year," Coal, February, pp. 48-52.
- Combs, Trigg H., 1992, "Longwall Productivity Reaches 2,372 tons/shift," Coal, February, pp. 36-37.
- Dahl, H. D., and Parsons, P. C., 1972, "Ground Control Studies in the Hampherey No.7 Mine," Trans, Soc. Min. Eng. AIME v. 252, pp. 211-222.
- Demarco, M. S., and Koehler, J. K., 1988, "Characterization of Chain Pillar Stability in a Deep Western Coal Mine-Case Study," SME Preprint Number 88-76, SME-AIME Annual Meeting, Phoenix, Arizona, January, 25-28.
- Dey, A., 1985, Orthogonal Fractional Factorial Design, John Wiley & Sons, Inc., New York, pp. 133.
- Dowdy, S., and Wearden, S., 1983, Statistics For Research, John Wiley & Sons, Inc., New York, pp. 537.
- Eyer, D. D., 1988. "Underground Mines Continue Evolution, Forgo Revolutionary Changes," Coal, V.25, No. 8, 1988, pp. 52-54(A).
- Fang, K. T., and Pan, E. P., 1982, Clustering Analysis, Series on Geological Mathematics, Geological Publishing House(in Chinese), pp. 281.
- Franklin, J. A., 1975, Safety and Economy of Tunneling, Proc. Tenth Canadian Rock Mechanics Symp., Kingstone, pp. 27-53.
- Gaddy, F. L., 1956, A Study of the Ultimate Strength of Coal as Related to the Absolute Size of the Cubical Specimens Tested, VPI Bull., No. 112, pp. 1-27.
- Gauna, M., Price, K. R. and Martin, E., 1985, "Yield Pillar Usage in Longwall Mining at Depth, No. 4 Mine, Brookwood, Alabama," 26th U. S. Symposium on Rock Mechanics, Rapid City, SD, June, pp. 695-702.
- Haramy, K. Y., 1989, "Comparative Study of Western U.S. Longwall Panel Entry System," Proceedings of the 30th U.S. Symposium on Rock Mechanics, pp. 125-132.
- Holland, C. T., 1963, "Pressure Arch Techniques," Mechanization, Vol. 27, No. 3, pp.

45-48.

Holland, C. T., 1973, "Mine Pillar Design," in SME Mining Engineering Handbook, 1st ed. edited by A. B. Cummins and I. A. Given, SME-AIME, pp. 13-96-13-118.

Hsiung, S. M., and Peng, S. S., 1985. "Chain Pillar Design for U.S. Longwall Panel," Mining Science and Technology, 2(4): pp. 279-305.

Hustrulid, W. A., 1976, A Review of Coal Pillar Strength Formulas, Rock Mechanics, Vol, 8, pp. 115-145.

Kempthorne, O., 1952, The Design and Analysis of Experiments, John Wiley & Sons Inc., New York, pp. 312.

King, H. J. and Whittaker, B. N., "A Review of Current Knowledge on Roadway Behavior," Paper in the Proceedings of the Symposium on Roadway Strata Control, Inst. of Min and Metal, pp. 73-78.

Mark, C. and Bieniawski, Z. T., 1986, "Field Measurements of Chain Pillar Response to Longwall Abutment Loads," Proceedings of 5th Conference on Ground Control in Mining. West Virginia University, Morgantown, WV, pp. 114-122.

Mark, C. and Bieniawski, Z. T., 1986, "An Empirical Method for Design of Chain Pillars in Longwall Mining," Proceedings of the 27th U.S. Symposium on Rock, Mechanics (Tuscaloosa, AL, July). Soc. Min. Eng. AIME, pp. 415-422.

Martin, E., Stehney, C., Gambrel, C., Guana, M., and Southerland, R., 1985, "Yield Pillar Applications--Impact on Strata Control & Coal Production," Proceedings 4th Conference on Ground Control in Mining, West Virginia University, Morgantown, WV, July 22-24, supplement, pp. 104.

Martin, E. and Carr, F., 1988, "Recent Strata Control Advances at Jim Walter Resources Mining Division--Case Studies," Proceedings of 7th International Conference on Ground Control in Mining, West Virginia University, Morgantown, WV, pp. 66-75.10.

Merritt, P. C., 1992, "Longwalls Having Their Ups and Downs," Coal, February, pp. 26-35.

Mukerjee, R., 1982, Universal Optimality of Fractional factorial Plans derivable Through

- Orthogonal Arrays, Cal. Stat. Assoc. Bull., 31, pp. 63-68.
- Obert, L. and Duvall, W. I., 1967, *Rock Mechanics and the Design of Structures in Rock*, John Wiley and Sons, New York, pp. 542-545.
- Pappas, D. M., 1987, "Roof and Rib Fall Accident and Cost Statistics: An In-Depth Study," U.S. BuMines IC 9151, pp. 20.
- Peng, S. S., 1986, *Coal Mine Ground Control*, John Wiley & Sons, Inc. New York, 2nd ed. pp. 491.
- Peng, S. S., and Chiang, H. S., 1984, *Longwall Mining*, John Wiley & Sons, Inc., New York, pp. 708.
- Peng, S. S., Matsuki, K., and Su, W. H., 1980, "3-D Structural Analysis of Longwall Panels," Proc. 21st U.S. Symp. on Rock Mech., University of Missouri, Rolla, pp. 44-56.
- Peng, S. S. and Su, W. H., 1980, "3-D Structural Analysis of Retreating Longwall Panel," Proc. 4th Joint Meeting of MMIJ/AIME, Tokyo, Japan, Vol. B4, pp 1-16.
- Potter, P. E., Shimp, N. F. and Witters, J. 1963, Trace elements in marine and fresh-water argillaceous sediments: *Geochimica et Cosmochimica Acta*, 27, pp. 669-694.
- Quenon, R. H., 1989, "Coal Markets in the 90's: Customers are the Key," *AMC Journal*, American Mining Congress, July, pp. 10-11.
- Rutledge, J. C. and Preston, R. L., 1978, Experience with Engineering Classifications of Rock for the Prediction of Tunnel Support. Proc. Int. Tunneling Symp., Tokyo, pp. a-3-17.
- Sanda, A. P., 1991, "Longwall Shearers Grow Powerful," *Coal*, December, pp. 36-39.
- SAS Institute, 1985, "SAS User's Guide: Statistics," Version 5 Edition
- Scott, G. B., 1986, "Microcomputer Analyzes Longwall Economics," *Coal Mining*, Feb, pp. 48-49.
- Serata, S., 1976, "Stress Control Technique--An Alternative to Roof Bolting?," *Mining Engineering*, May, pp. 51-56.

- Serata, S., 1982, "Stress Control Methods: Quantitative Approach to Stabilizing Mine Openings in Weak Ground," Proceedings of 1st International Conference on Stability in Underground Mining, August, pp. 52-93.
- Sprouls, M. W., 1989, "Producers Predict More Records," Coal, January, pp. 30-34.
- Sprouls, M. W., 1991, "Operators Foresee More Growth 1991," Coal, January, pp. 36-41.
- Tsang, P., and Peng, S. S., 1989, "Yield Pillar Application under Strong Roof and Strong Floor Condition-A Case Study," Proceedings of the 30th U. S. Symposium on Rock Mechanics, pp. 411-418.
- Wang, L. S., and Fang, D. S., 1979, Mathematical Handbook, Higher Education Publishing House(in Chinese), pp. 1398.
- Wilson, A. H., 1973, An Hypothesis Concerning Pillar Stability. Min. Eng. (London), v.131, No. 141, June, pp. 409-417.
- Wilson, A. H., 1983, "The Stability of Underground Workings in the Soft Rocks of the Coal Measures," Int. J. of Min. Eng., v. 1, pp. 91-187.
- Anonymous, 1986, "The MSC/NASTRAN User's Manual(Version 64, 1985)," The MacNeal-Schwendler Corporation, 1986. pp. 814.

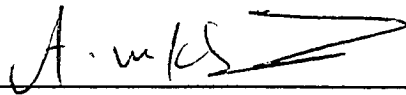
VITA

Po Tsang was born on December 1, 1960 in Shanghai, People's Republic of China. He attended Jiang-Xi Metallurgy Institute in China and received a Bachelor of Science Degree in Mining Engineering in June 1982.

In July 1982, he joined as an engineer in the Maanshan Metallurgy Research Institute, Maanshan, P. R. China and worked for two years. During that period, he was involved in various research projects including ventilation network analysis, control blasting design, etc.

He then entered the graduate school at West Virginia University in 1984, and obtained an M. S. Degree in Mining Engineering in 1986. In 1987, he enrolled in the Ph. D program in Mining Engineering at West Virginia University. Thereafter, he has been working as a Research/Teaching Assistant in the Department of Mining Engineering at West Virginia University.

APPROVAL OF EXAMINING COMMITTEE



Dr. A. W. Khair, Mining Engineering



Dr. C. Mark, U. S. Bureau of Mines



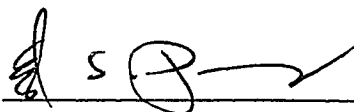
Dr. H. J. Siriwardane, Civil Engineering



Dr. N. T. Sivaneri, Mechanical & Aerospace Engineering

12-10-92

Date



Dr. S. S. Peng, Mining Engineering, Chairman